

**MORPHOLOGY CONTROL OF  
SELF-CONDENSED AROMATIC POLYIMIDES**

**自己縮合型芳香族ポリイミドの高次構造制御**

**MARCH 2014**

**Takashi Sawai**

**The Graduate School of Environmental Science**

**(Doctoral Program)**

**OKAYAMA UNIVERSITY**

**JAPAN**

## CONTENTS

INTRODUCTION	1
AIM AND STRATEGY OF THIS THESIS	5

### CHAPTER 1

#### MORPHOLOGY CONTROL WITH MOLECULAR CHAIN ORIENTATION OF POLY[4-(1,4-PHENYLENEOXY)PHTHALIMIDE]

1-1	INTRODUCTION	13
1-2	EXPERIMENTAL	14
1-2-1	Materials	14
1-2-2	Polymerization method	15
1-2-3	Measurements	15
1-3	RESULT AND DISCUSSION	16
1-3-1	Morphology of POPI	16
1-3-2	Morphology of P(OPI-co-PI)	30
1-4	CONCLUSIONS	39
1-5	REFERENCE	40

### CHAPTER 2

#### SYNTHESIS AND MORPHOLOGY CONTROL OF POLY(2,6-1H-BENZO[f]ISOINDOLE- 1,3(2H)-DIONE) AND EFFECT OF MONOMER STRUCTURE

2-1	INTRODUCTION	43
2-2	EXPERIMENTAL	45

2-2-1	Materials	45
2-2-2	Monomer synthesis	45
2-2-2-1	Synthesis of 3-ethoxycarbonyl-6-amino-2-naphthoic acid (6EAN)	46
2-2-2-2	Synthesis of 3-ethoxycarbonyl-7-amino-2-naphthoic acid (7EAN)	47
2-2-2-3	Synthesis of 6-amino- <i>N</i> -(2-pyridyl)naphthalene-2, 3-dicarboxylic imide (APNI)	49
2-2-2-4	Synthesis of 6-acetoaminonaphthalene-2, 3-dicarboxylic anhydride (ANDA)	48
2-2-3	Polymerization method	49
2-2-4	Measurements	49
2-3	RESULT AND DISCUSSION	50
2-3-1	Morphology of PBID prepared by 6EAN and 7EAN	50
2-3-2	Morphology of PBID prepared by APNI and ANDA	63
2-4	CONCLUSIONS	69
2-5	REFERENCE	70

## CHAPTER 3

### SYNTHESIS AND MORPHOLOGY CONTROL OF POLY(2,6-1H-BENZO[f]ISOINDOLE-1,3(2H)-DIONE-*co*-PHTHALIMIDE)

3-1	INTRODUCTION	73
3-2	EXPERIMENTAL	75
3-2-1	Materials	75
3-2-2	Polymerization method	75
3-2-3	Measurements	76
3-3	RESULT AND DISCUSSION	76
3-4	CONCLUSIONS	83
3-5	REFERENCE	84

CONCLUDING REMAREKS	86
LIST OF PUBLICATIONS	90
AKNOWLEDMENS	91

## INTRODUCTION AND AIM OF THIS STUDY

### INTRODUCTION

Aromatic polyimides are representative high performance polymer materials owing to prominent thermal stability, mechanical properties, chemical stability, low conductivity, and so on derived from their rigid structures. [1-5] Due to these excellent properties, various aromatic polyimides, for example KAPTON®, UPILEX® and so on, were used in industrial field as a thermally-stable resin, print circuit, photoresist resin and so on. [6-10] However, in most of polyimides, it is difficult to fabricate them to useful materials because of the infusibility and insolubility also derived from the rigid structures. Their intractable properties are trade-off relationship with high performance, and hence it is unfavorable to improve their processability by means of introduction of bulky pendant group or flexible linkage into the rigid main chains. [11-13] Therefore, aromatic polyimides are fabricated by traditional two-step method *via* the formation of corresponding poly(amic acid) as a soluble precursor. Tetracarboxylic dianhydride and diamine are reacted in an aprotic polar solvent to produce the poly(amic acid) and formed into fibers and films. Then poly(amic acid) materials are chemically or thermally imidized, resulting in the formation of the polyimide fibers and films. This method is superior in viewpoint of ease of handling and economy, but fatal defect is existed. In the imidization process, rigidity and planarity of the backbone structure increase owing to the change in the structure from poly(amic acid) to polyimide, simultaneously bringing about the decrease in molecular chain mobility. This structural development occurs rapidly, and desirable higher order structure including molecular orientation cannot be created.

Among many aromatic polyimides, self-condensed polyimides have been expected as

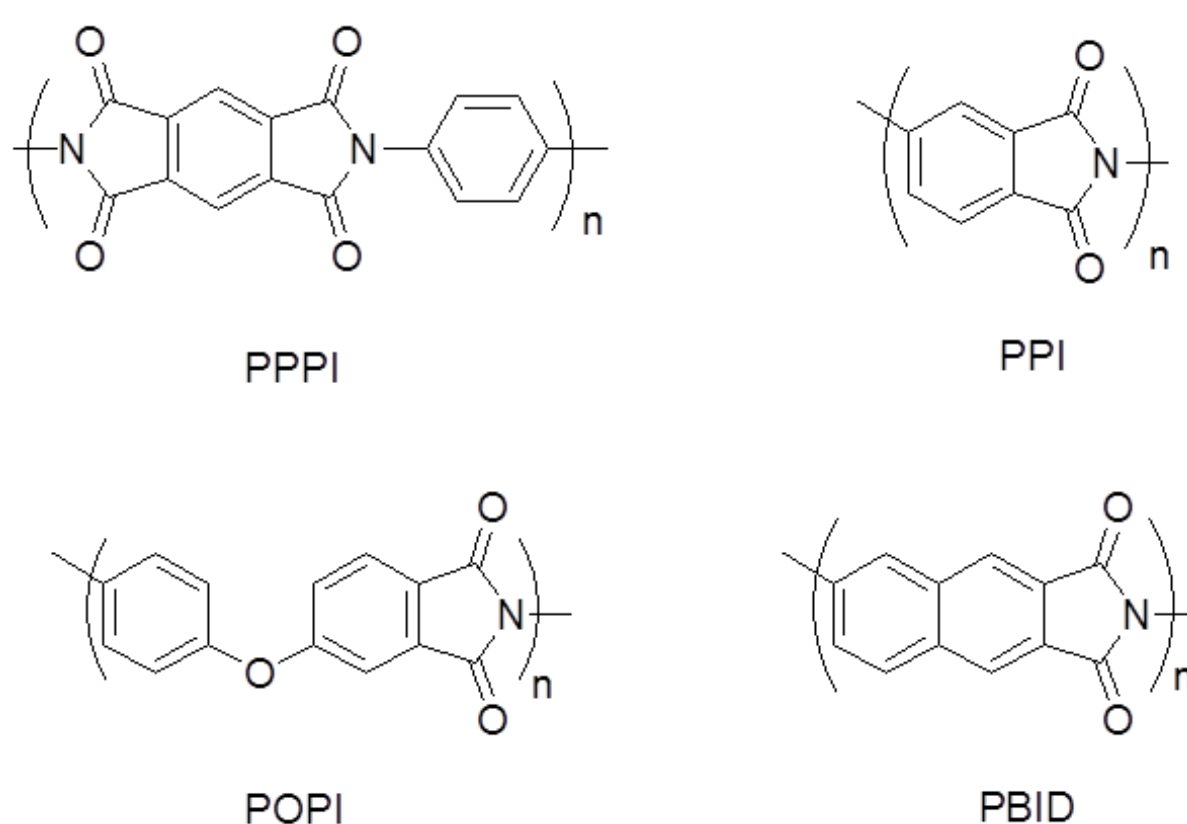
a hopeful candidate for not only the high-performance materials but also highly functional materials, because they possess polarization along the polymer molecules, resulting in the generation of hyperpolarizability. Even though the self-condensed polyimides are supposed to be synthesized from monomers containing two different functional groups, synthesis of the corresponding monomers is quite difficult. The imidization reaction of poly(amic acid) with elimination waters proceeds at relatively low temperature of below 100°C, and therefore highly reactive functional groups such as the combination of an amino group and a carboxylic anhydride group are required in the same molecule to prepare the poly(amic acid) precursor not containing imide groups under 100°C. However, the synthesis and purification of the monomer containing highly reactive groups, for example aromatic amino anhydride, are impossibly difficult because these groups react quickly and they are not isolated. In order to conquer this drawback, a few self-condensed polyimides were synthesized from amino aromatic dicarboxylic acids which were less reactive by using condensation agents as previously reported. [14] However, this preparative method is industrially and environmentally unfavorable because the condensation agent is required an equal or more amount of the functional group in the monomer, and process flow of remove the byproducts is entailed. For the preparation of the self-condensed polyimides, a novel methodology based on the different aspects is eagerly needed.

Morphology control of the polymer materials is of great importance to obtain the essential properties predicted from the polymer structure. However, the intractability of the rigid-rod polyimides makes them difficult to control the morphology by the conventional procedures as mentioned above. The research group of Okayama University has been studying the morphology control of wholly aromatic polymer by means of reaction-induced phase separation during phase separation, and the whisker of aromatic polyesters and a polythioester such as poly(*p*-oxybenzoyl) (POB), poly(2-oxy-6-nahtoyl)

(PON), poly[4-(4-oxyphenyl)benzoyl] and poly(*p*-mercaptobenzoyl) were successfully prepared by corresponding acetoxy carboxylic acid or *S*-acetylmercaptobenzoic acid [15-24]. The molecular chains are aligned along the long axis of these whiskers. It has been known that the one dimensional morphology such as needle-like crystals, fibers and ribbon-like crystals in which fully-extended molecular chains orient along the long direction of the crystal is the most desirable to withdraw the essential property of the polymers potentially predicted from the chemical structure. Therefore, these whiskers with the molecular chain orientation are ideal materials. This preparative procedure is beneficially applicable to the totally intractable polymers because the morphology is created by the self-assembling of oligomers during polymerization. These results afford the new methodology of the morphology control and its applicability is much broader for intractable rigid-rod polymers compared with the conventional methods.

There are only a few reports about the self-condensed polyimides [14, 25-34] as mentioned above, despite their potentials for advancement performance and emergence of new function. The preparative procedure using reaction-induced phase separation during polymerization can be used without the restriction of monomer, because the oligoimides, not oligo(amic acid)s, precipitate to form the morphology. Thus less reactive functional groups are able to be used for the fabrication of the aromatic polyimides. Structural homogeneity of oligomers significantly affects the morphology including both conversion of amic acid to imide and the structure of oligomer end-groups. And further, stoichiometry of two functional groups is very important factor for obtain high molecular weight polymer in the step-growth polymerization. The self-condensable monomers resolve these problems because the both end-groups of oligomers are stoichiometrically constant. Based on these viewpoints, poly(*p*-phenylenepyromelitimide) (PPPI) micro-flower of needle-like crystals and poly(4-phthalimide) (PPI) ribbon-like crystals were prepared by corresponding amino

dicarboxylic monoesters as self-condensable monomers [35, 36]. Molecular chains of PPPI and PPI are aligned along the long axis direction of the needle-like crystals and the ribbon-like crystals. These molecular orientations are desirable for the emergence of particular property attribute to self-condensed polymer such as second order non-linear optical properties owing to the hyperpolarization generated along the molecular chains. In fact, the PPI ribbon-like crystals exhibited second harmonic generation (SHG) activity [32]. Poly(2,6-1H-benzo[f]isoindole-1,3(2H)-dione) (PBID), which is a naphthalene ring containing self-condensed polyimide, has developed  $\pi$ -conjugate system. Due to this, strong non-linear optical property is expected, and hence the synthesis and morphology control of self-condensed polyimides by using reaction-induced phase separation during polymerization is a hopeful procedure to provide useful materials. But there still reminds unclear, for instance, adaptable molecular structure, influence of functional groups of monomers equal to the oligomer end-groups and copolymerization on higher-order structure and properties.



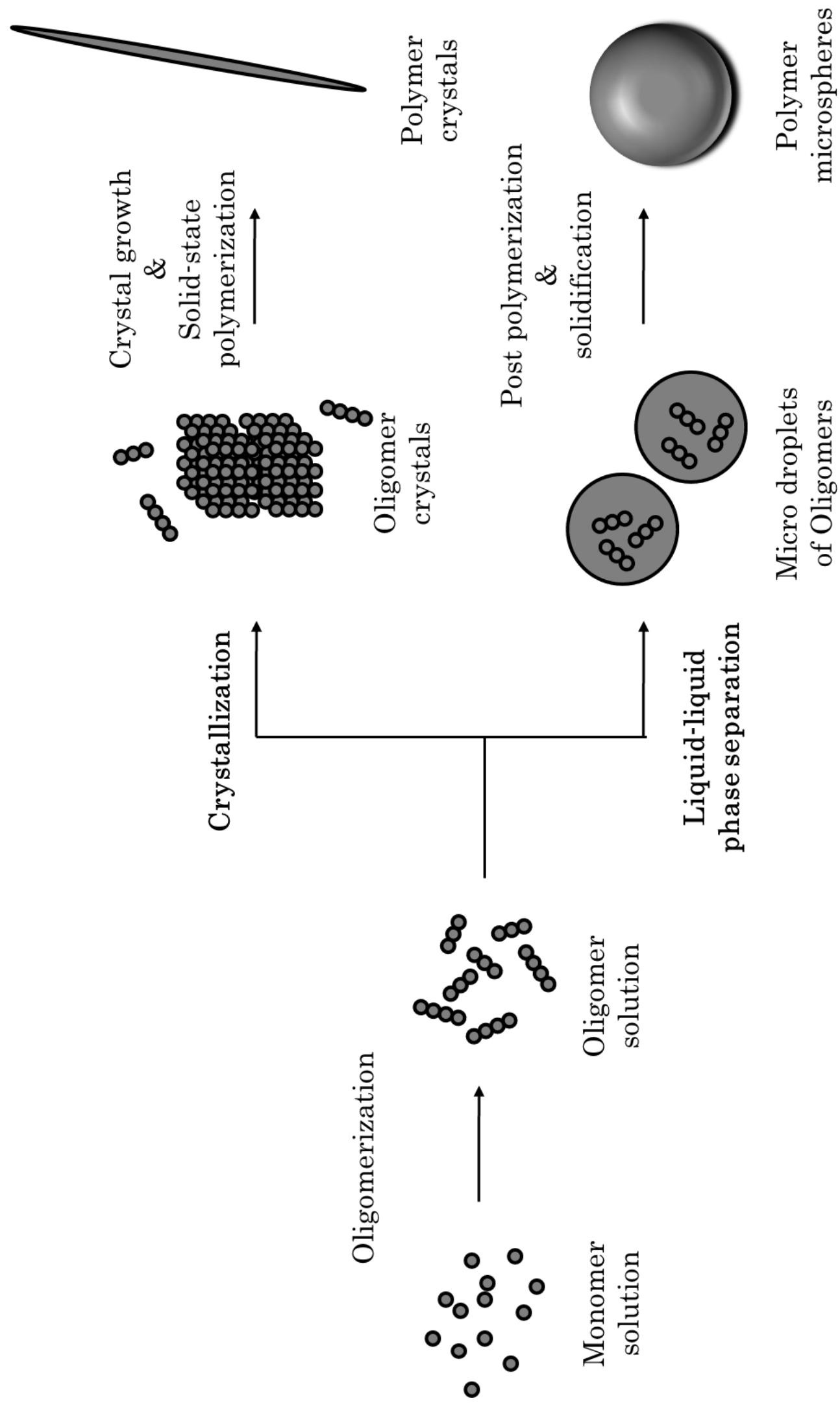
Scheme 1 Structure of various aromatic polyimides



## AIM AND STRATEGY OF THIS THESIS

On the basis of above discussion, the aim of this thesis is to develop the methodology for the synthesis and morphology control of self-condensed aromatic polyimides.

In order to accomplish this thesis, the strategy should be mapped out. The mechanism of the morphology control using reaction-induced phase separation during polymerization has been clarified by the previous studies, and basic principle of this method is schematically illustrated in Scheme 2. In this method, the solvents which are good to monomers and poor to polymers are used to induce the phase separation. Oligomers are formed in the solution and the degree of polymerization of them increases stepwise with time. Then the degree of polymerization exceeds a critical value, the oligomers start to be phase-separated. The phase separation diagram can be described in Figure 2, which is the analogous concentration-temperature ( $C$ - $T$ ) phase diagram to the partially miscible polymer-solvent system. [37, 38] The phase separation curve in the repulsive system in which here is no attractive interaction between oligomer and solvent is written as the combination of the freezing point curve of oligomers and the upper critical solution temperature type solubility curve. If the super-saturated oligomers precipitate across the freezing point curve, oligomers precipitate to form the crystals. Then subsequent crystal growth with simultaneously occurring solid-state polymerization in them accomplish the polymer crystals. On the other hand, if they precipitate across the consolution curve, polymer microspheres form *via* the formation of microdroplets of dense phase in the dilute phase by the liquid-liquid phase separation and following further polymerization in microdroplets, bringing about the solidification. The formation of the POB whisker as mentioned before and poly(*p*-oxycinnamoyl) microspheres are the typical examples of crystallization and liquid-liquid phase separation, respectively.



Scheme 2 Schematic illustrate of mechanism of reaction-induced phase separation during polymerization

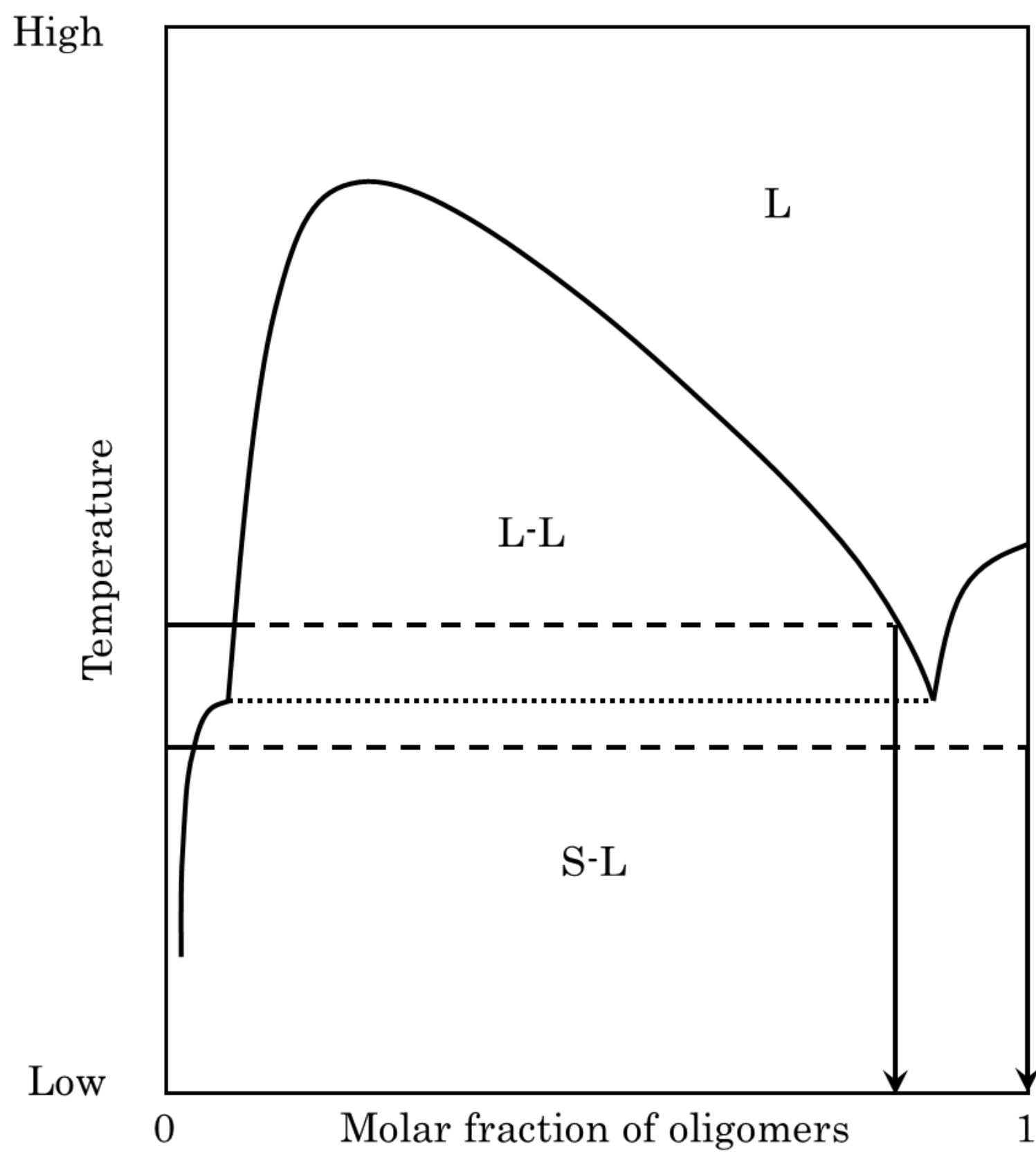


Figure 2 Schematic  $C$ - $T$  diagram for partially miscible oligomer and solvent system

L : miscible liquid phase

L-L : two immiscible liquid phase

S-L : liquid and solid phase

Rigid polymers possess strong interaction between molecules, and hence tend to crystallize laterally. Hence, alignment of rigid molecules along the long axis of the crystals requires other deserved mechanism. In the case of the POB whisker, it is clear that fully-extended molecular chains are aligned along the long direction by spiral growth of oligomers served as a screw dislocation on the oligomer lamellae. But the origin of screw dislocation is not cleared yet. Moreover, in the case of PPPI micro-flower of needle-like crystals and PPI ribbon-like crystals, even formation mechanism of these structures is unapparent. Therefore, control of molecular chain direction in the crystals is difficult. Here, in the reaction-induced phase separation during polymerization, it is reported that polymer whiskers comprised of *p*-oxybenzoyl and *p*-mercaptobenzoyl having graded composition were prepared by stepwise addition of 4-acetoxybenzoic acid to polymerization solution. [39] Based on this result, I thought that even though the direction molecular orientation cannot be controlled in the homopolymerization system, nuclei of other components would work as template in the copolymerization system resulting in the control of molecular orientation.

In the preparation of polyimide using reaction-induced phase separation during polymerization, it becomes clear that degree of imidization of precipitating oligomers greatly affects the morphology of precipitated products. The imide-rich oligomers, which possess higher freezing point and lower miscibility, have a tendency to crystallization. Reversely, imide-poor oligomers are prone to induce liquid-liquid phase separation by lower freezing point and higher miscibility. The microspheres formed by liquid-liquid phase separation are hard to control the molecular orientation. Hence, induction of the crystallization is preferable for synthesis and morphology control with molecular orientation of high performance materials. Furthermore, the non-cyclized imide-poor oligomers lose the crystallizability compared with the imide-rich oligomers because of not

only the essential crystallizability of amic acid but also existence of structural isomers. In the preparation of polyimide by amino dicarboxylic monoester, three kinds of reaction pathway exist in the formation of non-cyclized precursors. First one is the formation of dicarboxylic anhydride by dealcoholized cyclization, following the formation of amic acid. Others are the direct condensation reactions of amine and carboxylic acid or ester, resulting in the formation of amic acid or amic ester, respectively. The three non-cyclized structural isomers, two differential catenation amic acids and amic ester, are formed by three reaction pathways. The existence of structural isomers inhibits the formation of clear crystals. In previous study, it is reported that imide content of precipitation of imide-rich oligomers can control by polymerization condition [40]. However, if the miscibility between oligomers and solvent is quite low such as preparation of PBID, the degree of imidization of precipitation oligomers is more strongly dependent on monomer structure than polymerization conditions because it is predict that precipitation of oligomers is occurred in condensation-limited rather than imidization-limited. In order to clear these problems, I investigate using two kinds of one-step imide forming functional group combination that is dicarboxylic anhydride and acetoamido or 2-pyridylimide and amine. [41, 42]

This thesis consists of three chapters. Morphology control with molecular chain orientation of poly[4-(1,4-phenylene)oxyphthalimide] (POPI) by using reaction induced phase separation during polymerization by the aid of PPI nuclei as a template is reported in Chapter 1. Chapter 2 is described synthesis and morphology control of PBID as a novel self-condensed polyimide. In this chapter, influence of monomer functional groups for morphology is also discussed. In Chapter 3, synthesis and morphology control of P(BID-*co*-PI) is investigated with the comparison of P(OB-*co*-ON) which is well-known thermotropic wholly aromatic polyesters.

## REFERENCE

- [1] Sroog, C. E., *J. Polym. Sci., Macromol. Rev.* 1976, **11**, 161.
- [2] Bessonov, M. I.; Koton, M. M.; Kudryavtsev, V. V.; Laius, L. A., *Polyimides: Thermally Stable Polymers*; Consultants Bureau: New York, 1987.
- [3] Wilson, D.; Stenzenberger, H. D.; Hergenrother, P. M., *Polyimides*; Blackie: New York, 1990.
- [4] Eastmond, G. C.; Paprotny, J., *Reactive & Functional Polymers*, 1996, **30**, 27.
- [5] Takekoshi, T., *Adv. Polym. Sci.* 1990, **94**, 1.
- [6] Sroog, C. E.; Endrey, A. L.; Abramo, S. V.; Berr, C. E.; Edward, W. M.; Olivier, K. L., *J. Polym. Sci.: Part A: Polym. Chem.*, 1965, **3**, 1373.
- [7] Sato, R., *Purasuchikkusu*, 1983, **34**, 93.
- [8] Kerwin, R. E.; Goldrick, M. R., *Polymer Eng. & Sci.*, 1971, **11**, 426.
- [9] Ueda, M.; Nakayama, T., *Macromolecules*, 1996, **29**, 6427.
- [10] Jang, Y. M.; Seo, J. Y.; Chae, K. H., *Macromol. Res.*, 2006, **14**, 300.
- [11] For example Cassidy, P.E., *Thermally Stable Polymers, Syntheses and Properties*. Marcel Dekker: New York: 1980.
- [12] Jinta, T.; Matsuda, T., *Sen'i Gakkaishi* 1986, **42**, 554.
- [13] Mittal, K. L., *Polyimides, synthesis, characterization,; application*, Vol. 1. New York: Plenum Press; 1984.
- [14] Liu, X. Q.; Yamanaka, K.; Jikei, M.; Kakimoto, M., *Chem. Mater.*, 2000, **12**, 3885.
- [15] Kato, Y.; Endo, S.; Kimura, K.; Yamashita, Y.; Tsugita, H.; Monobe, K., *Koubunshi Ronbunshu*, 1987, **44**, 35.
- [16] Yamashita, Y.; Kato, Y.; Kimura, K.; Tsugita, H.; Monobe, K., *Koubunshi Ronbunshu*, 1987, **44**, 41.
- [17] Kato, Y.; Yamashita, Y.; Kimura, K.; Endo, S.; Kajisaki, K., *Koubunshi Ronbunshu*,

1988, **45**, 973.

[18] Yamashita, Y.; Kato, Y.; Endo, S.; Kimura, K., *Makromol. Chem. Rapid Commun.*, 1988, **9(9)**, 678.

[19] Kato, Y.; Yamashita, Y.; Kimura, K.; Endo, S.; Ohata, T., *Koubunshi Ronbunshu*, 1990, **47**, 583.

[20] Kimura, K.; Endo, S.; Kato, Y.; Yamashita, Y., *Polymer*, 1994, **35**, 123.

[21] Yamashita, Y.; Kimura, K., *Polymeric Materials Encyclopedia* (CRC Press), 1996, 8707.

[22] Kimura, K.; Kato, Y.; Endo, S.; Yamashita, Y., *Polymer*, 1993, **34**, 1054.

[23] Kimura, K.; Yamashita, Y., *Polymer*, 1994, **35**, 3311.

[24] Kimura, K.; Kato, Y.; Inaba, T.; Yamashita, Y., *Macromolecules*, 1995, **28**, 255.

[25] Im, J. K.; Jung, J. C., *J. Polym. Sci.: Part A: Polym. Chem.*, 2000, **38**, 402.

[26] Wang, Z. Y.; Qi, Y.; Bender, T. P.; Gao, J. P., *Macromolecules*, 1997, **30**, 764.

[27] Bender, T. P.; Qi, Y.; Gao, J. P.; Wang, Z. Y., *Macromolecules*, 1997, **30**, 6001.

[28] Im, J. K.; Jung, J. C., *Polym. Bull.*, 1998, **41**, 409.

[29] Im, J. K.; Jung, J. C., *J. Polym. Sci.: Part A: Polym. Chem.*, 1999, **37**, 3530.

[30] Im, J. K.; Jung, J. C., *Polym. Bull.*, 1999, **43**, 157.

[31] Thiruvassagam, P.; Venkatesan, D. J., *Macromol. Sci., Part A: Pure and Applied Chem.*, 2009, **46**, 419.

[32] Kawauchi, S.; Shirata, K.; Hattori, M.; Kaneko, S.; Miyawaki, R.; Watanabe, J.; Kimura, K., Preprints of *21th Polyimide & Aromatic Polymer conference, Japan*, 2013.

[33] Nosova, G. I.; Gofman, I. V.; Baklagina, Yu. G.; Kofanov, E. R.; Ovchinnikov, K. L.; Kolobov, L. V.; Kudryavtsev, V. V., Institute of Macromolecular Compounds, Russian Academy of Sciences, St. Petersburg, Russia. *Vysokomolekulyarnye Soedineniya, Seriya A i Seriya B*, 2000, **42(5)**, 725.

[34] Numata, S.; Ikeda, T.; Fujisaki, K.; Miwa, T.; Kinjo, N., *Eur. Pat. Appl.*, 1988,

JPS63159434 (A).

[35] Wakabayashi, K.; Uchida, T.; Yamazaki, S.; Kimura, K., *Polymer*, 2011, **52**, 837.

[36] Wakabayashi, K.; Uchida, T.; Yamazaki, S.; Kimura, K., *Macromolecules*, 2008, **41**, 4607.

[37] Rain, H.C.; Richard, R. B.; Ryder, H., *Trans. Faraday Soc.*, 1945, **41**, 56.

[38] Richard, R. B., *Trans. Faraday Soc.*, 1946, **42**, 10.

[39] Kobashi, K.; Kimura, K.; Yamashita, Y., *Macromolecules*, 2004, **37**, 7570.

[40] Wakabayashi, K.; Uchida, T.; Yamazaki, S.; Kimura, K.; Shimamura, K., *Macromolecules*, 2007, **40**, 239.

[41] Takekoshi, T.; Webb, J. L.; Anderson, P. P.; Olsen, C. E., *IUPAC 32nd International Symposium on Macromolecules*, 1988, 464.

[42] John, A. K., *Polymer*, 1995, **36**, 2089.



## CHAPTER 1

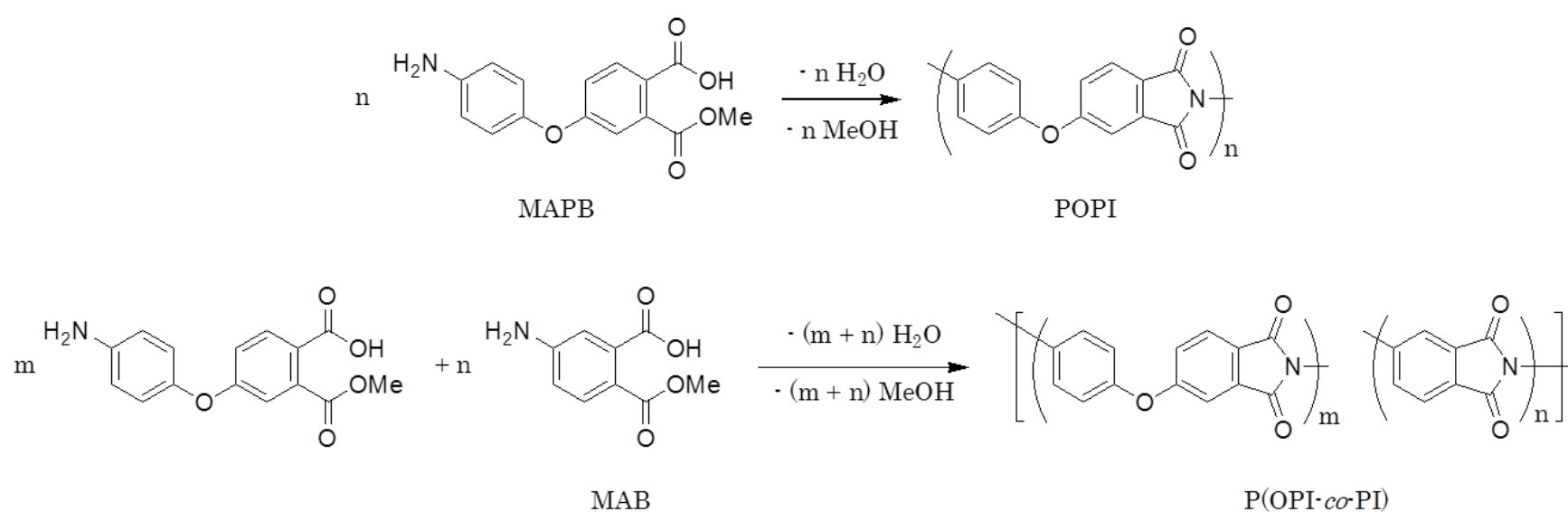
# MORPHOLOGY CONTROL WITH MOLECULAR CHAIN ORIENTATION OF POLY[4-(1,4-PHENYLENEOXY)PHTHALIMIDE]

### 1-1 INTRODUCTION

Wholly aromatic poly(ether-imide)s are in the class of high performance polymer materials [1-9] as represented by KAPTON®. It has been reported that poly[4-(1,4-phenylene)oxyphthalimide] (POPI) which is a self-condensed poly(ether-imide) was synthesized by using condensation agent. [3] However, creation of higher order structure has not been achieved because self-condensation polyimides cannot be synthesized by the two-step preparation method *via* the formation of poly(amic acid) precursor. Additionally, use of an equal amount of the condensation agent is atom-economically and environmentally unfavorable. Even though POPI showed low crystallinity, the film exhibited excellent thermal stability and good mechanical properties, suggesting that the POPI crystals having precise molecular orientation would become novel high performance materials. The method of reaction-induced phase separation during polymerization [10-17] explained in INTRODUCTION AND AIM is applicable to prepare morphologically controlled polyimides in one-pot procedure without condensation agents.

In this chapter, the morphology control of POPI was examined by using the reaction-induced phase separation during polymerization of 2-methoxycarbonyl-4-(4'-aminophenoxy)benzoic acid (MAPB). Further, the copolymerizations of MAPB and 2-methoxycarbonyl-5-aminobenzoic acid (MAB) were

examined as shown in Scheme 1-1 to investigate the influence of the copolymerization on the morphology of poly[4-(1,4-phenylene)oxyphthalimide-*co*-4-phthalimide] (P(OPI-*co*-PI)).



Scheme 1-1 Synthesis of POPI and P(OPI-*co*-PI)

## 1-2 EXPERIMENTAL

### 1-2-1 Materials

MAPB and MAB were synthesized according to the previously reported procedure [3, 18]. A mixture of isomers of dibenzyltoluene (DBT) was purchased from Matsumura Oil Co. Ltd. (Trade name: Barrel Therm 400, MW: 380, b.p.: 382°C) and purified by distillation under reduced pressure (170-180°C / 0.4 mmHg). Liquid paraffin (LPF) was purchased from Nacalai Tesque Co. Ltd. and purified by distillation under reduced pressure (185-215°C / 0.2 mmHg). Benzophenone (BPN) and diphenyl sulfone (DPS) were purchased from Tokyo Kasei Co. Ltd. BPN was purified by recrystallization from methanol. DPS was done from a mixture of methanol and water.

### 1-2-2 Polymerization method

DBT (10.5 g) was placed into a cylindrical flask equipped with gas inlet and outlet tubes and a thermometer, and then heated up to 330°C under nitrogen. MAPB (121 mg, 0.42 mmol) was added into DBT at 330°C, and the mixture was stirred for 5 second. And then the polymerization was carried out at 330°C for 6 h with no stirring. Concentration of the polymerization, defined as (calculated polymer weight / solvent volume)  $\times$  100 in this study, was 1.0%. The solution became turbid immediately due to the precipitation of oligomers and the POPI was formed as precipitates after 6 h. The POPI precipitates were collected by vacuum filtration at 330°C, washed with *n*-hexane and acetone, and then dried at 50°C for 12 h. Oligomers left in the solution at 330°C were recovered by pouring the filtrate into *n*-hexane at 25°C. The polymerizations of MAPB under other conditions were also carried out in a similar manner. But in the case of using BPN and DPS as a solvent, toluene and acetone used for washing precipitates. The copolymerizations of MAPB and MAB were also carried out in a similar manner to the polymerization of MAPB.

### 1-2-3 Measurements

Morphology of precipitates was observed on a HITACHI S-3500N scanning electron microscope at 20 kV. Samples were dried, sputtered with platinum/palladium and observed at 20kV. Average shape parameters of the products were determined by taking the average of over 100 observation values. Samples for transmission electron microscopy were prepared by depositing the precipitate suspension in acetone onto carbon grids and drying in air at 25°C. Bright field images, dark field images and selected area electron diffraction (SAED) patterns were recorded on Kodak SO-163 Film using JEM 2000EX (operated at

200 kV). Infrared (IR) spectra were recorded on a JASCO FT/IR-410 spectrometer. Wide angle X-ray scattering (WAXS) was performed on a Rigaku Gaiger Flex with nickel-filtered CuK $\alpha$  radiation (35 kV, 20 mA). Matrix assisted laser desorption ionization time-of-flight (MALDI-TOF) mass spectrometry was performed on a Bruker Daltonics AutoFLEX MALDI-TOF MS system operating with a 337 nm N<sub>2</sub> laser. Spectra were obtained in the linear positive mode with an accelerating potential of 20 kV. Mass calibration was performed with angiotensin I (MW 1296.69) and insulin B (MW 3496.96) from a Sequazyme peptide mass standard kit. Samples were then prepared by the evaporation-grinding method and ran in dithranol as a matrix doped with potassium trifluoroacetate according to previously reported procedures [19, 20]. Thermogravimetric analysis (TGA) was performed on a Perkin-Elmer TGA-7 with a scanning rate of 10°C·min<sup>-1</sup> in nitrogen atmosphere. Differential scanning calorimetry (DSC) was performed on a Perkin-Elmer DSC-7 with a scanning rate of 10°C·min<sup>-1</sup> in nitrogen atmosphere. Inherent viscosity ( $\eta_{inh}$ ) was measured in 97% sulfuric acid at a concentration of 0.5% at 30°C and it was adapted as a measure of molecular weight of POPI as generally used. The content of POPI moiety in the copolymers ( $\chi_p$ ) was determined by IR analysis.

## 1- 3 RESULT AND DISCUSSION

### 1-3-1 Morphology of POPI

The solvent is of importance to induce the phase separation during polymerization, and it is required that the solvent is miscible to a monomer and immiscible to a polymer. Further, they must possess boiling point higher than polymerization temperature. Based on these requirements, three kinds of the solvent such as DBT, BPN and DPS were used in this

study. And LPF was used for adjustment of miscibility in mixed with DBT. MAPB was insoluble in these solvents at 25°C, but it became dissolved at the polymerization temperature. In the case of the polymerization carried out in DBT, polymerization solution became turbid immediately after an addition of monomers due to the formation of the oligomers and following their precipitation, and products were obtained after 6 hours. The polymerizations were carried out under various conditions. Results of the polymerization in DBT are shown in Table 1-1. The polymerization of MAPB afforded pale yellow precipitates in yields of 83-91%. In the IR spectrum of precipitates prepared in DBT at 330°C at a concentration of 1.0% as shown in Figure 1-1, asymmetric and symmetric stretching of imide carbonyl C=O, stretching of imide C-N and deformation of imide ring were observed in 1776, 1717, 1378 and 743 cm<sup>-1</sup>, respectively. Additionally, the groups of amino, carboxyl, anhydride and methyl ester which were non-cyclized amic acid or amic ester and end-group were not visualized. This spectrum was identical with the previously reported POPI spectrum [3]. Inherent viscosities of precipitates were 0.39–0.99 dL·g<sup>-1</sup>, and high molecular weight POPIs were obtained at above 330°C. Inherent viscosity increased with the

Table 1-1 Results of polymerization of MAPB in DBT <sup>a</sup>

Run No.	Polymerization condition		Yield (%)	$\eta_{inh}^b$ (dL·g <sup>-1</sup> )	T <sub>10</sub> <sup>c</sup> (°C)	Morphology
	Temp. (°C)	Conc. (%)				
1	270	1.0	89	0.39	586	Unclear
2	330	0.5	83	0.99	564	Fiber, SP <sup>d</sup>
3	330	1.0	86	0.77	571	Fiber, SP
4	330	5.0	86	0.71	543	SP
5	350	1.0	91	0.85	571	Fiber, SP

<sup>a</sup> Polymerizations were carried out in DBT for 6 h. <sup>b</sup> Inherent viscosities were measured in 97% sulfuric acid at a concentration of 0.5 g · dL<sup>-1</sup> at 30°C. <sup>c</sup> Temperature of 10% weight loss in nitrogen atmosphere. <sup>d</sup> Spherical aggregates of plate-like crystals.

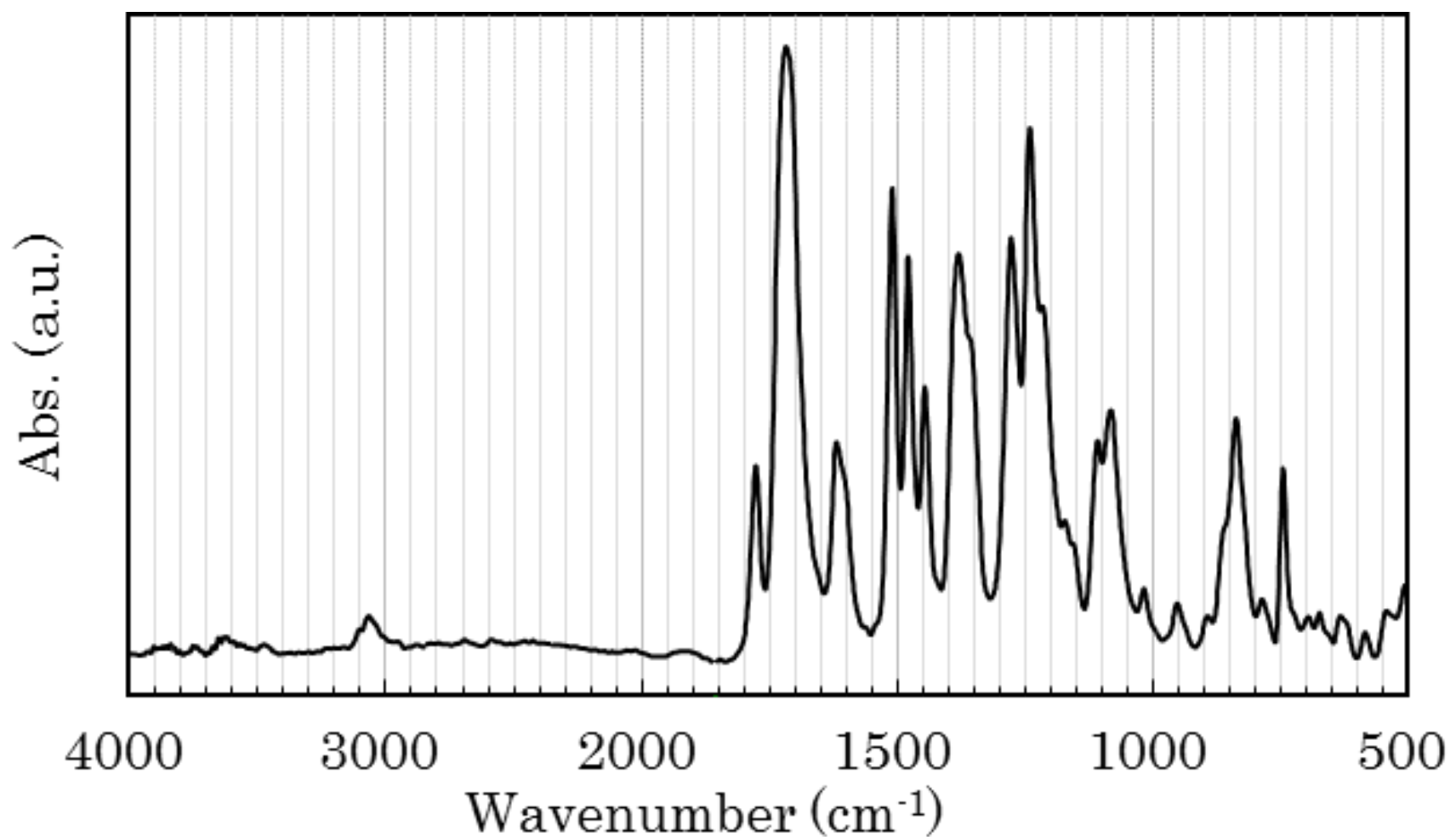


Figure 1-1 FT-IR spectrum of POPI precipitates prepared in DBT at 330°C at a concentration of 1.0% (Run No. 3)

polymerization temperature, and decreased with the polymerization concentration. It seems that higher polymerization temperature progress efficient solid-state polymerization, and higher polymerization concentration cause decrease molecular weight of precipitation oligomers. Morphology of POPI precipitates were shown in Figure 1-2. The polymerization at 270°C at a concentration of 1.0% produced unclear morphology as shown in Figure 1-2 (a). In the condition of lower polymerization temperature, molecular weight of oligomers precipitated from the polymerization solution decreased owing to the lower miscibility between oligomers and solvent. Hence, liquid-liquid phase separation and not crystallization was occurred because of lower freezing point of low molecular weight oligomers, spherical precipitates were formed. In contrast to this, spherical aggregates of plate-like crystals were observed in other conditions as shown in Figure 1-2 (b)-(e). The diameter of these aggregates is 2–3  $\mu\text{m}$ . The plate-like crystals showed clear crystal habit, and grew like crosshatch form in the spherical aggregates. This morphology is similar to a microsphere having rugged surface of PPPI from the polymerization of pyromellitic

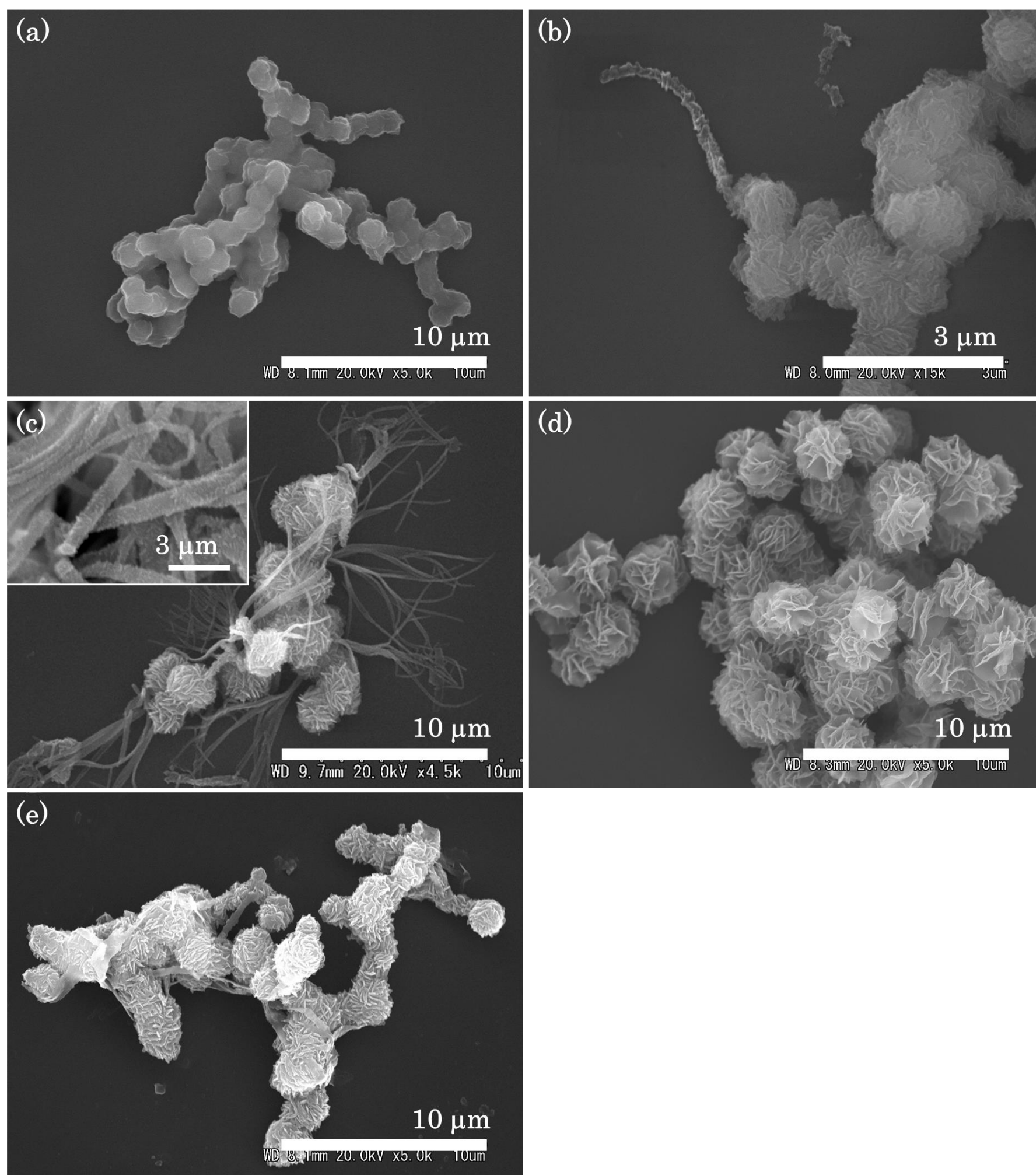


Figure 1-2 Morphology of POPI precipitates prepared in DBT (a) at 270°C at a conc. of 1.0% (Run No. 1), (b) at 330°C at a conc. of 0.5% (Run No. 2), (c) 330°C at a conc. of 1.0% (Run No. 3), (d) at 330°C at a conc. of 5.0% (Run No. 4) and (e) at 350°C at a conc. of 1.0% (Run No. 5)

dianhydride and *p*-phenylene diamine previously reported [21], and it is interesting as a functional microsphere and fillers. The polymerization at 330°C at a concentration of 1.0% afforded fiber crystals co-existed with spherical aggregates of plate-like crystals. This fiber is approximately 250 nm in width and 15 μm longer in length (Figure 1-2 (c)). The polymerization at 330°C at a concentration of 0.5% also yielded the fiber crystals as well as that at 350°C at a concentration of 1.0% (Figure 1-2 (b), (e)). But these fibers were quite short and scarce, the polymerization at 330°C at a concentration of 1.0% is a favorable condition for the formation of the POPI fibers in DBT.

Influence of the polymerization solvent on the POPI morphology was also investigated. In LPF, MAPB was not dissolved at 330°C entirely, thus the mixtures of DBT and LPF were used for the adjustment of miscibility between oligomers and solvents. The contents of each solvent in the mixed solvents are named by their weight ratios. Results of polymerization were represented in Table 1-2. In the case of the polymerizations in BPN and DPS, yields of product were slightly lower than polymerization in DBT. BPN and DPS are polar solvent that possess higher miscibility for oligomers, hence, greater amount of oligomers were remained in the solution. In the polymerization in DBT/LPF = 5/5, precipitates were short rod-like shown in Figure 1-3 (a) and the yield was 88%. This

Table 1-2 Results of polymerization of MAPB in various solvents <sup>a</sup>

Run No.	Polymerization condition		Yield (%)	$\eta_{inh}^b$ (dL·g <sup>-1</sup> )	T <sub>10</sub> <sup>c</sup> (°C)	Morphology
	Solvent	Temp. (°C)				
6	DBT/LPF = 5/5	330	88	0.48	569	Rod
7	DBT/LPF = 7/3	330	81	0.52	567	Fiber, Rod
8	BPN	300	78	0.30	492	SP
9	DPS	330	64	0.51	562	SP <sup>d</sup>

<sup>a</sup> Polymerizations were carried out at a concentration of 1.0%. <sup>b</sup> Inherent viscosities were measured in 97% sulfuric acid at a concentration of 0.5 g·dL<sup>-1</sup> at 30°C. <sup>c</sup> Temperature of 10% weight loss in nitrogen atmosphere. <sup>d</sup> Spherical aggregates of plate-like crystals.



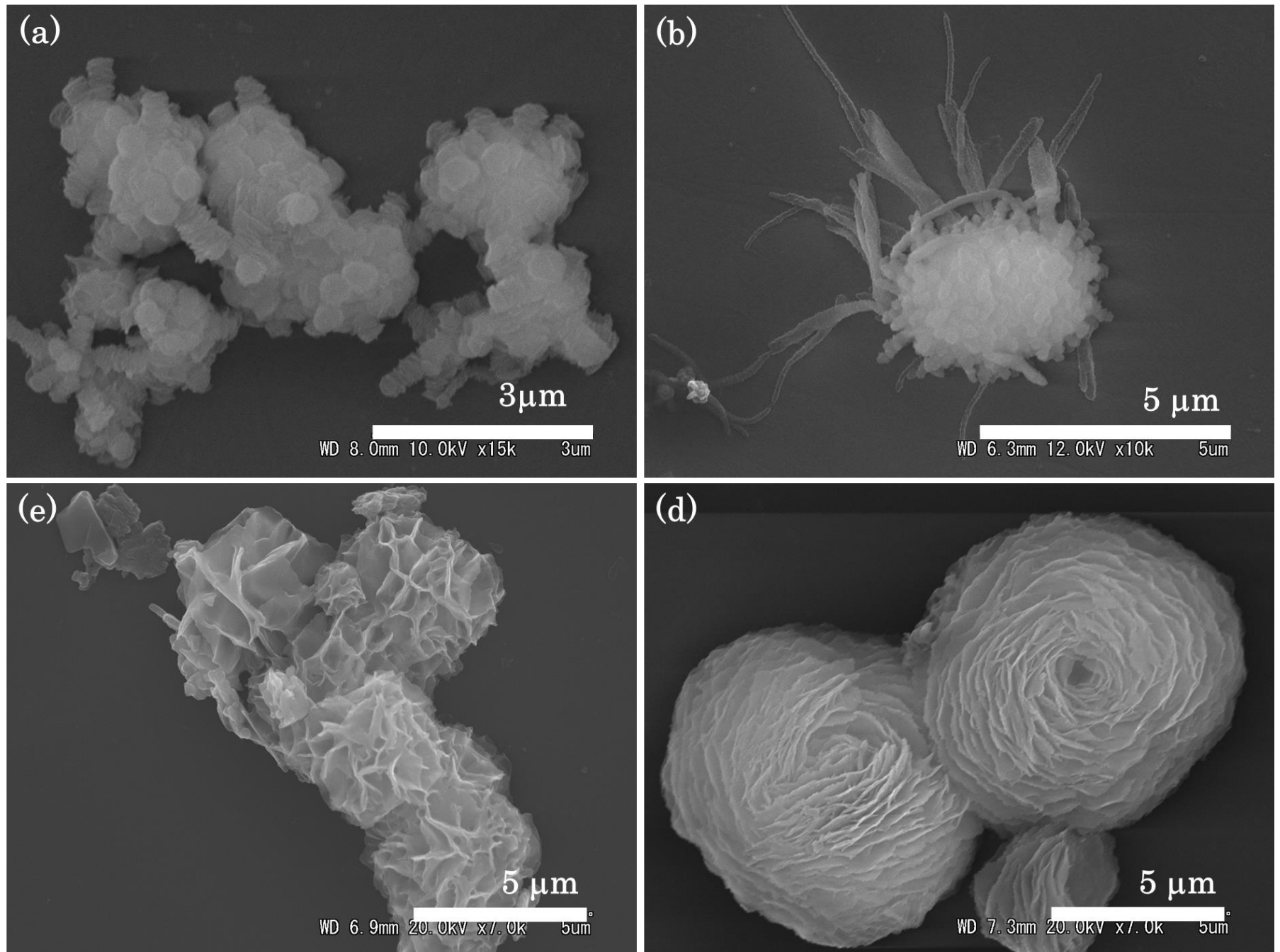


Figure 1-3 Morphology of POPI precipitates prepared at a concentration of 1.0% in (a) DBT/LPF = 5/5 (Run No. 6), (b) DBT/LPF = 7/3 (Run No. 7), (c) DPS (Run No. 8) and (d) BPN (Run No. 9)

rod-like structure looks like to be composed of small plate-like crystals stacked in rod long direction. This rod-like structure was also observed with the fiber crystals in the polymerization in DBT/LPF = 7/3 in yield of 81% (Figure 1-3 (b)). In this condition, the rod-like structure is sharper and longer than that prepared in DBT/LPF = 5/5. This sharper rod-like structure is very similar to the fiber, and it seems that these are quite similar structures. In the polymerization in DPS, the spherical aggregates of plate-like crystals were formed with the yield of 64% and the diameter of the spheres was ca. 8  $\mu\text{m}$  (Figure 1-3 (c)). It is interest that they were different from other spherical aggregates of the plate-like crystals prepared in DBT. The spherical aggregates prepared in DPS, plate-like crystals were circumferentially oriented. This morphology is similar to the inner structure of the poly(*p*-oxycinnamoyl) microspheres prepared by the reaction-induced liquid-liquid phase separation [22]. The polymerization in BPN was carried out at 300°C due to the boiling temperature of BPN and it gave the spherical aggregates of plate-like crystals with the yield of 78% (Figure 1-3 (d)). The precipitates of POPI prepared by the polymerizations in BPN and DPS were lower molecular weight. This fact is explained from the aspect of the POPI crystallinity. Figure 1-4 is WAXS intensity profiles of POPI precipitates prepared in DBT, BPN and DPS. In the profile of the precipitates prepared in DBT, six sharp peaks were found at  $2\theta = 10.4, 18.3, 24.2, 26.8, 28.0$  and  $31.4^\circ$  corresponding to  $d$ -spaces of 0.851, 0.486, 0.368, 0.333, 0.319, and 0.285 nm, respectively, indicating high crystallinity of the precipitates. In contrast to this, the crystallinity of the precipitates prepared in BPN and DPS was quite lower than that prepared in DBT. In the crude crystals, solid-state polymerization cannot occur efficiently because of the end-group position is unfavorable for the polycondensation.

In order to know the molecular orientation in the fiber, TEM and SAED were taken as shown in Figure 1-5. It was observed that the fiber crystal was composed of small

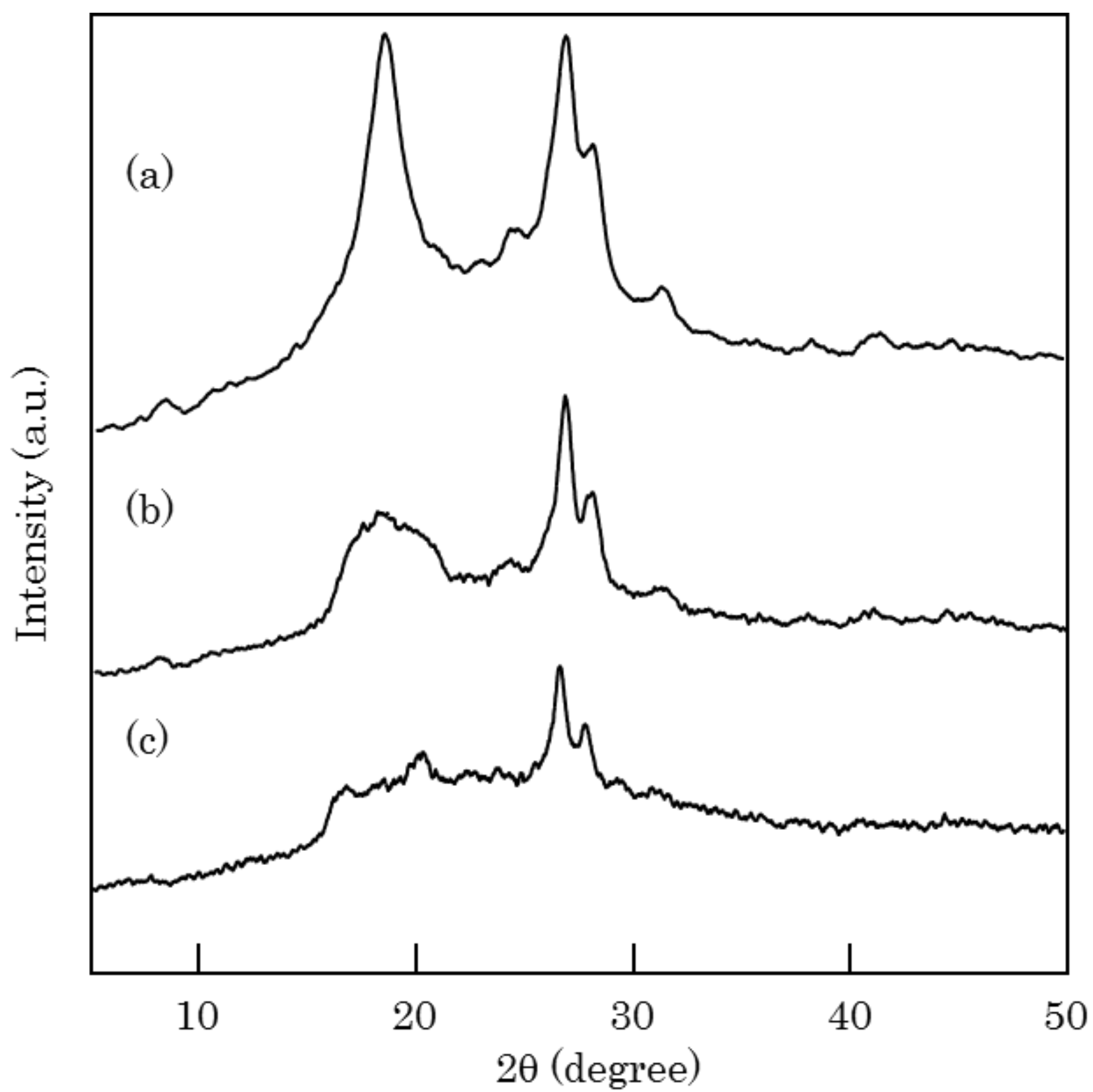


Figure 1-4 WAXS intensity profiles of POPI precipitates prepared at a concentration of 1.0 % (a) in DBT at 330°C (Run No. 3), (b) in BPN at 300°C (Run No. 8) and (c) in DPS at 330°C (Run No. 9)

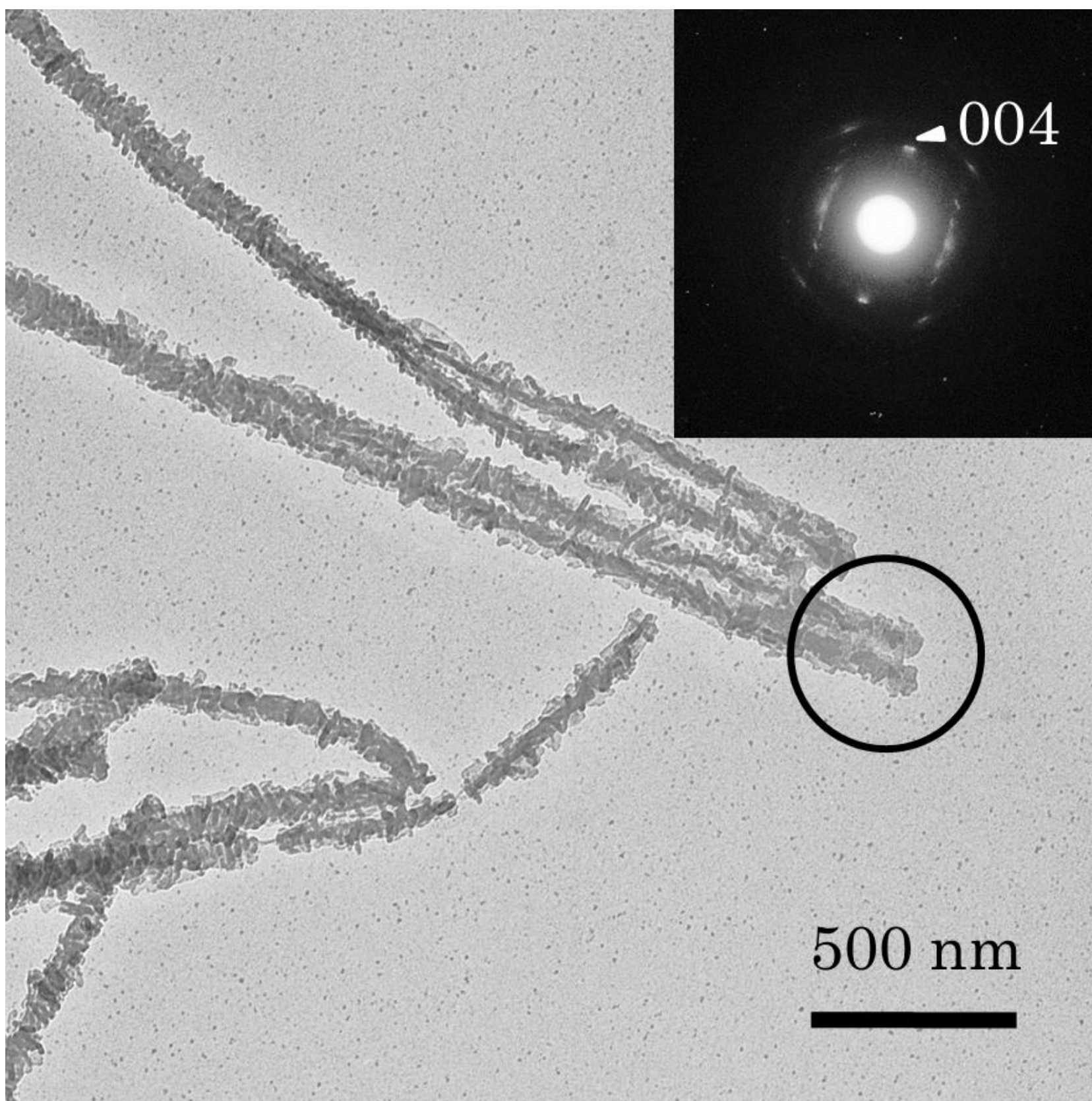


Figure 1-5 TEM image and SAED pattern of POPI fiber prepared in DBT at 330°C and a concentration of 1.0% (Run No. 3)

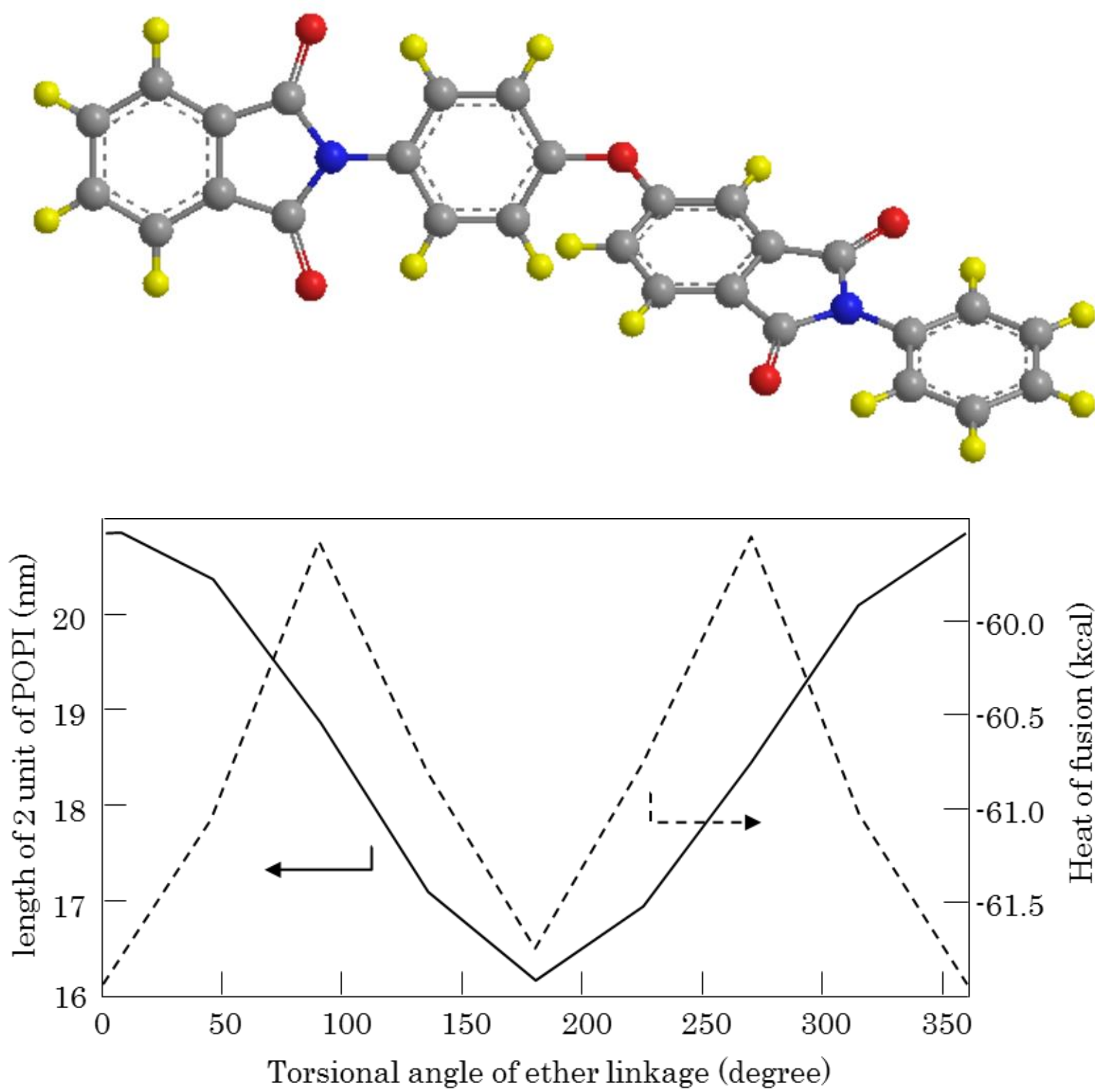


Figure 1-6 Plots of length of two units of POPI and heat of fusion as a function of torsional angle of ether linkage

rectangle crystals, of which the dimension was ca. 70 nm and 15 nm. The small rectangle crystals stacked laterally along the long axis of the fiber and their long direction was perpendicular to the long axis of the fiber. The edge of the fiber was flat and the both sides were jagged. This morphological feature resembles a well-known shish-kebab structure. However, the shish is not found in the center of the fiber, and this fiber is different from the shish-kebab structure. The SAED pattern taken from the encircled area was not a true fiber pattern of a cylindrical symmetry. Reflections were slightly diffuse, but many reflections were observed clearly. The bright reflections corresponding to  $d$ -space of 0.425 nm were observed on the meridian. Figure 1-6 is plots of length of two units of POPI and heat of fusion as a function of torsional angle of ether linkage. If the fiber identity period is assumed as 1.70 nm being in good agreement of the length of two POPI repeating units in which the torsional angle of ether linkage was  $135^\circ$ , the reflection of  $d$ -space of 0.425 nm can be indexed as 004 plane. In order to discuss the molecular orientation of the POPI fiber crystal, the crystal unit parameters were provisionally determined with the results of the SAED and the WAXS powder pattern. If an orthorhombic unit cell having  $a = 0.49$  nm,  $b = 0.54$  nm and  $c = 1.70$  nm was assumed, all diffractions appeared in WAXS and SAED of the POPI crystals can be assigned as shown in Table 1-3. The WAXS data of the oriented POPI fiber was not obtained yet because of the low processability of the POPI, and therefore the crystal spacing has not been determined. All the diffractions appeared in the SAED and the WAXS powder pattern enabled to be explained without difficulty, and this crystal parameter was used to estimate the molecular orientation. Based on this unit cell, the POPI molecules likely align perpendicular to the long axis of the fiber.

Even though the POPI crystal was soluble in concentrated sulfuric acid, the oligomers precipitated to form the crystal could not be directly analyzed because the further polymerization proceeded in the crystals followed by the crystallization. Therefore,

Table 1-3 Results of WAXS and ED of POPI crystals				
WAXS		ED	$d_{\text{calc}}$ (nm)	hkl <sup>a</sup>
$2\theta$ (degree)	$d_{\text{obs}}$ (nm)	$d_{\text{obs}}$ (nm)		
10.39	0.851		0.850	002
		0.540	0.540	010
18.25	0.486		0.486	100
		0.425	0.425	004
24.18	0.368		0.369	013
26.77	0.333		0.334	104
28.00	0.319		0.320	014
31.39	0.285		0.283	006
<sup>a</sup> POPI: orthorhombic, $a = 0.49$ nm, $b = 0.54$ nm, $c = 1.70$ nm.				

oligomers left in the solution were collected and analyzed by MALDI-TOF mass spectrometry to estimate the structure of the precipitated oligomers. The spectra and the peak assignments are presented in Figure 1-7 and Table 1-4, respectively. There were many unknown peaks, but it is cleared that the molecular weight of the oligomer increased from 10 sec to 10 min. Although the molecular weight of oligomers dissolved in the solution increased from 10 min to 6 h, the highest molecular weight oligomer was not changed during the polymerization, which was the cyclized ether-imide hexamer. This result suggests that the ether-imide oligomers higher than the hexamer, probably heptamer, might be mainly precipitated to form the crystals. The oligomers precipitated to form the crystals have the molecular weight distribution because they were formed by the step-growth polymerization. The polymerization occurred in the precipitates to yield high molecular weight POPI. The fibrous morphology with the molecular orientation is very similar to that of the poly(1,4-phenylene benzazole)s crystallized from the solution [23]. Rigid polymers possess a strong interaction between molecules, and hence they tend to

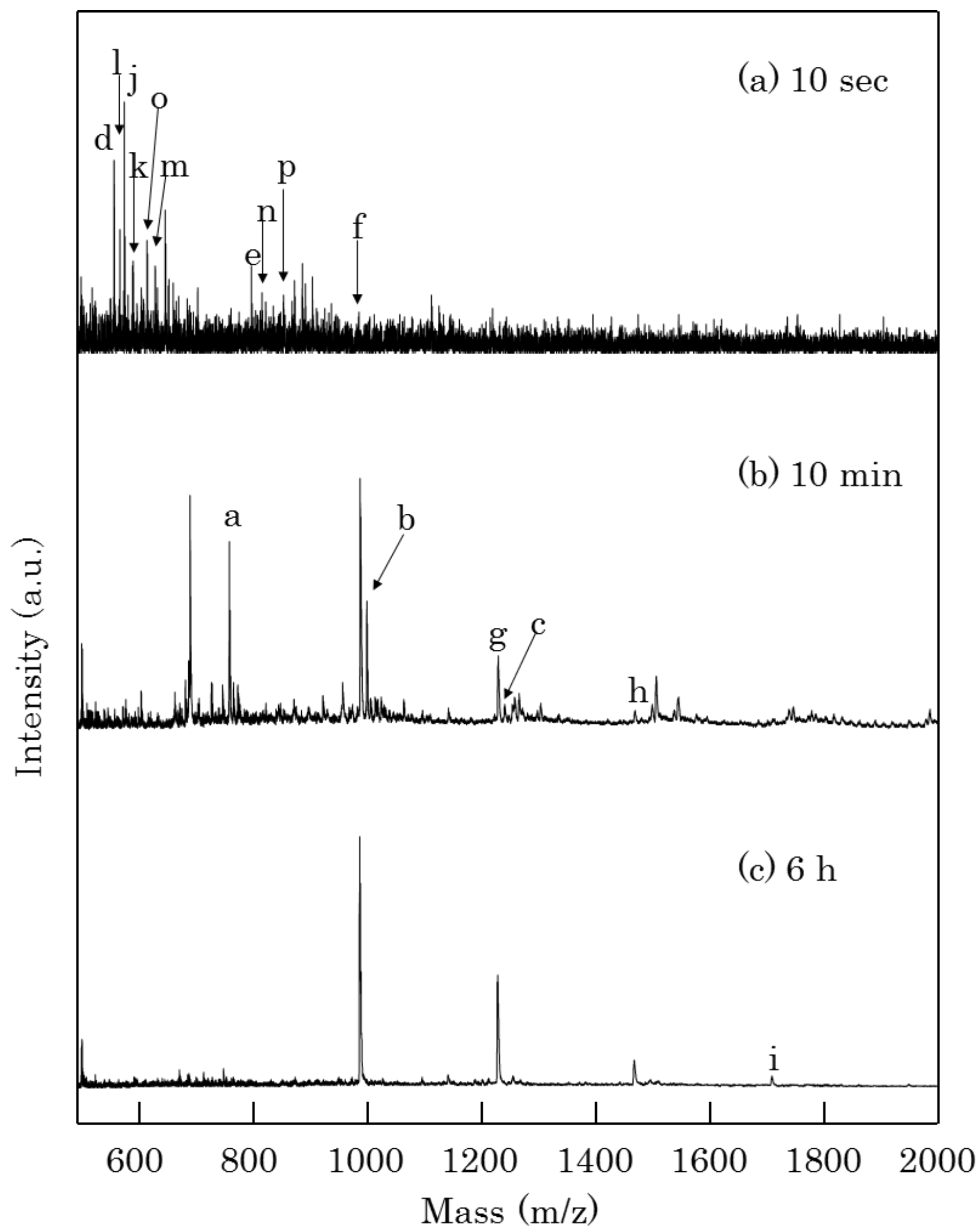
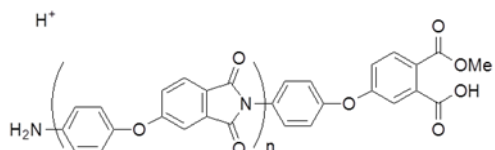
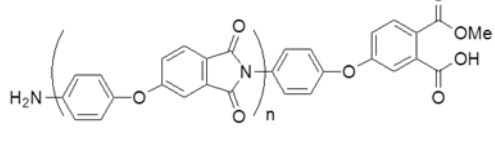

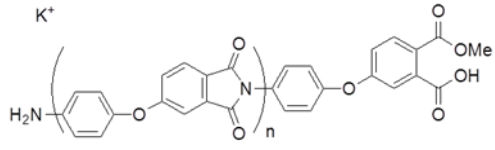
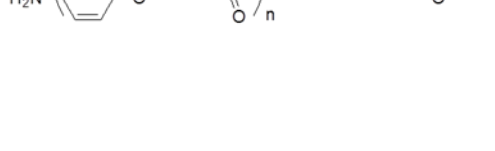

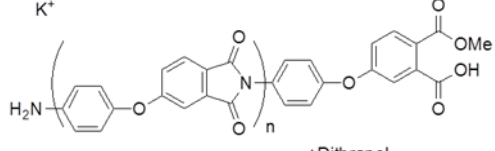
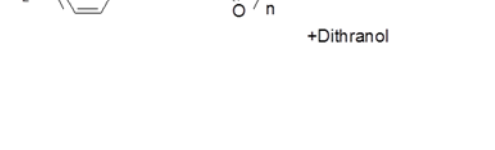
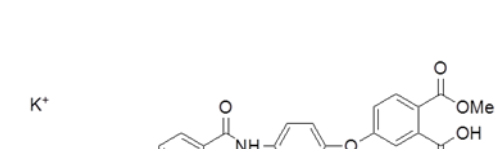
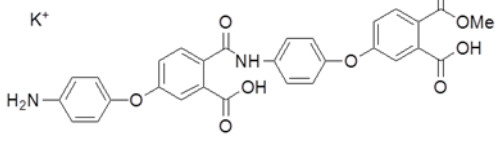
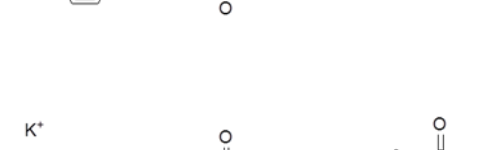
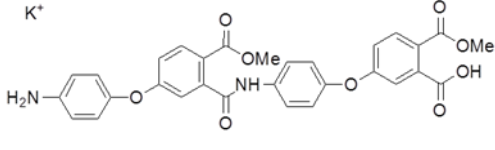
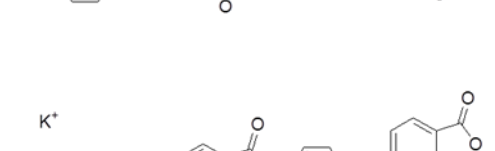
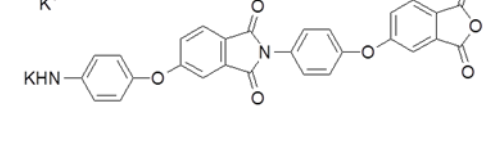
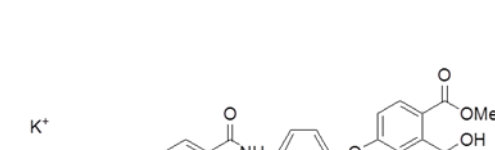
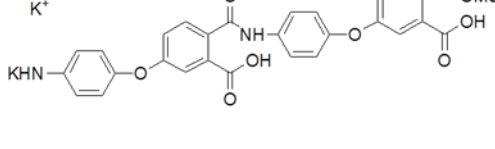


Figure 1-7 MALDI TOF mass spectra of POPI oligomers recovered after (a) 10 sec, (b) 10 min and (c) 6 h (Run No. 3). Polymerization was carried out in DBT at 330°C at a concentration of 1.0%.



Table 1-4 Structural assignments of peak in the MALDI-TOF Mass spectra in Figure 1-7

Peak code	Structure	n	Mass			
			Calculated	observed		
				10 sec	10 min	6 h
a		2	762.68	-	762.59	-
b		3	999.89	-	1000.2	-
c		4	1237.10	-	1237.7	-
d		1	563.57	562.66	-	-
e		2	800.78	799.92	-	-
f		2	989.90	-	989.02	988.30
g		3	1226.11	-	1227.4	1226.6
h		4	1463.32	-	1464.1	1463.6
i		5	1700.52	-	-	1700.5
j		-	581.59	580.69	583.28	-
k		-	593.61	594.65	-	-
l		-	569.66	571.82	-	-
m		-	631.70	632.80	-	-
n		-	818.79	817.86	-	-
o		0	619.68	618.81	-	-
p		1	856.88	856.03	-	-

crystallize laterally to form the fan-like crystals composed of several bundles in which the molecules aligned perpendicular to the long direction of the bundle. According to the formation of the POPI fibrillar crystals, the ether-imide oligomers higher than hexamer might possess strong  $\pi$ - $\pi$  stacking interaction, bringing about the tendency of the lateral crystallization. Thermal stabilities of the precipitate were measured by a TGA in nitrogen atmosphere. Temperatures of 10 wt% loss ( $T_{10}$ ) presented in Table 1-1 were in the range of 543 – 586°C. The POPI precipitates exhibited the outstanding thermal stability.

### 1-3-2 Morphology of P(OPI-*co*-PI)

The copolymerization influences significantly the morphology and the molecular orientation, and the clear morphology is generally damaged by the copolymerization because of the structural irregularity [17, 24-27]. However, if the oligomers composed of particular composition are selectively precipitated due to the difference in the solubility of the oligomer, crystals having clear habits would be created even in a copolymerization system by means of the crystallization of oligomers. The formation of the needle-like crystals of aromatic polyesters with molecular orientation had been previously reported by the aid of the copolymerization [28]. Ribbon-like PPI crystals had been previously prepared by the polymerization of monoalkyl-4-aminophthalate in DBT and the PPI molecules oriented along the long direction of the ribbon as aforesaid. If the nuclei of the PPI ribbon acts as a template to guide the orientation of POPI molecules in this copolymerization system, the P(OPI-*co*-PI) fiber can be prepared with the desirable molecular orientation. From the viewpoint of this, the copolymerization of MAPB with MAB was performed in DBT at 330°C at a concentration of 1.0% for 6 h. Results of the copolymerization are presented in Table 1-5 and the morphologies of the precipitates are shown in Figure 1-8.

Run No.	Polymer code	$\chi_f^b$ (mol%)	Yield (%)	$\chi_p^c$ (mol%)	T <sub>10</sub> <sup>d</sup> (°C)	Morphology
10	PPI	0	59	0	650	Ribbon
11	P(OPI- <i>co</i> -PI)-10	10	64	8	678	Plate
12	P(OPI- <i>co</i> -PI)-30	30	75	21	622	Cone
13	P(OPI- <i>co</i> -PI)-50	50	76	42	592	Cone
14	P(OPI- <i>co</i> -PI)-70	70	78	65	580	Rod
15	P(OPI- <i>co</i> -PI)-90	90	79	95	572	Fiber, SP <sup>e</sup>

<sup>a</sup> Copolymerizations were carried out in DBT at 330°C at a concentration of 1.0% for 6 h. <sup>b</sup> Molar ratio of POPI moiety in feed <sup>c</sup> Molar ratio of POPI moiety in product <sup>d</sup> Temperature of 10% weight loss in nitrogen atmosphere <sup>e</sup> Spherical aggregates of plate-like crystals

Polymer codes of the copolymer are named using the molar ratio of MAPB in feed ( $\chi_f$ ). For example, P(OPI-*co*-PI)-30 stands for the copolymer prepared at  $\chi_f$  of 30 mol%. The precipitates were dissolved in 97% sulfuric acid, but the solutions of the copolymer were not enough stable during the viscosity measurement because of the hydrolysis. Therefore, the viscosity of the copolymer could not be measured. The  $\chi_p$  is defined as the molar ratio of POPI moiety in precipitates and determined by IR spectra. The calibration curve to determine the  $\chi_p$  was made by the intensity ratio of aromatic rings C=C stretching of POPI and PPI at 1478 and 1488 cm<sup>-1</sup>, respectively. The  $\chi_p$  values of the precipitates were slightly lower than the corresponding  $\chi_f$  values except P(OPI-*co*-PI)-90, and the yields of the precipitates become higher with increasing  $\chi_f$  values. The morphology of PPI prepared from MAB was ribbon-like identical to that prepared in previous report [18] (Figure 1-8 (a)). The morphology of precipitates of P(OPI-*co*-PI)-10 and P(OPI-*co*-PI)-90 was similar to each homopolymers. The morphology of P(OPI-*co*-PI)-10 shown in Figure 1-8 (b) was thin plates. Plate surface was very smooth, and these look like shorter ribbons. In the case of P(OPI-*co*-PI)-90, the precipitates was fibers and spherical aggregates of plate-like crystals.

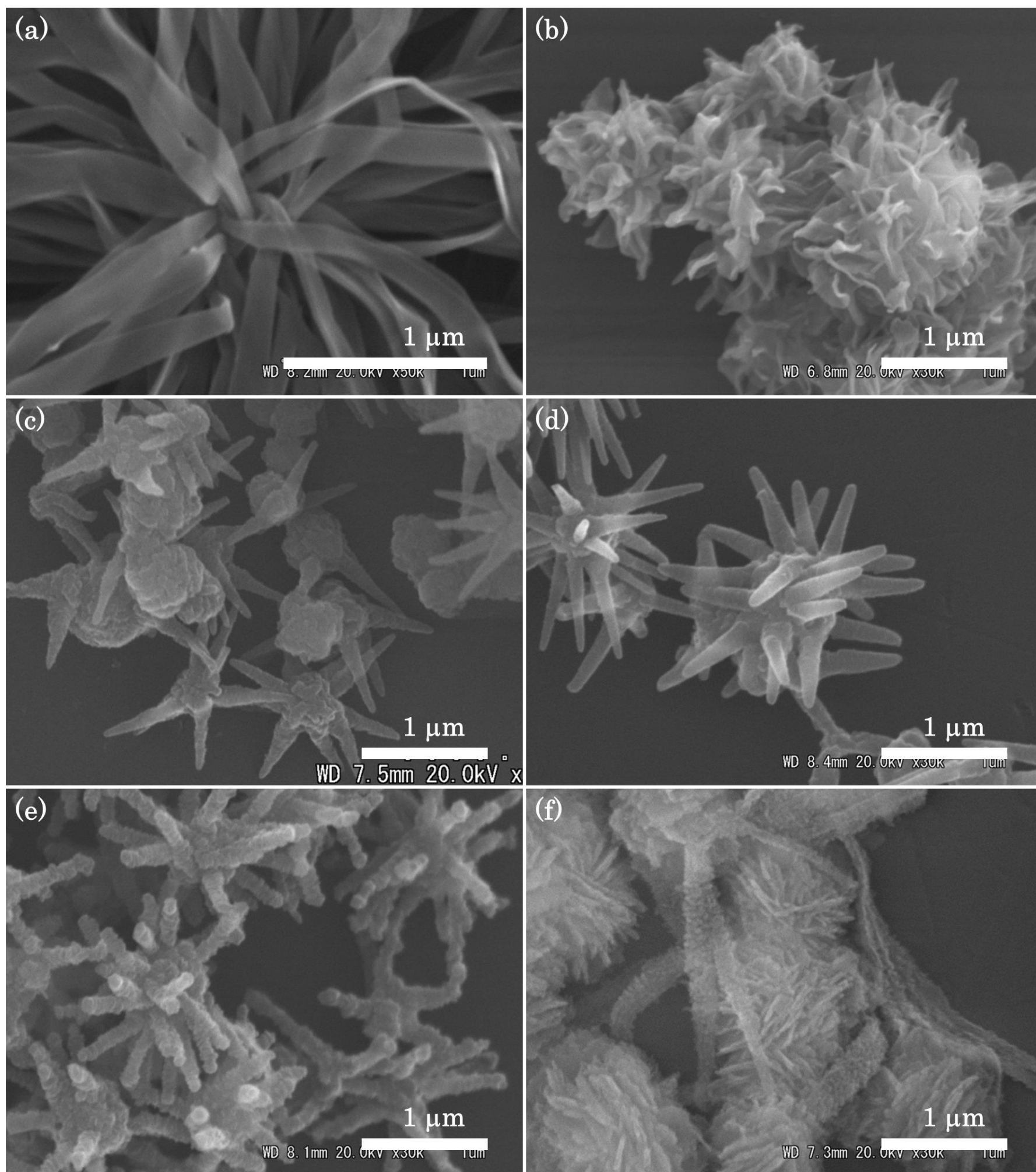


Figure 1-8 Morphology of (a) PPI (Run No. 10), (b) P(OPI-*co*-PI)-10 (Run No. 11), (c) P(OPI-*co*-PI)-30 (Run No. 12) , (d) P(OPI-*co*-PI)-50 (Run No.13), (e) P(OPI-*co*-PI)-70 (Run No. 14) and (f) P(OPI-*co*-PI)-90 (Run No. 15)

In the middle copolymerization ratios, the morphology was usually damaged and clear crystal habit disappeared. But precipitates of P(OPI-*co*-PI) prepared in the middle copolymerization ratio exhibited clear morphology. P(OPI-*co*-PI)-30 and P(OPI-*co*-PI)-50 exhibited cone-like morphology, and P(OPI-*co*-PI)-70 exhibited rod-like morphology similar to that of prepared in DBT/LPF = 7/3. The cone-like crystals and the rod-like crystals were not individually separated, and they grew radially from the center part. The length and width of the cone-like crystals of P(OPI-*co*-PI)-30 were 700 and 100 nm, respectively. Those of the cone-like crystals of P(OPI-*co*-PI)-50 were 800 and 200 nm, respectively. The tips of cone-like crystals of P(OPI-*co*-PI)-30 and P(OPI-*co*-PI)-50 were sharp, whereas those of rod-like crystals of P(OPI-*co*-PI)-70 were flat and many striations ran perpendicular to the long direction of the rod-like crystals. WAXS intensity profiles of the P(OPI-*co*-PI) precipitates are shown in Figure 1-9. Copolymerization lowered the crystallinity, but some crystalline peaks were detected even in P(OPI-*co*-PI)-50. Even though the peak intensity became weaker, the diffraction peaks of PPI were clearly visualized in P(OPI-*co*-PI)-10 and P(OPI-*co*-PI)-30 (marked by black solid circle), and those of POPI were observed in P(OPI-*co*-PI)-70 and P(OPI-*co*-PI)-90 (marked by open circles). In the profiles of the precipitates prepared at the middle copolymerization ratios, a new diffraction peak was seen at  $2\theta = 19.1^\circ$  ( $d$ -space = 0.462 nm) characterizing the copolymer crystals (marked by black solid triangle). This result suggests that the crystal structure of copolymer was newly generated at the middle copolymerization ratio, which was different from that of the each homopolymer.

In order to estimate the molecular orientation in the copolymer crystals, TEM and SAED were taken as shown in Figure 1-10. The several diffuse reflections were observed on the equator in the ED pattern of P(OPI-*co*-PI)-30. The 010 and 100 reflections of the PPI

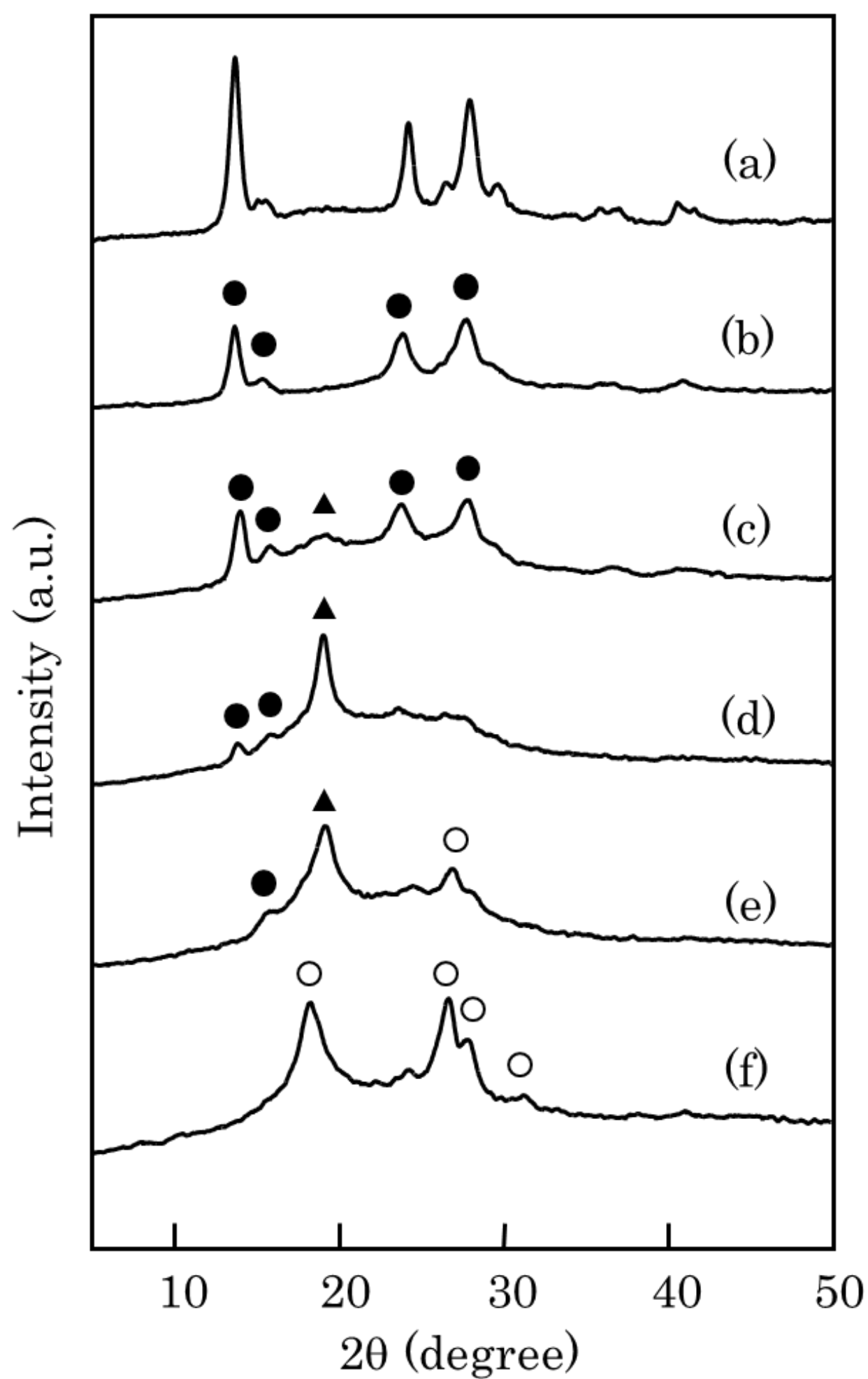


Figure 1-9 WAXS intensity profiles of (a) PPI (Run No. 10), (b) P(OPI-*co*-PI)-10 (Run No. 11), (c) P(OPI-*co*-PI)-30 (Run No. 12), (d) P(OPI-*co*-PI)-50 (Run No. 13), (e) P(OPI-*co*-PI)-70 (Run No. 14) and (f) P(OPI-*co*-PI)-90 (Run No. 1). ● : reflection of PPI crystal, ▲ : reflection of P(OPI-*co*-PI) crystal, ○ : reflection of POPI crystal

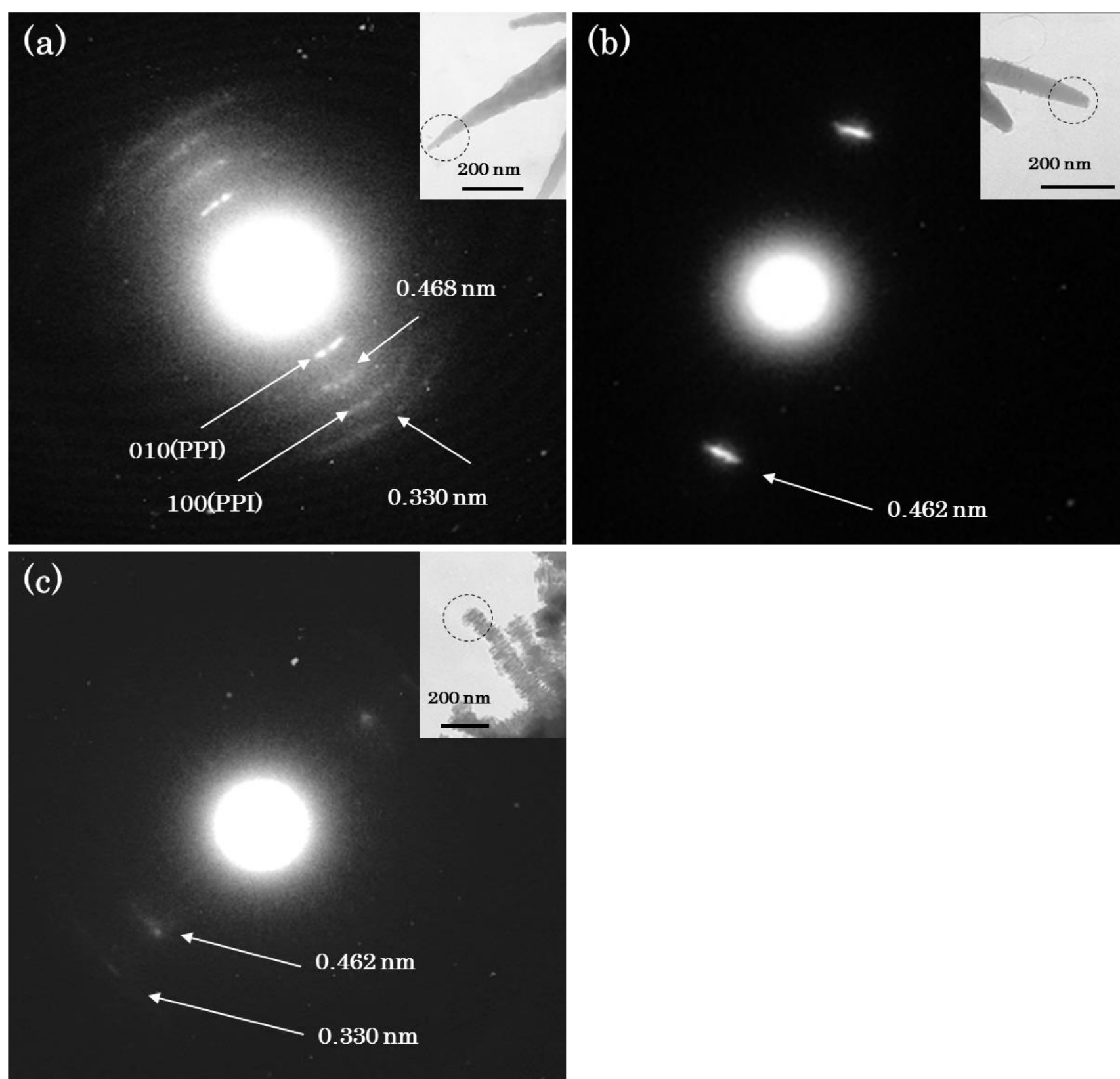


Figure 1-10 TEM and SAED patterns taken from circled area of (a) P(OPI-*co*-PI)-30 (Run No. 12), (b) P(OPI-*co*-PI)-50 (Run No. 13) and (c) P(OPI-*co*-PI)-70 (Run No. 14)



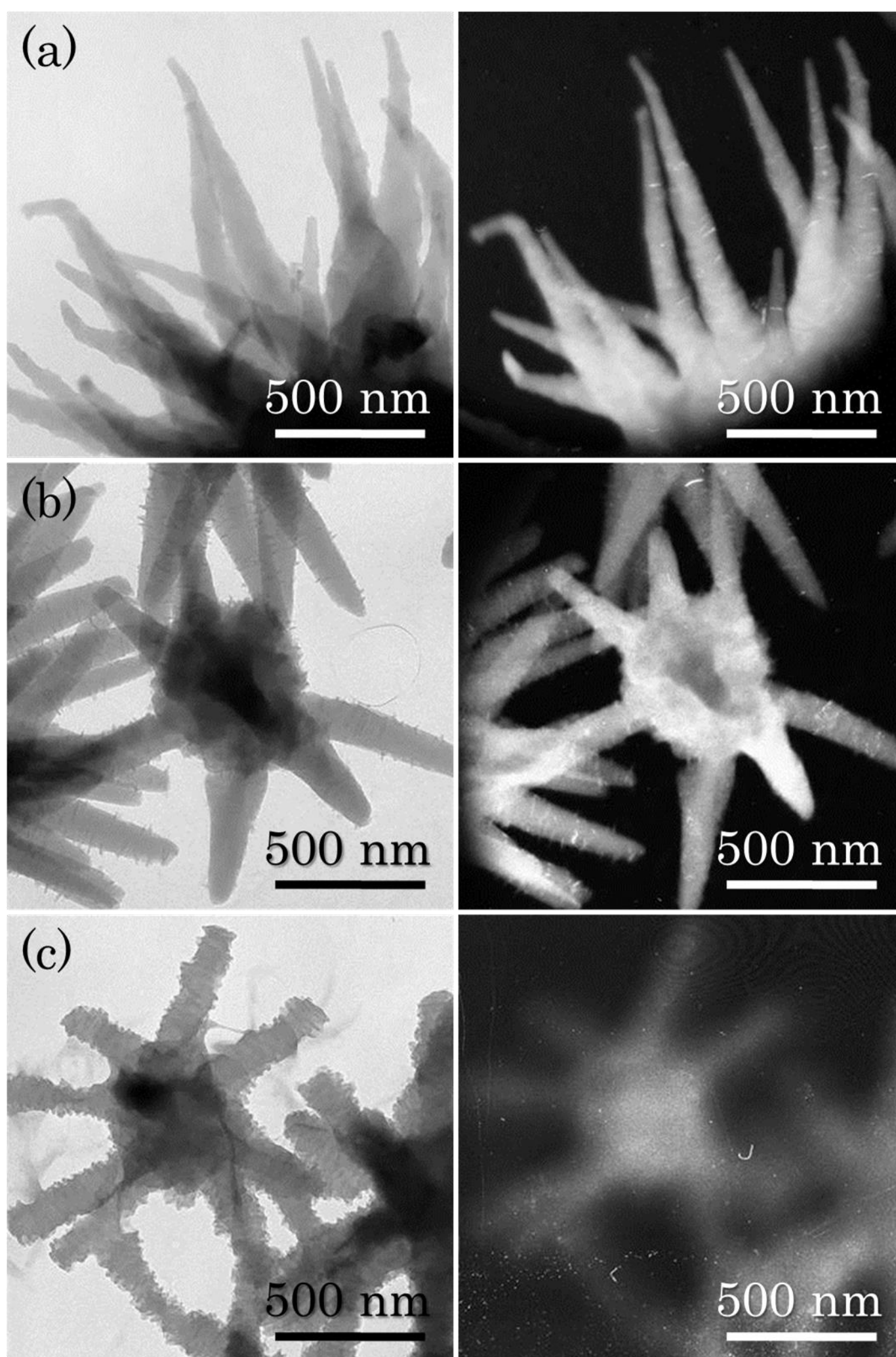


Figure 1-11 Bright and dark field images of (a) P(OPI-*co*-PI)-30 (Run No. 13), (b) P(OPI-*co*-PI)-50 (Run No. 14) and (c) P(OPI-*co*-PI)-70 (Run No. 15). Dark field image of P(OPI-*co*-PI)-30 was taken by using 010 reflection of PPI, and those of P(OPI-*co*-PI)-50 and 70 were taken by using reflection of  $d$ -space = 0.462 nm.



crystals were clearly observed, revealing that the PPI molecules aligned along the long direction of the cone-like crystals. Other reflection was observed at  $d$ -space of 0.462 nm which was observed in the WAXS profile, being characterized as the copolymer crystal. The reflection characterized by the POPI crystals did not appear at all because of low content. It can be speculated that the copolymer molecules might be oriented roughly to the long direction of the cone-like crystals. Bright and corresponding dark field images of the P(OPI-*co*-PI) precipitates are shown in Figure 1-11. The dark field image of P(OPI-*co*-PI)-30 was taken by using 010 reflection. The crystal was not uniformly bright and fluctuation of brightness was observed in many places. Many bright striations ran in the horizontal direction of cone-like crystals, suggesting that some regions of internal distortions were present within the crystal. Changes in the yield, the  $\chi_p$  value and the morphology were examined in the early stage of the polymerization. The results are shown in Figure 1-12. The yield increased rapidly within 10 min and then very slowly with time. The  $\chi_p$  value also increased largely within 10 min and then slowly with the yield. After 1 min, the yield and the  $\chi_p$  value reached to 22% and 7.3 mol%, and then they increased to 29% and 9.8 mol% after 3 min. The oligomers which were rich in the PPI moiety were precipitated to form the nuclei in the very beginning of the polymerization, and then those containing larger amount of the POPI moieties were gradually precipitated. According to the morphology, the precipitates after 1 min were spheres having rugged surface of which the diameter was in the range of 100–400 nm. The cone-like crystals were formed from the surface of the spheres after 3 min, and then they grew gradually with maintaining the cone-like morphology. The nucleation occurred very rapidly from a super-saturated state of oligomers, and hence the generated nuclei aggregated spherically. The nucleus was mainly composed of the PPI moieties and the cone-like morphology was developed from the nucleus by the consecutive supply of oligomers. In the case of P(OPI-*co*-PI)-50 and P(OPI-*co*-PI)-70,

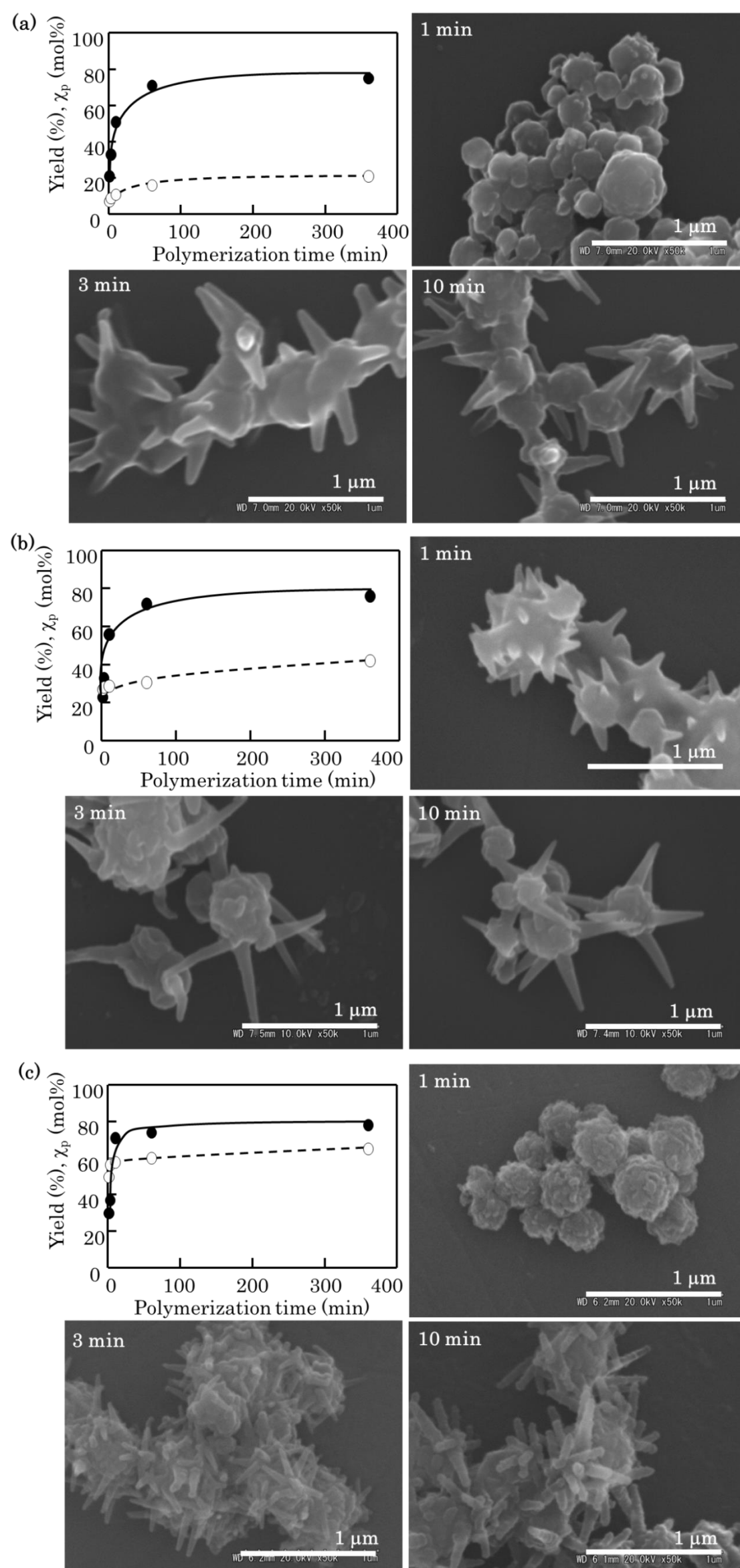


Figure 1-12 Polymerization time dependencies of yield,  $\chi_p$  and morphology of (a) P(OPI-*co*-PI)-30, (b) P(OPI-*co*-PI)-50 and (c) P(OPI-*co*-PI)-70

changes in the yield, the  $\chi_p$  value and the morphology showed same tendency of P(OPI-*co*-PI)-30 basically. Morphology of P(OPI-*co*-PI)-70 at 3 min was cone-like similar to P(OPI-*co*-PI)-30 and P(OPI-*co*-PI)-50, and then the rod-like morphology formed in course of time. In the ED patterns of P(OPI-*co*-PI)-50 and P(OPI-*co*-PI)-70, the reflection of  $d$ -space = 0.462 nm was clearly observed, which came from the copolymer crystal. The dark field image of P(OPI-*co*-PI)-50 and P(OPI-*co*-PI)-70 were taken by using the reflection of  $d$ -space = 0.462 nm. That of P(OPI-*co*-PI)-50 was quite similar to that of P(OPI-*co*-PI)-30 as shown in Figure 1-9, indicating that some regions of internal distortions are present in the crystal. In contrast to these, the dark field image of P(OPI-*co*-PI)-70 was not bright and it was vague due to the lack of crystallinity, being identical with the result of WAXS measurement. The molecular orientations in P(OPI-*co*-PI)-50 and P(OPI-*co*-PI)-70 were not clarified because the unit cell of the P(OPI-*co*-PI) crystal could not be determined, but it is expected that the molecular chains might align along the long axis direction of cone or rod-like morphology because positional relationship of reflection of  $d$ -space = 0.462 nm.

Thermal stability of the P(OPI-*co*-PI) precipitates was also measured by a TGA in nitrogen atmosphere and  $T_{10}$ s are summarized in Table 1-3. The  $T_{10}$  values were in the range of 572-678°C. The  $T_{10}$  values were highly dependent on the  $\chi_p$  values and they increased with the content of the PPI. The P(OPI-*co*-PI) precipitates exhibited the outstanding thermal stability and they are more stable than the POPI precipitates.

#### 1-4 CONCLUSIONS

The POPI fibrillar crystals were obtained as the precipitates with the spherical aggregates of the plate-like crystals by the polymerization of MAPB in DBT at 330-350°C at a concentration of 0.5-1.0% and in DBT/LPF = 7/3 at 330°C at a concentration of 1%. The

fibers were approximately 250 nm in width and some of them were longer than 15  $\mu\text{m}$ . They possessed high crystallinity and the POPI molecules aligned perpendicular to the long direction of the fibers. In contrast to this, the POPI microspheres having ragged surface were formed in DBT at 330°C at a higher concentration of 5.0%. The solvent also influenced the morphology and the fibers were not formed in other solvents. The copolymerization usually distinguished the clear morphology, but the precipitates having the clear morphology were formed even at the middle  $\chi_f$  values. The precipitates of one-dimensional structure such as ribbon, cone, rod and fiber were formed by the polymerization in DBT. The oligomers rich in the PPI moiety were initially precipitated to form the crystals served as the nuclei, because the solubility of the oligomers rich in the PPI moiety was lower than that of the oligomers containing the POPI moiety in DBT. The copolymer molecules might align along the long direction of the one-dimensional crystals. The POPI crystals and the P(OPI-*co*-PI) crystals were infusible under their decomposition temperature and they exhibited outstanding thermal stability.

## 1-5 REFERENCE

- [1] Eastmond, G. C.; Paprotny, J., *Reactive & Functional Polymers*, 1996, **30**, 27.
- [2] Takekoshi, T., *Adv. Polym. Sci.*, 1990, **94**, 1.
- [3] Liu, X. Q.; Yamanaka, K.; Jikei, M.; Kakimoto, M., *Chem. Mater.*, 2000, **12**, 3885.
- [4] Im, J. K.; Jung, J. C., *J. Polym. Sci.: Part A: Polym. Chem.*, 2000, **38**, 402.
- [5] Wang, Z. Y.; Qi, Y.; Bender, T. P.; Gao, J. P., *Macromolecules*, 1997, **30**, 764.
- [6] Bender, T. P.; Qi, Y.; Gao, J. P.; Wang, Z. Y., *Macromolecules*, 1997, **30**, 6001.
- [7] Im, J. K.; Jung, J. C., *Polym. Bull.*, 1998, **41**, 409-416.
- [8] Im, J. K.; Jung, J. C., *J. Polym. Sci.: Part A: Polym. Chem.*, 1999, **37**, 3530.

- [9] Im, J. K.; Jung, J. C., *Polym. Bull.*, 1999, **43**, 157.
- [10] Thiruvassagam, P.; Venkatesan, D., *J. Macromol. Sci., Part A: Pure and Applied Chem.*, 2009, **46**, 419.
- [11] Nephew, J. B.; Nihei, T. C.; Carter, S. A., *Phys. Rev. Lett.*, 1998, **80**, 3276.
- [12] Tran-Cong, Q.; Harada, A., *Phys. Rev. Lett.*, 1996, **76**, 1162.
- [13] Kyu, T.; Lee, J. H., *Phys. Rev. Lett.*, 1996, **76**, 3746.
- [14] Williams, R. J. J.; Rozenberg, B. A.; Pascault, J.-P., *Adv. Polym. Sci.*, 1997, **128**, 95.
- [15] Luo, K., *Eur. Polym. J.*, 2006, **42**, 1499.
- [16] Wang, X.; Okada, M.; Matsushita, Y.; Furukawa, H.; Han, C. C., *Macromolecules*, 2005, **38**, 7127.
- [17] Kimura, K.; Kohama, S.; Yamazaki, S., *Polym. J.*, 2006, **38**, 1005.
- [18] Wakabayashi, K.; Uchida, T.; Yamazaki, S.; Kimura, K., *Macromolecules*, 2008, **41**, 4607.
- [19] Wakabayashi, K.; Uchida, T.; Yamazaki, S.; Kimura, K.; Shimamura, K., *Macromolecules*, 2007, **40**, 239.
- [20] Gies, A. P.; Nonidez, W. K.; Anthamatten, M.; Cook, R. C.; Mays, J. W., *Rapid Commun Mass Spectrom.*, 2002, **16**, 1903.
- [21] Wakabayashi, K.; Uchida, T.; Yamazaki, S.; Kimura, K., *Macromol. Chem. Phys.*, 2011, **212**, 159.
- [22] Kimura, K.; Inoue, H.; Kohama, S.; Yamashita, Y.; Sakaguchi, Y., *Macromolecules*, 2003, **36**, 7721.
- [23] Shimamura, K.; Uchida, T., *J. Macromol. Sci. Phys.: Part B: Physics*, 2000, **39**, 667.
- [24] Schwarz, G.; Zemmann, U.; Kricheldorf, H. R., *High Perform. Polym.*, 1997, **9**, 61.
- [25] Kricheldorf, H. R.; Adebahr, T., *J. Polym. Sci., Part A: Polym. Chem.*, 1994, **32**, 159.

- [26] Kricheldorf, H. R.; Loehden, G.; Wilson, D. J., *Macromolecules*, 1994, **27**, 1669.
- [27] Kimura, K.; Nakajima, D.; Kobashi, K.; Yamashita, Y.; Yokoyama, F.; Uchida, T.; Sakaguchi, Y., *Polym. Adv. Tech.*, 2000, **11**, 747.
- [28] Yoshida, N.; Kurihara, Y.; Kohama, S.; Uchida, T.; Yamazaki, S.; Kimura, K., *Macromolecules*, 2008, **41**, 7571.

## CHAPTER 2

### SYNTHESIS AND MORPHOLOGY CONTROL OF POLY(2,6-1H-BENZO[f]ISOINDOLE-1,3(2H)-DIONE) AND EFFECT OF MONOMER STRUCTURE

#### 2-1 INTRODUCTION

Many AA-BB types of aromatic polyimides containing naphthalene moiety have been prepared to improve the heat resistance [1-4] and the linear coefficients of thermal expansion. [5, 6] It is well known that six-membered imide ring has higher stability for hydrolysis compared with five-membered imide ring. Hence, the naphthalene moiety is also introduced into the aromatic polyimides as a part of the six-membered imide ring [7-9] and these polyimides have been applied for polymer electrolyte membrane of fuel cell, [10-15] as well as high-performance materials. Although many naphthalene-containing polyimides have been synthesized two-step method *via* the poly(amic acid), the self-condensed naphthalene-containing polyimide has not been synthesized because of the instability of monomers due to the facile reaction between the amino group and the anhydride group attached in the same molecule as described in Chapter 1. Poly(2,6-1H-benzo[f]isoindole-1,3(2H)-dione) (PBID) has been designed as a novel self-condensed aromatic polyimide containing naphthalene ring, but it has not been prepared.

Morphology control of the polymer materials is of great importance to obtain the essential properties predicted from the polymer structure. However, the intractability of the rigid-rod polyimides makes them difficult to control the morphology by the conventional procedures. An isothermal polymerization can induce phase separation from

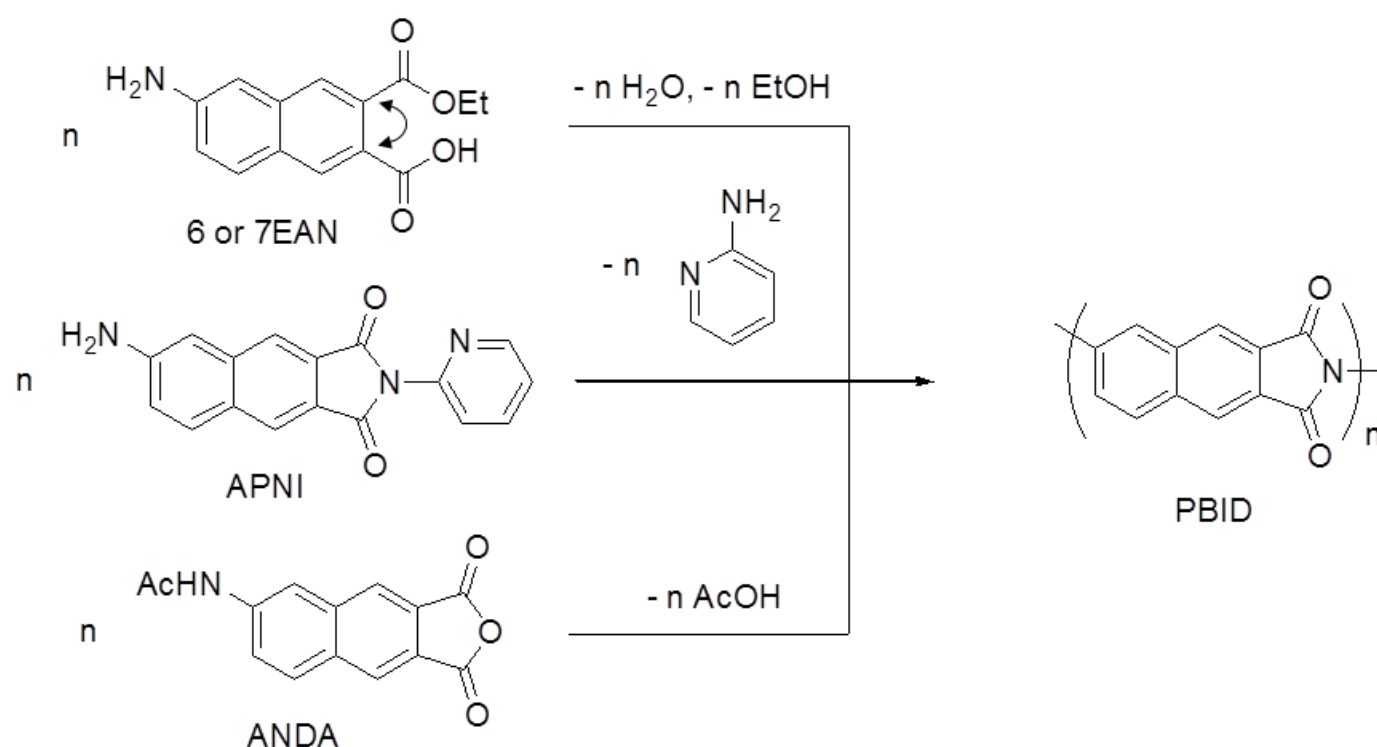
homogeneous solution. [16-23] Nanoribbons of PPI, which was a self-condensed polyimide, were prepared from polymerization of 1-alkylcarbonyl-4-aminobenzoic acid and 2-alkylcarbonyl-4-aminobenzoic acid as the self-condensable monomer by means of the reaction-induced phase separation during polymerization. [24] The obtained PPI nanoribbons were highly crystalline and molecular chains aligned along the long direction of the ribbon, suggesting not only high-performance materials but also functional materials as non-linear optical devices. [25, 26] PBID comprised of naphthalene moiety and imide linkage is analogous to PPI. If the morphology of PBID with molecular orientation will be precisely controlled, it is expected to be high-performance and high functional materials as non-linear optical property by reason of their developed  $\pi$ -conjugate system by injection of naphthalene ring.

In the reaction-induced phase separation during polymerization, monomer structure is an important factor to affect the morphology though reaction rate, miscibility between precipitating oligomers and solvent, interaction between oligomers, and homogeneity of oligomers structure including degree of imidization in the polymerization system. Due to the strong interaction of naphthalene ring in PBDI, the miscibility between oligomers and solvent is decreased, predicting that low molecular weight oligomers will precipitate. The molecular weight of the precipitated oligomers significantly influences the morphology of PBID crystals, and hence the influence of end-group of oligomers depending on the structure of functional groups of the monomer is of great importance to examine.

Based on the above discussion, the synthesis and morphology control of PBID was examined by using the reaction-induced phase separation during polymerization. And effect of monomer functional group was mainly investigated using four kinds of monomers such as 3-ethoxycarbonyl-6-amino-2-naphthoic acid (6EAN), 3-ethoxycarbonyl-7-amino-2-naphthoic acid (7EAN), 6-amino-*N*-(2-pyridyl)naphthalene-2,3-dicarboxylic



imide (APNI), and 6-acetoaminonaphthalene-2,3-dicarboxylic anhydride (ANDA) as shown in Scheme 2-1.



Scheme 2-1 Synthesis of PBID

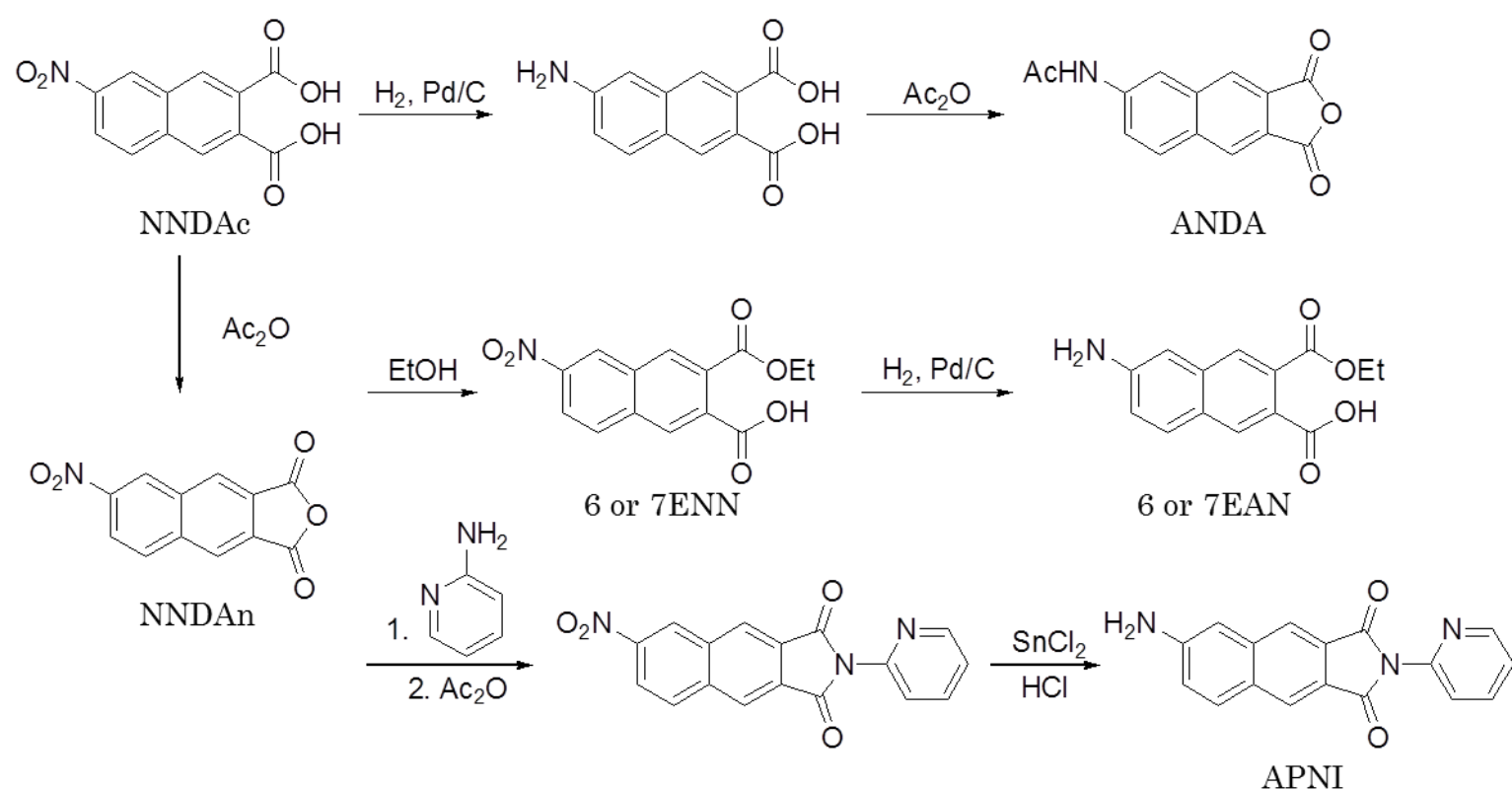
## 2-2 EXPERIMENTAL

### 2-2-1 Materials

DBT and DPS used in this Chapter were the same as those in Chapter 1. 1,3,5-Triphenyl benzene (TPB) was purchased from Alfa Aesar Co. Ltd. and purified by recrystallization from toluene with activated carbon.

### 2-2-2 Monomer synthesis

The monomers using prepared of PBID were synthesized according to Scheme 2-2.



Scheme 2-2 Synthesis of monomers

#### 2-2-2-1 Synthesis of 3-ethoxycarbonyl-6-amino-2-naphthoic acid (6EAN)

6-Nitronaphthalene-2,3-dicarboxylic acid (NNDAc) was synthesized according to the previously reported procedure. [27] NNDAc (10.4 g, 40 mmol) and acetic anhydride (200 mL) were stirred at 120°C for 2 h, and then excess of acetic anhydride and by-produced acetic acid were stripped off under reduced pressure. The obtained 6-nitronaphthalene-2,3-dicarboxylic anhydride (NNDAn) was refluxed in dried ethanol for 24 h. Recrystallization of the crude solid, which was a mixture of 3-ethoxycarbonyl-6-nitro-2-naphthoic acid (6ENN) and 3-ethoxycarbonyl-7-nitro-2-naphthoic acid (7ENN), from ethanol gave 6ENN with the yield of 27%. Pd/C (500 mg) was added into the suspension of 6ENN (0.5 g, 1.73 mmol) and dried methanol (150 mL), and then the mixture was stirred at 25°C for 6 h under H<sub>2</sub> atmosphere. After filtration of Pd/C, methanol was evaporated from the filtrate and the obtained solids were dried in vacuum to give yellow solids of 6EAN with yield of 97%. mp: 181°C. Anal.

Calc. for C<sub>14</sub>H<sub>13</sub>O<sub>4</sub>N (259.26): C, 64.86; H, 5.05; N, 5.40. Found: C, 64.31; H, 5.35; N, 5.22.

<sup>1</sup>H NMR (300 MHz, DMSO-*d*<sub>6</sub>): δ 8.24 (s, 1H), 7.76 (s, 1H), 7.75 (d, 1H, *J*=9.3), 7.04 (dd, 1H, *J*= 8.4 Hz), 6.88 (d, 1H, *J*= 1.8 Hz), 5.86 (s, 2H), 4.23 (q, 2H, *J*=7.1), 1.28 (t, 3H, *J*=7.1). IR (KBr): 3416, 3334, 2977, 2596, 1938, 1714, 1627, 1534, 1501, 1474, 1390, 1366, 1289, 1257, 1206, 1133, 1039, 911, 849, 795, 601.

#### 2-2-2-2 Synthesis of 3-ethoxycarbonyl-7-amino-2-naphthoic acid (7EAN)

Recrystallization of the mixture of 6ENN and 7ENN obtained by the same procedure described above from THF gave 7ENN with the yield of 34%. Then, 7EAN was converted from 7ENN by the procedure similar to 6EAN with yield of 99%. Anal. Calc. for C<sub>14</sub>H<sub>13</sub>O<sub>4</sub>N (259.26): C, 64.86; H, 5.05; N, 5.40. Found: C, 64.22; H, 5.02; N, 5.30. mp: 192°C. <sup>1</sup>H NMR (300 MHz, DMSO-*d*<sub>6</sub>): δ 8.14 (s, 1H), 7.76 (s, 1H), 7.65 (s, 1H), 7.04 (d, 1H, *J*= 8.4 Hz), 6.87 (s, 1H), 5.87 (s, 2H), 4.24 (q, 2H, *J*=7.1), 1.27 (t, 3H, *J*=7.1). IR (KBr): 3487, 3381, 2871, 1721, 1675, 1624, 1473, 1395, 1306, 1281, 1257, 1210, 1151, 1131, 1041, 911, 889, 822, 786, 653, 628, 611, 545, 522.

#### 2-2-2-3 Synthesis of 6-amino-*N*-(2-pyridyl)naphthalene-2, 3-dicarboxylic imide (APNI)

NNDA<sub>n</sub> (1.3 g, 5.3 mmol) was added into the solution of 2-aminopyridin (0.75 g, 8.0 mmol) in THF (20 mL) and the mixture was refluxed for 2 h. Then acetic anhydride (10 mL) was additionally added and refluxed for 3 h. The mixture was allowed to cool to 25°C and the precipitated 6-nitro-*N*-(2-pyridyl)naphthalene-2,3-dicarboxylic imide (1.45 g) was obtained by filtration with the yield of 85%. Into the flask, 6-nitro-*N*-(2-pyridyl)naphthalene-2,3-dicarboxylic imide (0.50 g, 1.6 mmol), SnCl<sub>2</sub> (1.2 g),

35% *aq.* HCl (2.0 mL) and distilled water (0.3 mL) were placed and the mixture was heated at 85°C for 2 h. APNI (0.29 g) was obtained after filtration and washing with water with the yield of 64%. <sup>1</sup>H NMR (300 MHz, DMSO-*d*<sub>6</sub>): δ 8.71 (m, 1H), 8.38 (s, 1H), 8.22 (s, 1H), 8.11 (m, 2H), 8.02 (d, 2H, *J* = 8.8 Hz), 7.60 (m, 2H), 7.20 (m, 2H), 6.24 (s, 2H). IR (KBr): 3416, 3304, 3212, 1776, 1711, 1631, 1616, 1587, 1518, 1472, 1439, 1372, 1285, 1209, 1127, 1103, 998, 908, 893, 860, 845, 821, 786, 764, 742, 647, 632.

#### 2-2-2-4 Synthesis of 6-acetoaminonaphthalene-2, 3-dicarboxylic anhydride (ANDA)

NNDAc (4.0 g, 15.3 mmol) and dried THF (300mL) were placed into the flask and 10% Pd/C (0.4 g) was added. Then the mixture was stirred at 25°C under slow stream of hydrogen gas (3 mL·min<sup>-1</sup>) for 6 h. Pd/C was filtrated and 6-aminonaphthalene-2,3-dicarboxylic acid (2.2 g) was obtained after stripping off the THF with the yield of 62%. 6-Aminonaphthalene-2,3-dicarboxylic acid (1.9 g, 8.2 mmol) and acetic anhydride (100 mL) was placed into a flask and the mixture was stirred at 25°C for 2 h and then at 120°C for 3 h. After being allowed to cool at 25°C, ANDA (1.8 g) was obtained with the yield of 87%. <sup>1</sup>H NMR (300 MHz, DMSO-*d*<sub>6</sub>): δ 10.60 (s, 1H), 8.75 (s, 2H), 8.71 (s, 1H), 8.34 (d, 1H, *J* = 9.0 Hz), 7.98 (dd, 1H, *J* = 8.8 Hz), 2.22 (s, 3H). IR (KBr): 3353, 3093, 3019, 1838, 1766, 1696, 1627, 1611, 1551, 1501, 468, 1387, 1321, 1261, 1209, 1159, 1091, 938, 890, 826, 740, 629, 595.

### 2-2-3 Polymerization method

DBT (10.5 g) was placed in a cylindrical flask equipped with gas inlet and outlet tubes and a thermometer, and heat up to 330°C under a slow stream of N<sub>2</sub>. 6EAN (133 mg, 0.51 mmol) was added to DBT at 330°C, and the mixture was stirred for 5 sec to dissolve 6EAN entirely. Then the stirring was stopped and the polymerization was carried out at 330°C for 6 h. Concentration of the polymerization, defined as (calculated polymer weight / solvent volume) ×100, was 1.0% in this polymerization. The yellow precipitates of PBID were collected by filtration at 330°C to avoid a disturbance of the morphology by the crystallization of oligomers dissolved in the solution during cooling, and then washed with *n*-hexane and acetone. The obtained crystals were dried at 50°C for 12 h in vacuum. The filtrate was poured into *n*-hexane to precipitate the oligomers dissolved in the solution at 330°C. The precipitated oligomers were collected by centrifugation and washed with *n*-hexane. Polymerizations of other monomers were also carried out in a similar manner. When TPB and DPS were used as a solvent, precipitates were washed with hot toluene and acetone.

### 2-2-4 Measurements

Characterizations by SEM, IR, WAXS, TGA and DSC were examined in the same manner to Chapter 1. Inherent viscosities ( $\eta_{inh}$ ) were measured in 97% sulfuric acid at a concentration of 0.1 g·dL<sup>-1</sup> at 30°C. <sup>1</sup>H NMR spectra were recorded on a JEOL JNM-AL spectrometer operating at 300 MHz. A solid-state <sup>13</sup>C NMR spectrum was measured on a Bruker AVANCE300WB spectrometer operating at 75.48 MHz.

## 2-3 RESULTS AND DISCUSSION

### 2-3-1 Morphology of PBID prepared by 6EAN and 7EAN

6EAN and 7EAN which are structural isomers mutually were synthesized as the self-condensable monomers for PBID. These monomers were insoluble into the solvents at 25°C, but they were dissolved at the polymerization temperature. In order to induce the isothermal crystallization, the monomers were added into the solvent at the polymerization temperature and polymerized without stirring. The solution became turbid several minutes after the addition of monomers due to the phase separation, and then the yellow precipitates were obtained after 6 h. Results of the polymerization in DBT are presented in Table 2-1. The polymerizations of 6EAN and 7EAN afforded precipitates with the yields of 25-92%. When super-saturation is lower than need of precipitation of oligomer, certain amount of oligomers was always left in the solution in spite of the polymerization concentration, and thus the yields of precipitates were increased with weight of additional monomer. The yields of precipitates were also increased according to polymerization temperature, it is understood that effect of increase of reaction rate outweigh the increase of miscibility. The chemical structure of precipitates was analyzed by the solid-state  $^{13}\text{C}$  NMR and the IR spectroscopy. In a CP/MAS/TOSS  $^{13}\text{C}$  NMR spectrum of precipitates shown in Figure 2-1, corresponding imide carbons and other naphthalene carbons were observed, confirming the formation of the PBID structure. Figure 2-2 is IR spectra of the precipitates. The imide asymmetry and symmetry C=O stretching, imide C-N stretching, and the deformation of the imide ring are observed at 1776 and 1716, 1344 and 736  $\text{cm}^{-1}$ , respectively, formation of PBID is confirmed again. But when the polymerizations were occurred in DBT or TPB at below 350°C, a weak peak was observed at 1846  $\text{cm}^{-1}$  attributed

Table 2-1 Results of polymerization of 6EAN and 7EAN <sup>a</sup>

Run No.	Polymerization condition				Yield (%)	$\eta_{inh}^b$ (dL·g <sup>-1</sup> )	T <sub>10</sub> <sup>c</sup> (°C)	Morpholgy
	Monomer	Solvent	Temp. (°C)	Conc. (%)				
1	6EAN	DBT	330	1.0	45	0.20	581	Rod, Unclear
2				2.0	71	0.26	610	Rod
3			350	1.0	79	0.57	628	PP <sup>d</sup>
4				2.0	91	0.55	647	SP <sup>e</sup>
5			350	0.5	25	0.31	598	PP
6				2.0	66	0.67	593	Lath, PP
7		TPB	370	0.5	48	0.33	588	PP
8				1.0	60	0.53	622	PP
9		DPS	400	1.0	92	1.01	572	Unclear
10			350	1.0	81	0.30	580	Plate
11	7EAN	DBT	330	2.0	57	0.25	612	SP
12			350	2.0	81	0.46	615	SP

<sup>a</sup> Polymerizations were carried out for 6 h. <sup>b</sup> Inherent viscosities were measured in 97% sulfuric acid at 30°C at a concentration of 0.1 g·dL<sup>-1</sup>. <sup>c</sup> Temperature of 10% weight loss recorded on a TGA at a heating rate of 10°C·min<sup>-1</sup> in nitrogen. <sup>d</sup> Plate-like crystal having protuberances on surface <sup>e</sup> Spherical aggregate of plate-like crystals

to the symmetry C=O stretching of dicarboxylic anhydride end-groups (Figure 2-2 (a)-(c)).

Additionally, the shoulder peak of acid, ester or amide C=O stretching was also observed at around 1700 cm<sup>-1</sup>, implying that PBID was not so high molecular weight and degree of imidization. In the case of the PPI nanoribbon and POPI fiber crystals prepared at 330°C, the anhydride end-group did not appear at all. [20] The PBID molecule is more rigid than the PPI or POPI molecule, thus higher temperature is needed for the effective polymerization in the crystals because mobility of oligomers in crystal are lower. The precipitates were insoluble in the common organic solvents but dissolved for sulfuric acid, and therefore solution viscosity was adopted as a criterion to discuss the molecular weight

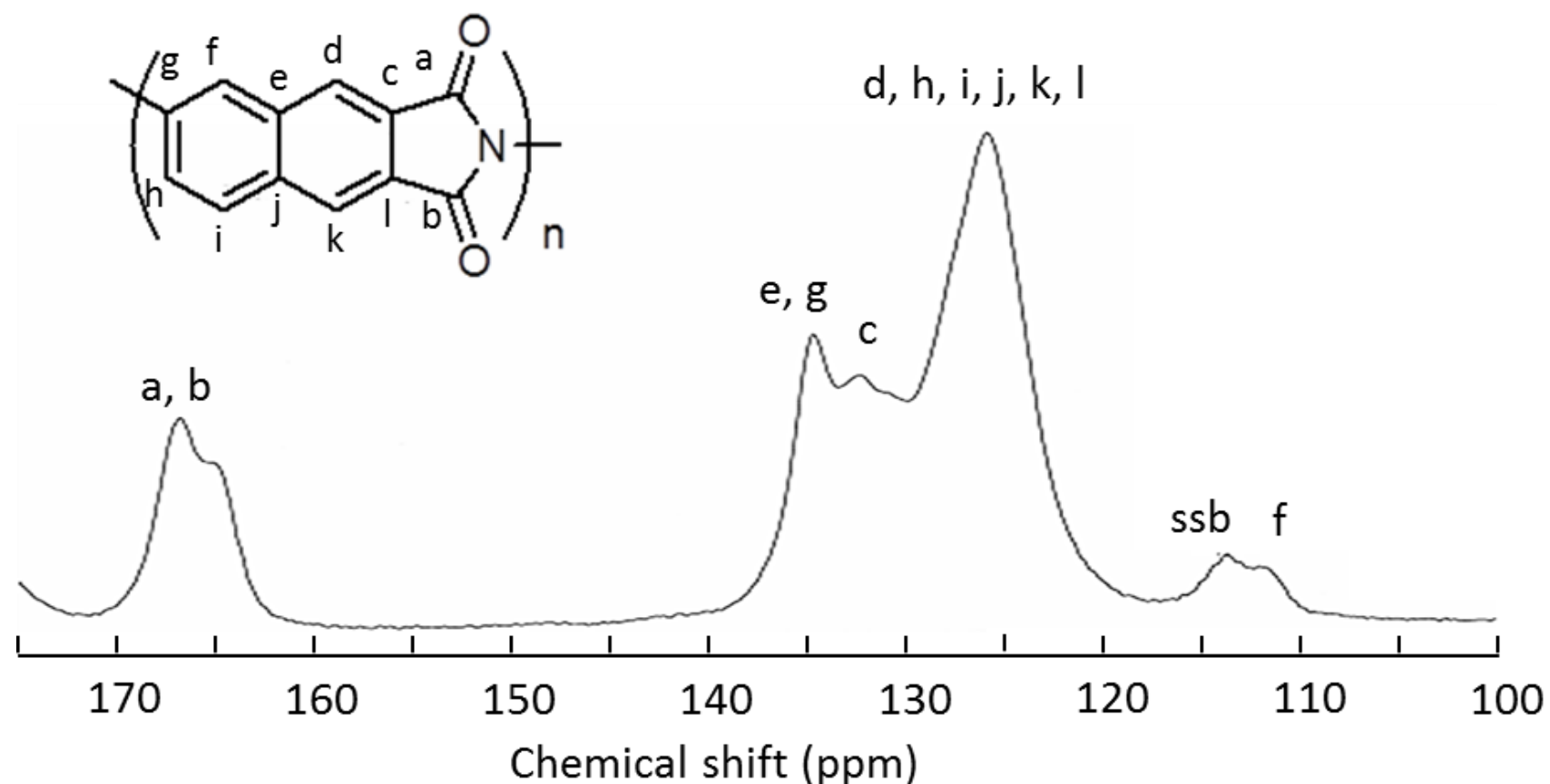


Figure 2-1 CP/MAS/TOSS  $^{13}\text{C}$  NMR spectrum of PBID precipitates prepared by 6EAN in TPB at  $350^\circ\text{C}$  at a concentrated of 2.0% (Run No. 6)

as commonly used. The  $\eta_{\text{inh}}$  values of the precipitates measured in 97% sulfuric acid were 0.20-1.01  $\text{dL}\cdot\text{g}^{-1}$ . The higher polymerization temperature made the  $\eta_{\text{inh}}$  values higher, due to efficient solid-state polymerization. This increase of  $\eta_{\text{inh}}$  values were assented to decrease of end-group peak intensity in IR spectra as shown in Figure 2-2 (a) and (b). Morphology of precipitates prepared in DBT was shown in Figure 2-3. In the polymerization using 6EAN in DBT at  $330^\circ\text{C}$  at a concentration of 1.0%, rod-like structure is observed with unclear spheres as shown in Figure 2-3 (a). And when the polymerization concentration increased 2.0%, rod-like structure observed more frequency (Figure 2-3 (b)). This rod-like structure is ca. 4  $\mu\text{m}$  length and 200-500 nm width, and they have many striations that ran perpendicular to the long direction suggesting the trace of the stacking lamellae of oligomers. These morphological features resemble the incipient crystals of poly(*p*-oxybenzoyl) whiskers, [23] implying that these crystals might be formed by the spiral growth of lamellae caused by the screw dislocation. It is considerable from the trace of the stacking lamellae that the polymerization did not occur effectively between the



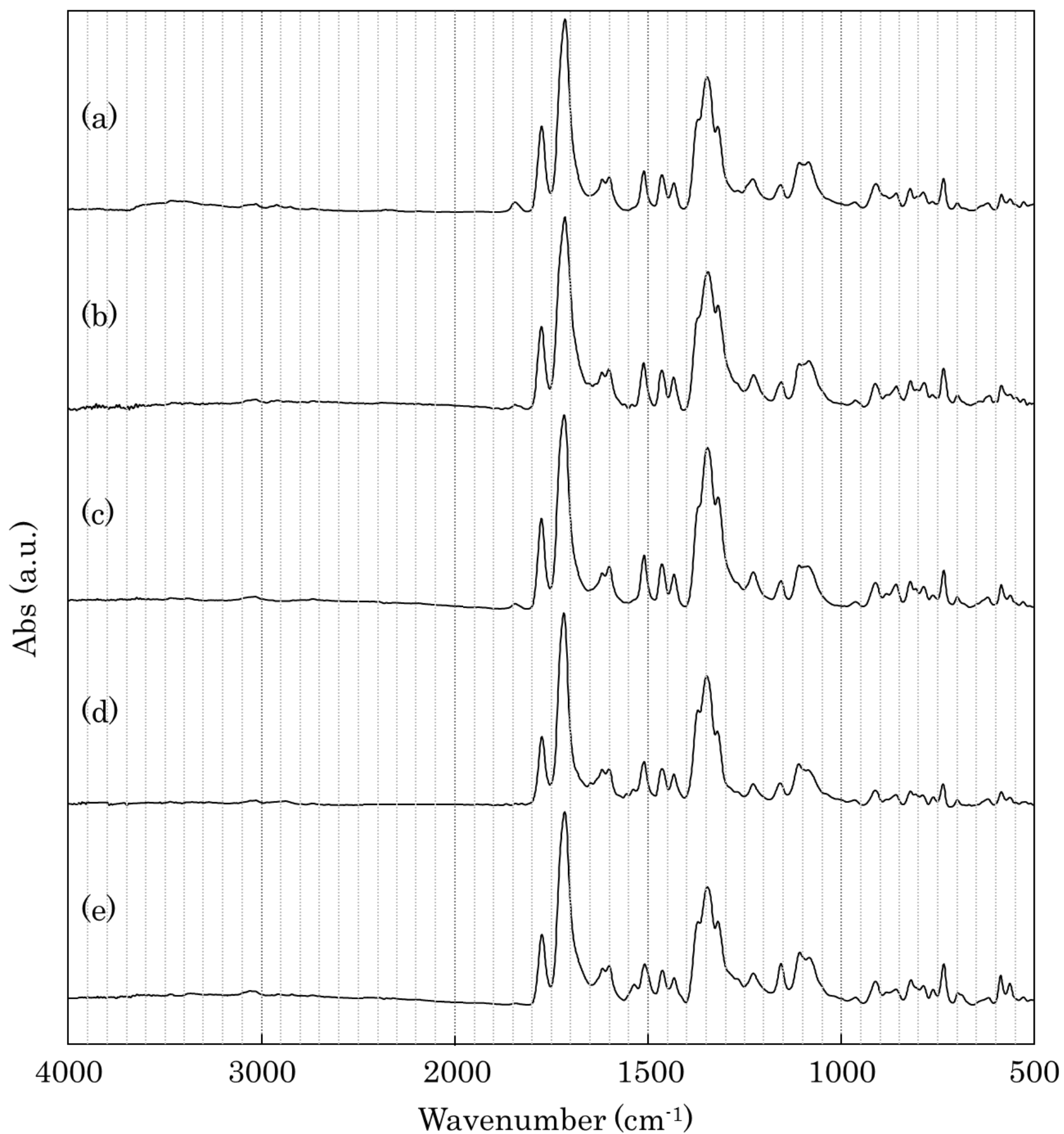


Figure 2-2 FT-IR spectra of PBID precipitates of prepared by 6EAN (a) in DBT at 330°C at a conc. of 1.0% (Run No. 1), (b) in DBT at 350°C at a conc. of 1.0% (Run No. 3), (c) in TPB at 350°C at a conc. of 2.0% (Run No. 6), (d) in TPB at 400°C at a conc. of 1.0% (Run No. 9) and (e) in DPS at 350°C at a conc. of 1.0% (Run No. 10)

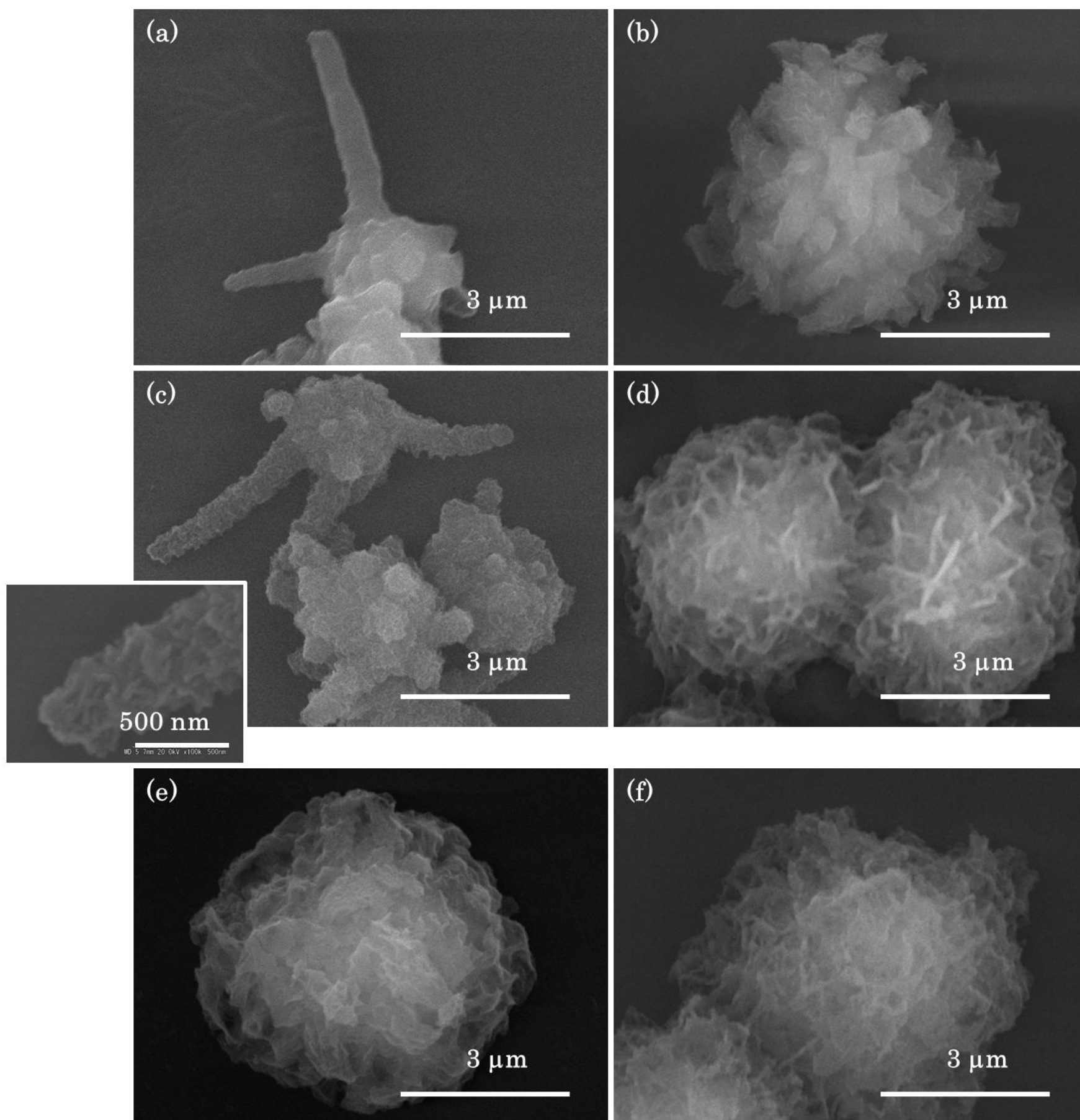


Figure 2-3 Morphology of PBID precipitates of prepared by 6EAN in DBT (a) at 330°C at a conc. of 1.0% (Run No. 1), (b) at 330°C at a conc. of 2.0% (Run No. 2), (c) at 350°C, at a conc. of 1.0% (Run No. 3) and (d) at 350°C at a conc. of 2.0% (Run No. 4). Those prepared by 7EAN in DBT (e) at 330°C, at a conc. of 2.0% (Run No. 11) and (f) at 350°C at a conc. of 2.0% (Run No.12).

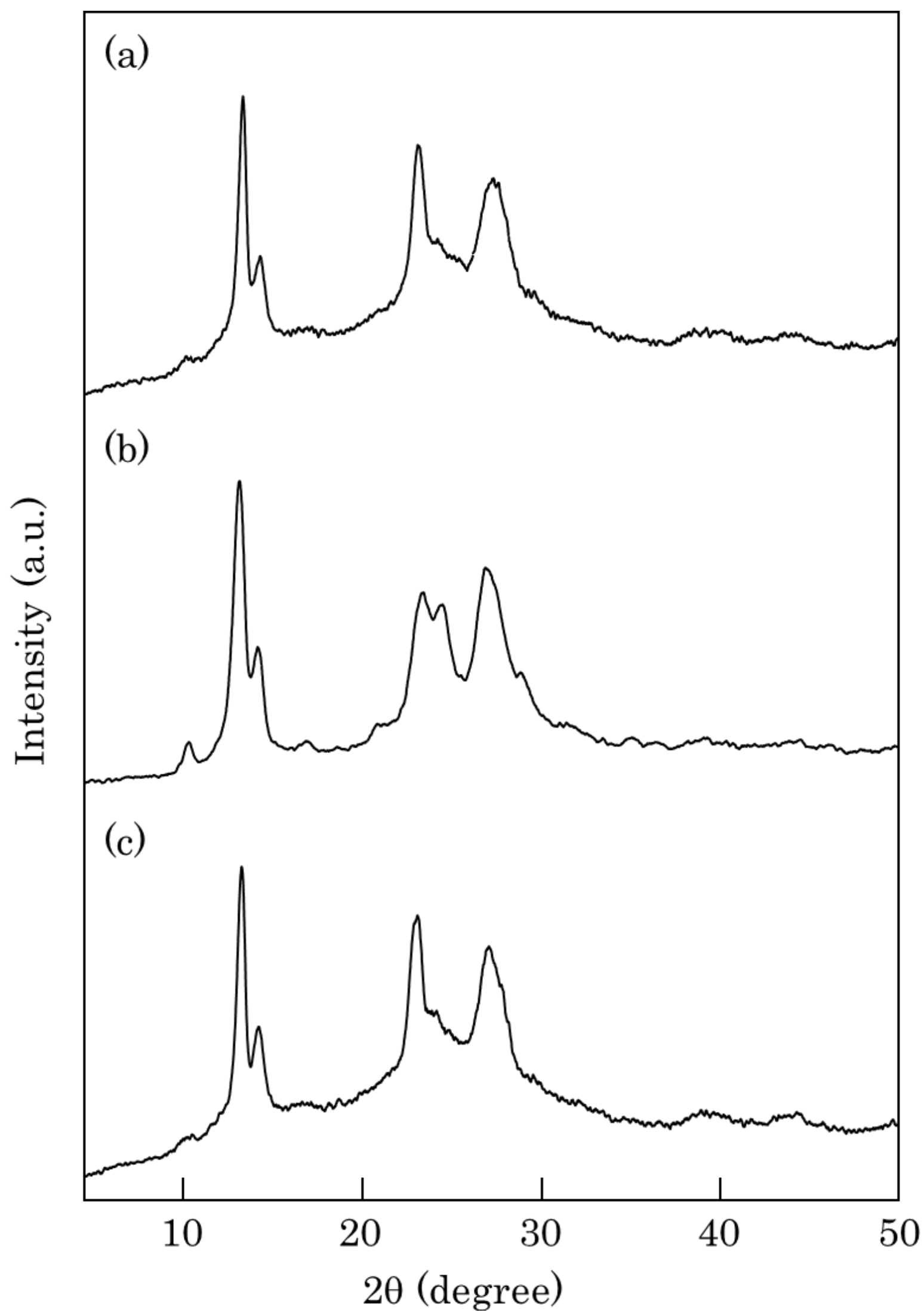


Figure 2-4 WAXS intensity profiles of PBID precipitates of prepared by 6EAN (a) in DBT at 330°C at a concentration of 2.0% (Run No. 1), (b) in DBT at 350°C at a concentration of 2.0% (Run No. 3) and (c) in TPB at 370°C at a concentration of 0.5% (Run No. 7)

lamellae in the crystals owing to the rigid molecular structure. The polymerizations were next carried out in DBT at 350°C. The morphology changed drastically, and the precipitates were spherical aggregate of plate-like crystals as shown in Figure 2-3 (b) and (d). It is noteworthy that the plate-like crystals prepared at a concentration of 1.0% possessed many small protuberances on the surface. The higher molecular weight oligomers were precipitated at 350°C owing to higher miscibility than 330°C, and they might suppress the occurrence of the screw dislocation, resulting in the formation of the plate-like crystals. The plate-like crystals having protuberances on the surface will be discussed later. Figure 2-4 is WAXS intensity profiles of precipitates, five sharp peaks were clearly observed at  $2\theta = 10.8$ ,  $13.5$ ,  $14.5$ ,  $23.7$  and  $27.1$  degree corresponding to  $d = 0.823$ ,  $0.656$ ,  $0.611$ ,  $0.375$  and  $0.329$  nm. Even though the diffuse halo attributed from amorphous region was slightly observed, these crystals possess high crystallinity. And it is indicating that precipitates of prepared at 350°C possess the higher crystallinity than that prepared at 330°C, the molecular

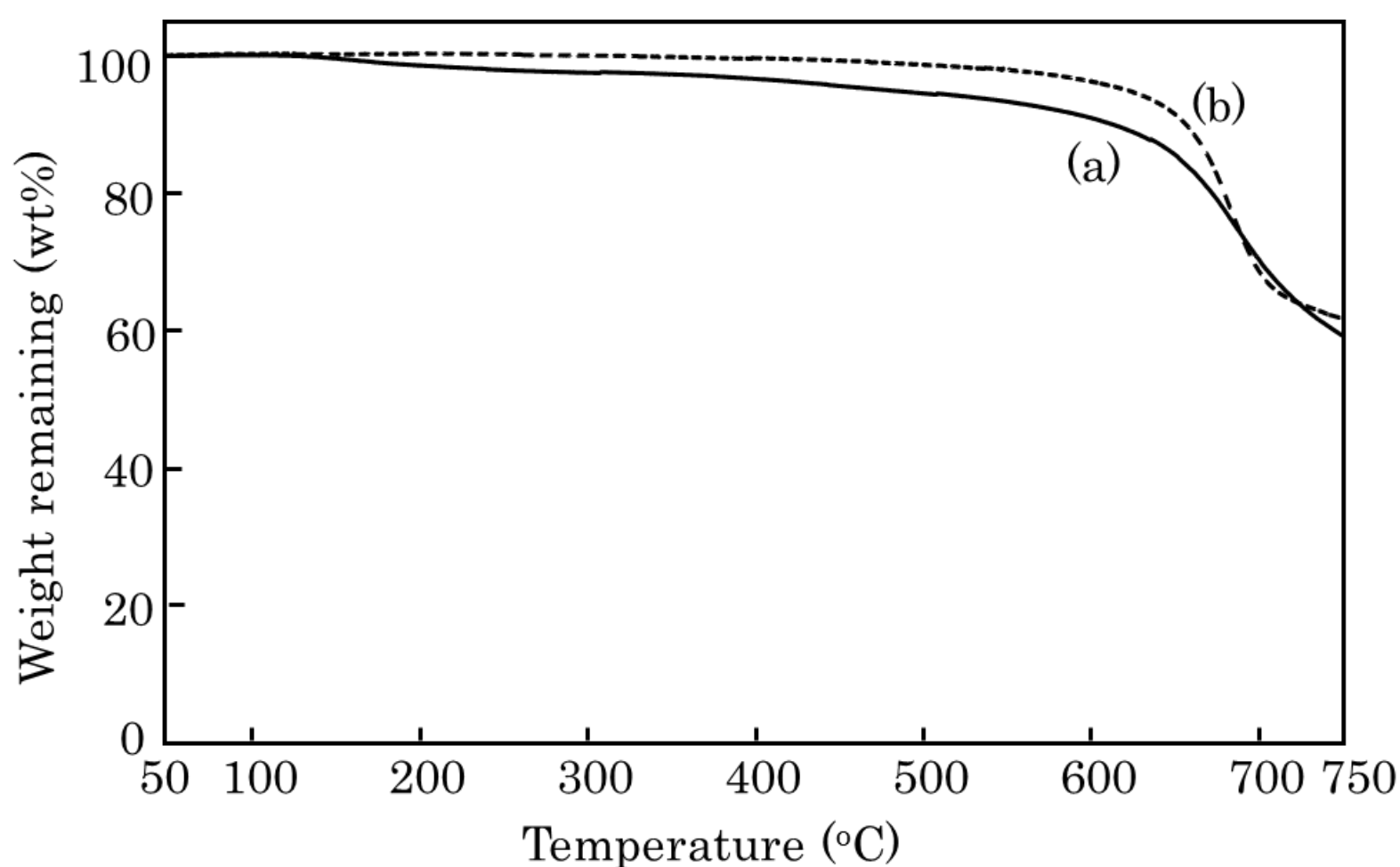


Figure 2-5 TGA profiles of PBID prepared by 6EAN in DBT at a concentration of 2.0% (a) at 330°C (Run No. 1) and (b) 350°C (Run No. 3)

chains packed more densely owing to both the optimum mobility of oligomer molecules and the lower degree of super-cooling. TGA profiles of the PBID crystals measured in nitrogen atmosphere are shown in Figure 2-5. Temperature of 5% and 10% weight loss ( $T_5$  and  $T_{10}$ ) of the PBID crystals prepared by 6EAN in DBT at 330°C at a concentration of 2.0% were 474 and 610°C, respectively. The degradation occurred gradually from about 150°C due to the low molecular weight. In contrast to this, the  $T_5$  and  $T_{10}$  values of the PBID crystals prepared by 6EAN in DBT at 350°C at a concentration of 2.0% were 617 and 647°C, respectively, and weight loss was not observed until 400°C. Further, the char yield at 700°C was over 60%. The PBID having higher molecular weight and higher crystallinity possess excellent thermal stability.

In the preparation of polyimide by amino dicarboxylic monoester, three kind of reaction pathway exist in the formation of non-cyclized precursors. First, formation of

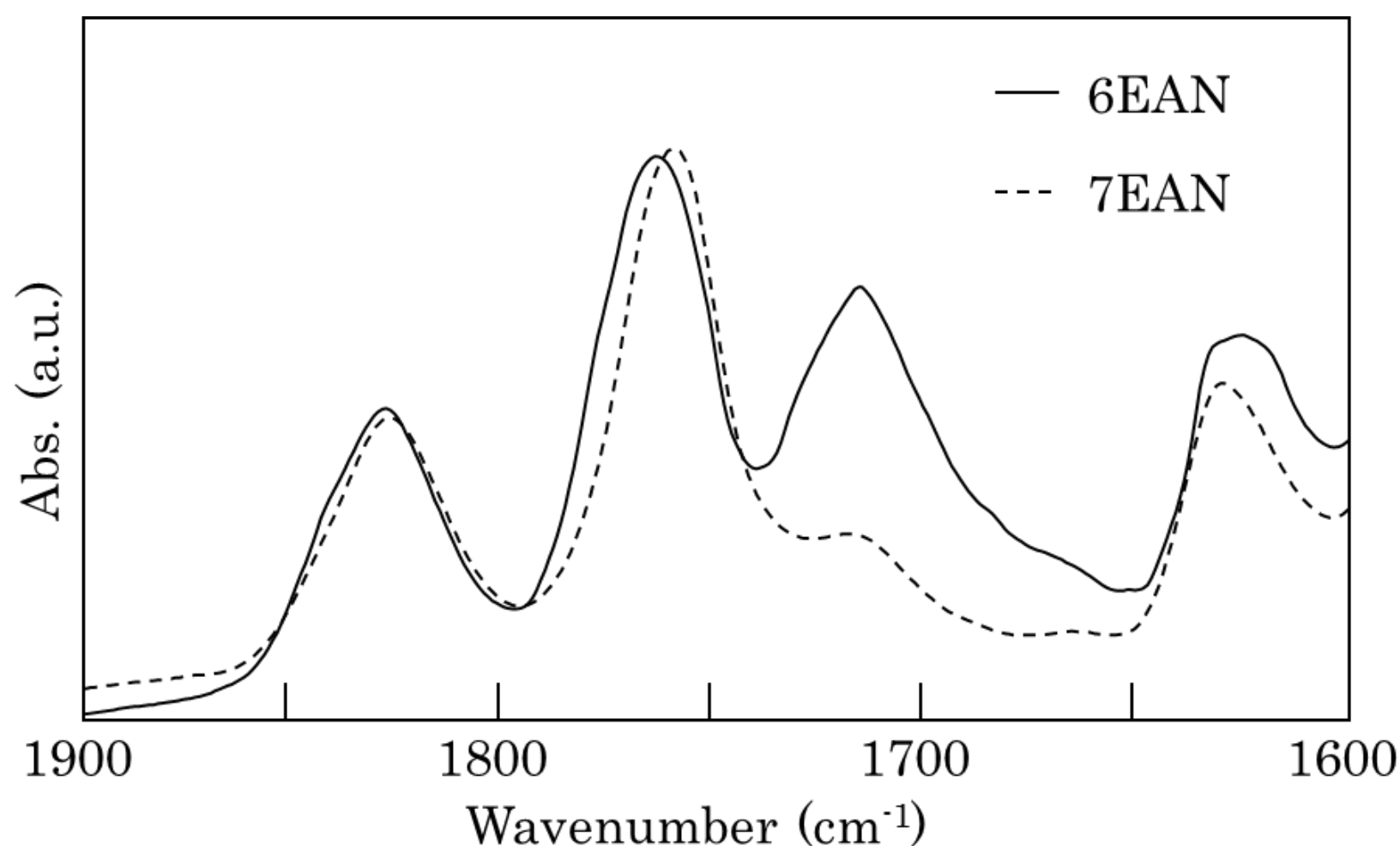


Figure 2-6 FT-IR spectra of oligomers recovered from the solution prepared from 6EAN and 7EAN after 30 min. Polymerizations were carried out in DBT at 330°C at a concentration of 2.0%.

dicarboxylic anhydride by dealcoholized cyclization and following formation of amic acid from reaction to amine. Others, it is direct condensation reaction of amine and carboxylic acid or ester, amic acid and amic ester are formed respectively. In the case of formation of imide linkage is later pathway, non-cyclized amic acid and amic ester contents were differed by using monomer, and thus affect to cyclization reaction rate and phase separation. The polymerization using 7EAN that is structural isomer of ethylation carbonyl position for 6EAN was investigated. In the polymerization in DBT at 330 and 350°C, the yields and  $\eta_{inh}$  values were slightly lower than in the case of using 6EAN. And morphology of these precipitates was spherical aggregates of plate-like crystals in both condition, rod-like crystals were not observed even 330°C different from in the case of using 6EAN. In order to deliberation of this contrast, oligomers dissolved in the solution at 330°C after 30 min were recovered and estimated the structure. IR spectra of oligomers were shown in Figure 2-6. The content of imide structure in oligomers prepared by 6EAN was quite higher than by 7EAN as shown peaks of imide symmetry C=O stretching  $1716\text{ cm}^{-1}$ . This difference in the oligomer structure makes the morphological difference understandable as follows; the rod-like crystals were formed by the spiral growth caused by the screw dislocation in the polymerization of 6EAN, but the strong interaction between the oligomers though hydrogen bonding owing to amic acid and amic ester stricter prevented the screw dislocation and the plate-like crystals are mainly formed by the lateral growth of the oligomers from 7EAN.

TPB have higher boiling point than DBT, thus able to polymerization at the higher temperature that expect for more efficiently solid-state polymerization. First, in order to compare to DBT, polymerization at 350°C were investigated. Spherical aggregates of plate-like crystals having protuberances on surface were formed at concentrations of 0.5% and 2.0% as shown in Figure 2-7 (a) and (b). The yields and  $\eta_{inh}$  values were 25, 66% and

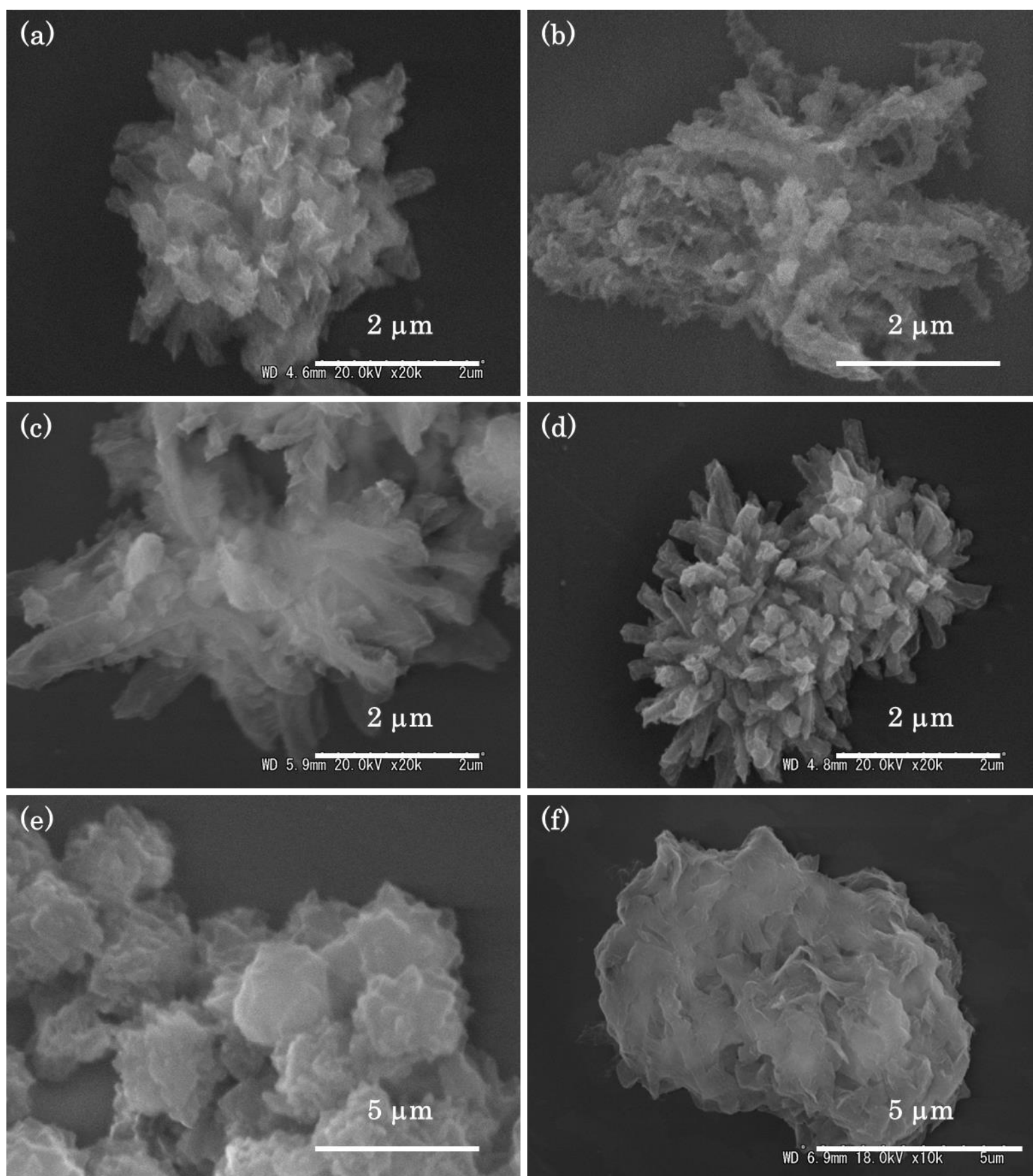


Figure 2-7 Morphology of PBID precipitates of prepared by 6EAN (a) in TPB at 350°C at a conc. of 0.5 % (Run No. 5), (b) in TPB at 350°C at a conc. of 2.0% (Run No. 6), (c) in TPB at 370°C at a conc. of 0.5% (Run No. 7), (d) in TPB at 370°C at a conc. of 1.0% (Run No. 8), (e) in TPB at 400°C at a conc. of 1.0% (Run No. 9) and (f) in DPS at 350°C at a conc. of 1.0% (Run No. 10).

0.31, 0.67 dL·g<sup>-1</sup>, respectively. Lath-like structure that is observed at a concentration of 2.0% was disappeared at a concentration of 0.5%. Also in TPB at 370°C, spherical aggregates of plate-like crystals having protuberances on surface were formed at concentrations of 0.5% and 1.0% as shown in Figure 2-2 (d) and (e). The yields and the  $\eta_{inh}$  values were 48, 60% and 0.33, 0.55 dL·g<sup>-1</sup>, respectively. In TPB at 370°C at a concentration of 1.0%, exhibit most clearly crystal habit and highest  $T_{10}$ . The plate-like crystals having protuberances on the surface were the most distinctive morphology, and therefore TEM and SEAD of these crystals were examined as shown in Figure 2-8. It is clearly observed that many fine plate-like crystals were formed on the surface of the mother plate-like crystal as the protuberances. The mother plate-like crystals were ca. 2  $\mu$ m in length, ca. 600 nm in width and ca. 100 nm in thickness. The length and the width of the fine plate-like crystals were approximately 100 and 20 nm, respectively, and they were very thin, of which the thickness was roughly 8 nm. In the SAED pattern, several sharp spots were observed, suggesting high crystallinity. Among them, the spots of  $d$ -spacing 0.635 nm and 0.385 nm were intensively strong. The length of two repeating PBID units is estimated at 1.64 nm by using MMFF94 (Chem. draw 3D, 12.0). The peak observed at  $2\theta$  of 10.8 degree ( $d = 0.823$  nm) in the WAXS profile shown in Figure 2-4 (c) is reasonably assigned as 002 reflection. With the assumption that the PBID crystal has some analogy of the PPI crystal structure, [24] the spots of  $d$ -spacing of 0.635 nm and 0.385 nm might be assignable as 100 and 010 reflection, respectively. According to this speculation, the PBID molecules might align perpendicular to the plate plane. From the TEM of the side view and the SAED taken from the edge direction, the fine plate-like crystals of the protuberances possess the same crystal structure as the mother plate-like crystal. A dark field image was taken from the edge direction by using the reflection of  $d$ -spacing of 0.635 nm as shown in Figure 2-8 (c).



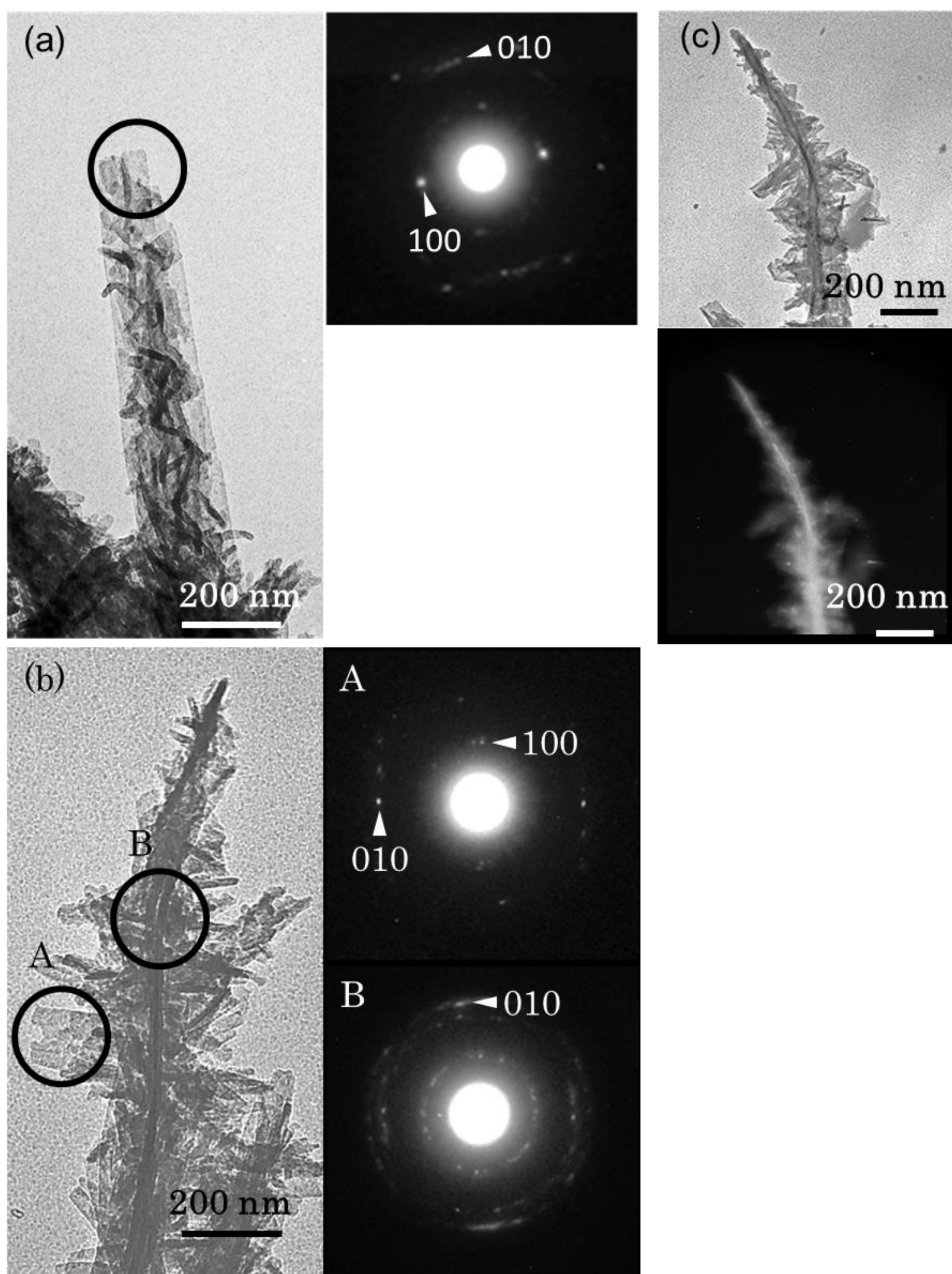


Figure 2-8 TEM and SAED of plate-like PBID crystals having protuberances on surface prepared in TPB at 370°C at a conc. of 0.5% (Run No. 5) taken from (a) though direction and (b) (c) edge direction. Dark-field image (c) was taken by using a reflection of d-spacing of 0.63<sub>5</sub> nm.

The crystal is not uniformly bright. The mother plate-like crystal is bright, but the brightness of other fine plate-like crystals is fluctuated, suggesting that some regions of internal distortions are present within the crystal and the fine plate-like crystals did not grow with specific crystallographic orientations on the mother plate-like crystal. The plate-like crystals having protuberances on the surface resembles the morphology of polybenzimidazole crystals prepared by using reaction-induced crystallization during polymerization. [28] According to the previous study, this unique morphology might be generated by the heterogeneous epitaxial mechanism. However, the orientation of the molecular chains of PBID in the crystals has not been determined yet, and the details in the formation mechanism cannot be proposed. In TPB at 400°C at a concentration of 1.0%, the yield was 92%. The  $\eta_{inh}$  value was 1.01 dL·g<sup>-1</sup> which is highest. And in IR spectrum in Figure 2-2 (d), anhydride C=O peak was disappeared and imide C=O peak was sharpest, high molecular weight PBID was prepared. But their morphology is obscured because increase of miscibility cause liquid-liquid phase separation perhaps. In DPS at a concentration of 1.0%, plate-like crystals having smooth surface were formed as shown in Figure 2-7 (f) with 81% yield and 0.30 dL·g<sup>-1</sup> of  $\eta_{inh}$  value. In IR spectrum of precipitates, the anhydride C=O peak was disappeared, but the peak attributed to amide II band was clearly observed at 1539 cm<sup>-1</sup> as shown in Figure 2-2 (e). DPS is more polar solvent than DBT or TPB, and thereby the amide or carboxyl group might be existed more stably. This suggest that amide-rich oligomers were generated in solution, therefore, crystals were grown laterally to formation of plate-like crystals having smooth surface owing to the strong hydrogen bond.

## 2-3-2 Morphology of PBID prepared by APNI and ANDA

In the reaction-induced phase separation during polymerization, absence of non-cyclized precursor is favorable for the growth of precise crystals. It has been reported that imide linkage is formed by the imide-amine exchange reaction or the condensation of acetoamino group and dicarboxylic anhydride with elimination of acetic acid in one-step. [29, 30] These reactions have moderate activity, and thus synthesis and purification of self-condensable monomers are possible. Hence, APNI and ANDA were synthesized and used for morphology control of PBID. Results of polymerization of APNI are presented in Table 2-2. The polymerizations of APNI afforded precipitates with yields of 44-97%. IR spectrum of precipitates was shown in Figure 2-9 (a), peak of imide C=O was observed sharply without shoulder peaks attribute to non-cyclized precursor. In the polymerization in DBT at a concentration of 0.25%, thin ribbon-like crystals were obtained with 78% yield and  $0.51 \text{ dL} \cdot \text{g}^{-1}$   $\eta_{\text{inh}}$  value as shown in Figure 2-10 (a). The ribbon-like crystals were 2-15  $\mu\text{m}$  in length and 400-800 nm in width. The thickness was approximately 150 nm. In the WAXS intensity

Table 2-2 Results of polymerization of APNI <sup>a</sup>

Run No.	Polymerization condition			Yield (%)	$\eta_{\text{inh}}^b$ ( $\text{dL} \cdot \text{g}^{-1}$ )	Morphology
	Solvent	Temp. (°C)	Conc. (%)			
13	DBT	350	0.25	78	0.51	Ribbon
14			1.00	97	0.32	Twisted ribbon
15	TPB	350	0.25	54	0.14	Unclear
16			1.00	96	0.37	Lath
17		370	0.25	44	0.24	Unclear
18			1.00	80	0.46	Lath

<sup>a</sup> Polymerizations were carried out for 6h. <sup>b</sup> Inherent viscosities were measured in 97% sulfuric acid at 30°C at a concentration of  $0.1 \text{ g} \cdot \text{dL}^{-1}$ .

profile of the ribbon-like crystals shown in Figure 2-11 (a), nine sharp and strong peaks were clearly observed at  $2\theta$  of 13.7, 14.7, 23.6, 25.5, 26.8, 27.4, 29.7, 30.5 and 31.9 degree corresponding to  $d$ -spacing 0.646, 0.603, 0.377, 0.349, 0.333, 0.325, 0.301, 0.293 and 0.281 nm. If the crystal unit cell is assumed as orthorhombic,  $a = 0.65$  nm,  $b = 0.38$  nm and  $c = 1.66$  nm, these diffractions can be indexed as shown in Figure 2-11. Even though the diffuse halo attributed from amorphous region was slightly observed, these crystals possessed high crystallinity. Polymerization was next carried out in DBT at a concentration of 1.00%, twisted ribbon-like crystals were obtained with 97% yield and  $0.32 \text{ dL}\cdot\text{g}^{-1} \eta_{\text{inh}}$  value. The twisted ribbon-like crystals were 1-2  $\mu\text{m}$  in length and ca. 100 nm in width. The twist pitch was ca. 150 nm. This kind of discriminating structures were found in self-condensed poly(ester imide) and poly(oxazole ester) previously, [31, 32] it is anticipated that developed planarity and large dipole moment along molecular chain direction of precipitated oligomers are important factor in the formation of these structure. It seems that exclusion of non-cyclized oligomers by one-step imide formation was permitted to satisfy this

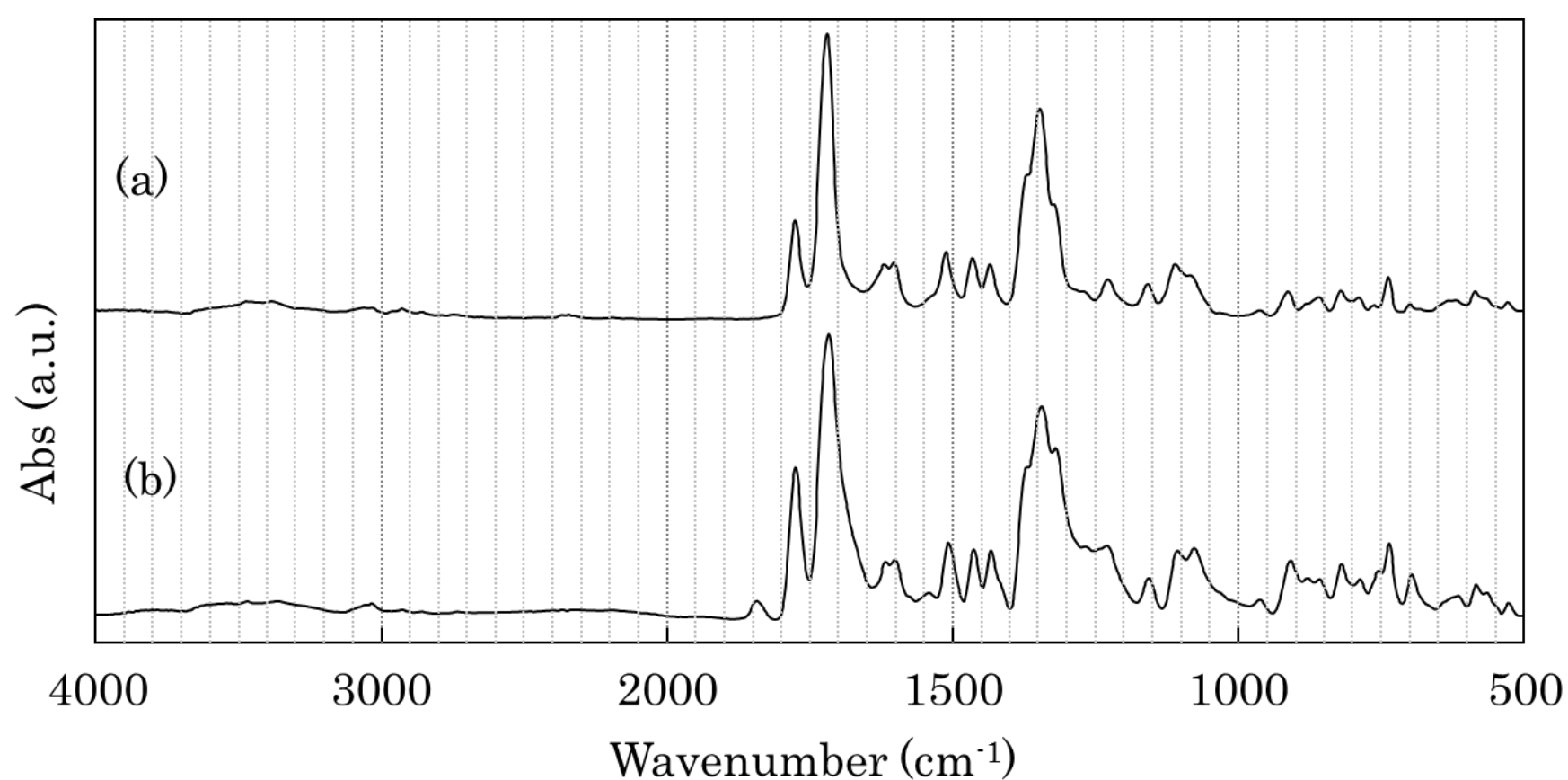


Figure 2-9 FT-IR spectra of PBID precipitates of prepared in DBT at 350°C at a concentration of 1.00% from (a) APNI (Run No. 14) and (b) ANDA (Run No. 20)

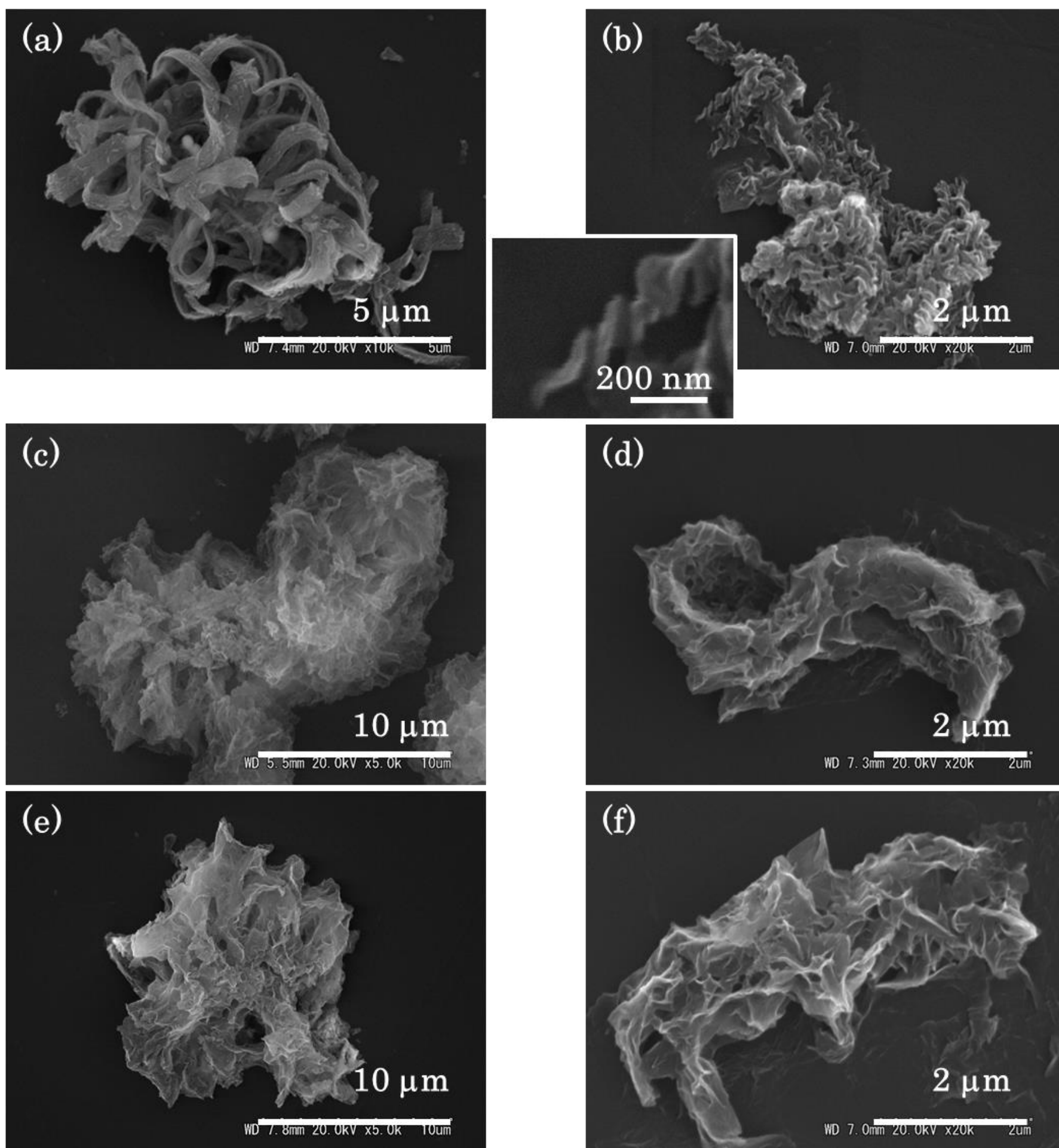


Figure 2-10 Morphology of PBID precipitates prepared by APNI (a) in DBT at 350°C at a conc. of 0.25% (Run No. 13), (b) in DBT at 350°C at a conc. of 1.00% (Run No. 14), (c) in TPB at 350°C at a conc. of 0.25% (Run No. 15), (d) in TPB at 350°C at a conc. of 1.00% (Run No. 16), (e) in DBT at 370°C at a conc. of 0.25% (Run No. 17) and (f) in TPB at 350°C at a conc. of 1.00% (Run No. 18)

requirement. In TPB, at a concentration of 1.00% at 350 and 370°C, lath-like crystals formed in yields of 96, 80% and 0.37, 0.46 dL·g<sup>-1</sup>  $\eta_{inh}$  values as shown in Figure 2-10 (d) and (f), respectively. TPB have higher miscibility than DBT as suggested by change of yields. Therefore, molecular weight of the precipitated oligomers was increase, and cause lateral grows to formed lath-like crystals. In TPB at a concentration of 0.25% at 350 and 370°C, further increase of molecular weight of the precipitated oligomers afforded produce unclear morphology (Figure 2-10 (c) and (e))in yield of 54 and 44%, respectively by reason of crystallizability of oligomers were lowered. The  $\eta_{inh}$  values of precipitates prepared in TPB at a concentration of 0.25% were 0.14 and 0.24 dL·g<sup>-1</sup>, lower than at a concentration of 1.00% reflecting niggardly condensation of end-group.

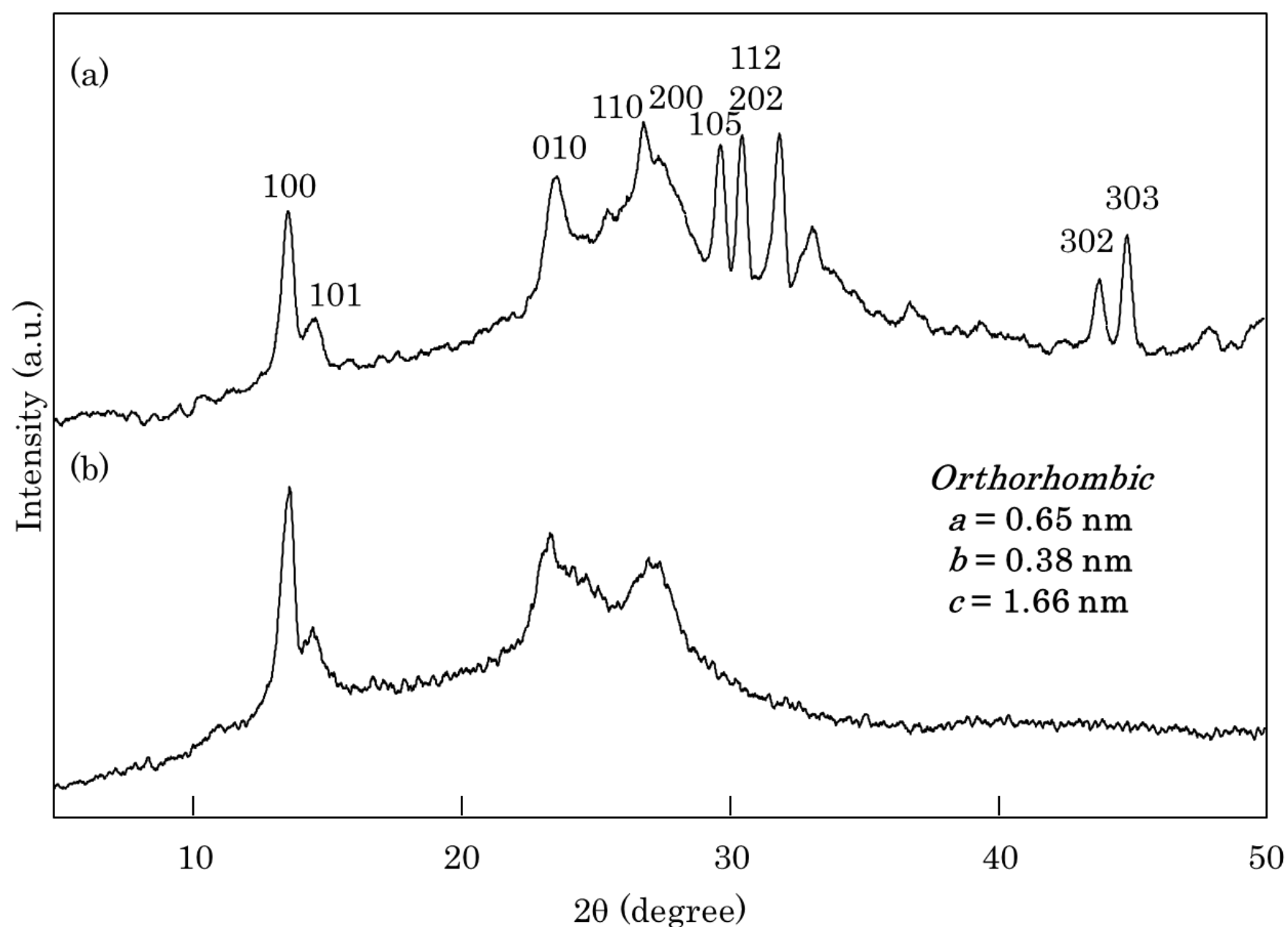


Figure 2-11 WAXS intensity profiles of PBID precipitates of prepared in DBT at 350°C (a) at a concentration of 0.25% from APNI and (b) at a concentration of 1.00% from ANDA

Polymerizations of ANDA were next carried out. The reaction of ANDA with the elimination of acetic acid occurs more slowly than that of APNI with the elimination of 2-aminopyridine. Due to this, the polymerization time of ANDA was 24 h. Results of polymerization of ANDA are presented in Table 2-3. PBID precipitates were obtained yields of 14-73 %. In DBT at 350°C at a concentration of 0.25%, obtained precipitates did not exhibit clear morphology. In DBT at a concentration of 1.0%, small needle-like crystals were obtained with the yield of 73% as shown in Figure 2-12 (c). The small needles, of which the length and the width were ca. 2  $\mu\text{m}$  and 400 nm, was grew radially from the center parts. The tip of the needle-like crystal was sharp. These morphological features were similar to Run No. 2. In IR spectra as shown in Figure 2-9 (a), peaks of anhydride and amide C=O were observed, molecular weight of these precipitates were predicted to not so high. However, these precipitates were insoluble for 97% sulfuric acid. In the WAXS intensity profile of the needle-like crystals shown in Figure 2-11 (b), four sharp and strong peaks were clearly observed at  $2\theta$  of 13.8, 14.6, 23.5 and 27.5 corresponding to  $d$ -spacing of 0.630, 0.596, 0.372, and 0.319 nm. Even though the crystals contained slightly the amorphous region, these crystals also possessed high crystallinity. The needle-like crystals prepared from ANDA was lower crystallinity but denser than the ribbon-like crystals

Table 2-3 Results of polymerization of ANDA <sup>a</sup>

Run No.	Polymerization condition			Yield (%)	Morphology
	Solvent	Temp. (°C)	Conc. (%)		
19	DBT	350	0.25	26	Unclear
20			1.00	73	Needle
21	TPB	350	0.25	22	Fiber, Sphere
22			1.00	47	Sphere
23		370	0.25	14	Unclear
24			1.00	36	Plate, Sphere

<sup>a</sup> Polymerizations were carried out for 24 h.



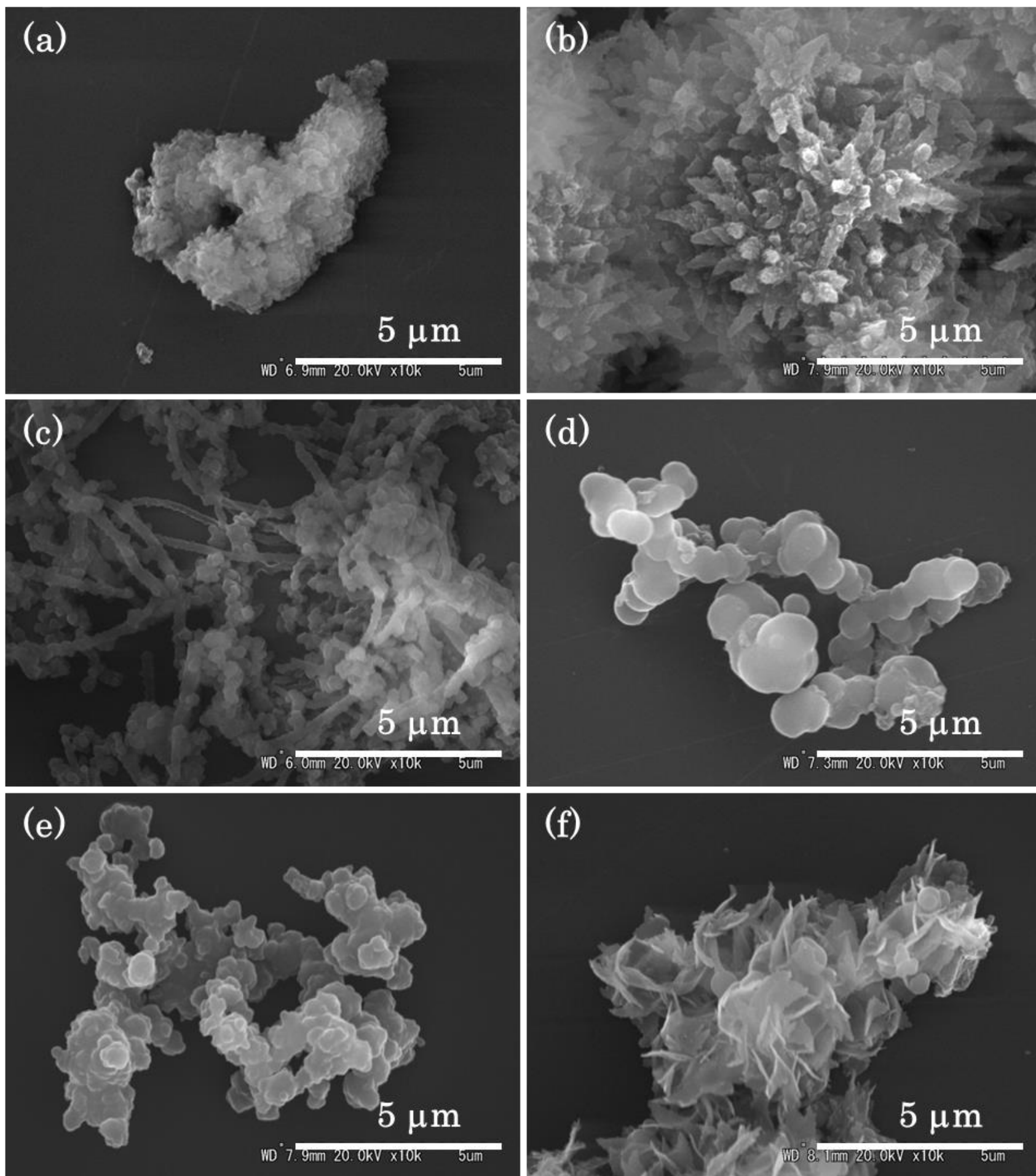


Figure 2-12 Morphology of PBID precipitates prepared by ANDA (a) in DBT at 350°C at a conc. of 0.25% (Run No. 19), (b) in DBT at 350°C at a conc. of 1.00% (Run No. 20), (c) in TPB at 350°C at a conc. of 0.25% (Run No. 21), (d) in TPB at 350°C at a conc. of 1.00% (Run No. 22), (e) in DBT at 370°C at a conc. of 0.25% (Run No. 23) and (f) in TPB at 350°C at a conc. of 1.00% (Run No. 24)



prepared from APNI. Conceivably, three dimensional interactions were formed by acetoamide end-group. The polymerization of ANDA in TPB at 350°C at a concentration of 0.25% for 24 h afforded fibrillar crystals with the yields of 22% as shown 12 (c). The width of the fibrillar crystals was ca. 200 nm. In contrast to these, the polymerization in TPB at 350°C at a concentration of 1.0% did not give crystals having clear habits at all, and the microspheres having smooth surface were only formed with the yield of 47%, of which the diameter was 3-4  $\mu\text{m}$  as shown in Figure 2-12 (d). The spherical morphology implies that the microspheres were formed *via* liquid-liquid phase separation rather than crystallization. At higher concentration, the molecular weight of the precipitated oligomers became lower leading to the lower freezing temperature of the oligomers. Due to this, the liquid-liquid phase separation is induced. In TPB at 370°C at a concentration of 0.25 and 1.00 %, unclear structure and plate-like crystals were obtained in yield of 14 and 36%, respectively. Increase of molecular weight of the precipitated oligomers cause this change of morphology in a similar way to the polymerizations of APNI.

The obtained PBID was dissolved only in 97% sulfuric acid as aforesaid. Owing to the rigid-rod structure, the PBID is expected to exhibit lyotropicity. However, maximum concentration of PBID was ca. 2%, and therefore the lyotropicity was not observed in the 97% sulfuric acid solution. And PBID was neither exhibited  $T_g$  nor  $T_m$  under the decomposition temperature, they showed excellent thermal stability.

## 2-4 CONCLUSIONS

PBID was synthesized as precipitated crystals from 6EAN, 7EAN, APNI and ANDA by using reaction-induced phase separation during polymerization. Various morphology of the PBID such as rods, plates have protuberances perpendicular or flat surface, lathes, twisted

and non-twisted ribbons, needles, fibers and spheres were fabricated. The morphology of PBID was highly influenced by not only polymerization conditions but also the structure of the monomer. The rod-like crystals and the spherical aggregates of plate-like crystals were formed in DBT at 330°C from 6EAN and 7EAN that is structural isomer mutually. This morphological difference was attributed to degree of imidizations of the precipitated oligomers. The plate-like crystals having protuberances on the surface were formed in TPB from 6EAN. It is suggest that the PBID molecules might align perpendicular to the plate plane. The twisted ribbon-like crystals were formed in DBT from APNI owing to precipitation of fully imidized oligomers. These PBID precipitates possessed high crystallinity, and they showed excellent thermal stability and chemical resistance.

## 2-5 REFERENCE

- [1] Yang, C. P.; Chen, W. T., *J. Polym. Sci. Part A: Polym. Chem.*, 1993, **31**, 2799.
- [2] Leua, T.; Wang, C., *Polymer*, 2002, **43**, 7069.
- [3] Le, N. L.; Wang, T.; Chung, T. S., *J. Membr. Sci.*, 2012, **415–416**, 109.
- [4] Barikani, M.; Ataei, S. M., *J. Polym. Sci. Part A: Polym. Chem.*, 1999, **37**, 2245.
- [5] Hasegawa, M.; Horii, S., *Polym. J.*, 2007, **39**, 610.
- [6] Ishii, J.; Takata, A.; Oami, Y.; Yokota, R.; Vladimirov, L.; Hasegawa, M., *Eur. Polym. J.*, 2010, **46**, 681.
- [7] Mittal, K. L., *Plenum Press: New York*, 1984, Vol. 1.
- [8] Cassidy, P. E., *Marcel Dekker, New York*, 1980.
- [9] For example, Sek, D.; Pijet, P.; Wanic, A., *Polymer*, 1992, **33**, 190 or Rehman, S.; Li, P.; Zhou, H.; Zhao, X.; Dang, G.; Chen, C., *Polym. Degrad. Stab.*, 2012, **97**, 1581.

- [10] Chen, X.; Yin, Y.; Chen, P.; Kita, H.; Okamoto, K., *J. Membr. Sci.*, 2008, **313**, 106.
- [11] Besse, S.; Capron, P.; Diat, O.; Gebel, G.; Jousse, F.; Marsacq, D.; Pin'eri, M.; Marestin, C.; Mercier, R., *J. New Mater. Electrochem. Syst.*, 2002, **5**, 109.
- [12] Badami, A. S.; Roy, A.; Lee, H. S.; Li, Y.; McGrath, J. E., *J. Membr. Sci.*, 2009, **328**, 156.
- [13] Liua, C.; Li, L.; Liua, Z.; Guoa, M.; Jing, L.; Liua, B.; Jianga, Z.; Matsumotob, T.; Guiverc, M. D., *J. Membr. Sci.*, 2011, **366**, 73.
- [14] Yang, C. P.; Su, Y. Y.; Guo, W.; Hsiao, S.H., *Eur. Polym. J.*, 2009, **45**, 721.
- [15] Bruma, M.; Damaceanu, M. D.; Rusu, R. D., *High Perform. Polym.*, 2012, **24**, 31.
- [16] Thiruvassagam, P.; Venkatesan, D., *J. Macromol. Sci., Part A: Pure and Applied Chem.*, 2009, **46**, 419.
- [17] Nephew, J. B.; Nihei, T. C.; Carter, S. A., *Phys. Rev. Lett.*, 1998, **80**, 3276.
- [18] Tran-Cong, Q. Harada, A., *Phys. Rev. Lett.*, 1996, **76**, 1162.
- [19] Kyu, T.; Lee, J. H., *Phys. Rev. Lett.*, 1996, **76**, 3746.
- [20] Williams, R. J. J.; Rozenberg, B. A.; Pascault, J. P., *Adv. Polym. Sci.*, 1997, **128**, 95.
- [21] Luo, K., *Eur. Polym. J.*, 2006, **42**, 1499.
- [22] Wang, X.; Okada, M.; Matsushita, Y.; Furukawa, H.; Han, C.C., *Macromolecules*, 2005, **38**, 7127.
- [23] Kimura, K.; Kohama, S.; Yamazaki, S., *Polym. J.*, 2006, **38**, 1005.
- [24] Wakabayashi, K.; Uchida, T.; Yamazaki, S.; Kimura, K., *Macromolecules*, 2008, **41**, 4607.
- [25] Kawauchi, S.; Shirata, K.; Hattori, M.; Kaneko, S.; Miyawaki, R.; Watanabe, J.; Kimura, K., *Preprints of 21th Polyimide & Aromatic Polymer conference, Japan*, 2013.
- [26] Sawai, T.; Uchida, T.; Yamazaki, S.; Kimura, K.; *Fiber Preprints, Japan*, 2013.
- [27] Baathulaa, K.; Xu, Y.; Qian, X., *J. Photochem. Photobiology A: Chem.*, 2010, **216**, 24.

- [28] Gong, J.; Uchida, T.; Yamazaki, S.; Kimura, K., *Macromol. Chem. Phys.*, 2010, **211**, 2226.
- [29] Takekoshi, T.; Webb, J. L.; Anderson, P. P.; Olsen, C. E., *IUPAC 32nd International Symposium on Macromolecules*, 1988, 464.
- [30] John, A. K., *Polymer*, 1995, **36**, 2089.
- [31] Ohnishi, T.; Uchida, T.; Yamazaki, S.; Kimura, K., *Preprints of 61th SPSJ Annual Meeting*, Japan, 2012.
- [32] Maki, Y.; Ohnishi, T.; Uchida, T.; Yamazaki, S.; Kimura, K., *Preprints of International Discussion Meeting on Polymer Crystallization 2013*, Japan, 2013.

## CHAPTER 3

### SYNTHESIS AND MORPHOLOGY CONTROL OF POLY(2,6-1H-BENZO[f]ISOINDOLE-1,3(2H)-DIONE-*co*-PHTHALIMIDE)

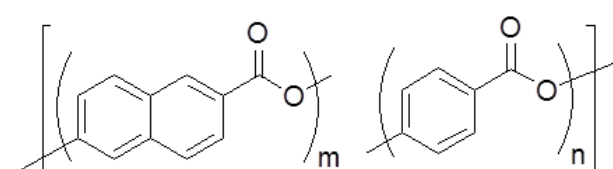
#### 3-1 INTRODUCTION

In reaction-induced phase separation during polymerization, copolymerization greatly effect on morphology due to lack of crystallizability and lowering freezing point, the clear crystal habit is generally damaged but some copolymers prepared maintain high crystallinity such as P(OPI-*co*-PI) shown in Chapter 1 and so on. [1-3] Preparation and morphology control of self-condensed copolyimide by the reaction-induced phase separation during polymerization using copolymerization is also an interesting investigation target. In Chapter 2, significant low mobility attributed to cohesion force of naphthalene ring inhibited preparation of high molecular weight PBID. In the polymerization at 400°C, increase of molecular weight was exhibit, but crystal habit disappeared. It is required another methodology to prepare high molecular weight morphology controlled naphthalene containing self-condensed polyimide. It is one of prospective method for this problem to reduce cohesion force by introduce of copolymerization component.

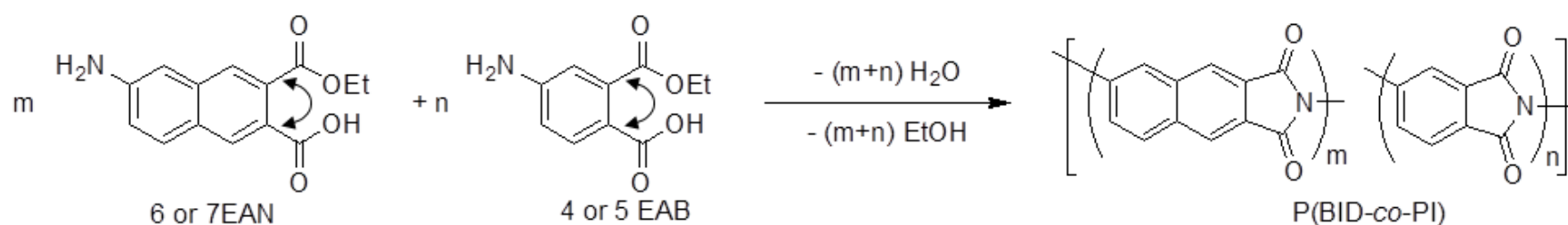
Additionally, copolymerization is useful method to reduce  $T_m$ , especially it is desirable to prepare the moldable rigid-rod polymers with maintaining high-performance such as thermal stability, chemical resistance and so on. The copolymers of 2-oxy-6-naphthoyl and *p*-oxybenzoyl moiety (P(ON-*co*-OB), shown in Scheme 3-1, were well-known. Both PON and POB are totally intractable, and they had been given up to use as processable materials. However, in the certain copolymerization ratio, the P(ON-*co*-OB)

exhibit the melting behavior under the decomposition temperature, and additionally they possess thermotropicity due to their rigid structures. P(ON-*co*-OB)s which are commercially well known as Vectra® are widely and industrially used as structural materials. [4-6] This thermotropicity is attributed to the crankshaft effect caused by the naphthalene moiety. Although the imide linkage is more rigid and straight than ester linkage, the structure of copolymer from PBID and PPI (P(BID-*co*-PI)) can be recognized to be analogous to that of P(ON-*co*-OB). If the crankshaft effect of naphthalene moiety in P(BID-*co*-PI), bringing about the reduction of the melting point under the decomposition temperature, the formation of thermotropic polyimide will be expected.

In this chapter, preparation and morphology control of P(BID-*co*-PI) were examined by using reaction-induced phase separation during polymerization from 6EAN and 2-ethoxycarbonyl-4-aminobenzoic acid (4EAB) or 7EAN and 2-ethoxycarbonyl-5-aminobenzoic acid (5EAB) as shown in Scheme 3-2.



Scheme 3-1 Structure of P(ON-*co*-OB)



Scheme 3-2 Synthesis of P(BID-*co*-PI)

## 3-2 EXPERIMENTAL

### 3-2-1 Materials

6EAN and 7EAN were synthesized in the same manner described in the Chapter 2. 4EAB and 5EAB were synthesized according to the previously reported procedure. [7] A mixture of isomers of dibenzyltoluene (DBT) used in this Chapter was the same as that in Chapter 1.

### 3-2-2 Polymerization method

DBT (10.5 g) was placed into a cylindrical flask equipped with gas inlet and outlet tubes and a thermometer, and then heated up to 330°C under nitrogen. 6EAN (202 mg, 0.78 mmol) and 4EAB (68 mg, 0.34mmol) were added into DBT at 330°C, and the mixture was stirred for 5 second. And then the polymerization was carried out at 330°C for 6 h with no stirring. Concentration of the polymerization, defined as (calculated polymer weight / solvent volume)  $\times$  100 in this study, was 2.0%. The solution became turbid several minutes after the addition of monomers due to the precipitation of oligomers and the P(BID-*co*-PI) was formed as precipitates after 6 h. The P(BID-*co*-PI) precipitates were collected by vacuum filtration at 330°C, washed with *n*-hexane and acetone, and then dried at 50°C for 12 h. Oligomers left in the solution at 330°C were recovered by pouring the filtrate into *n*-hexane at 25°C. The copolymerizations of EAN and EAB under other conditions were also carried out in a similar manner.

### 3-2-3 Measurements

Characterizations by SEM, IR, WAXS, TGA and DSC were examined in the same manner of the Chapter 1. Inherent viscosities were measured in the same manner to the Chapter 2. The content of PBID moiety in the copolymers ( $\chi_p$ ) was determined by IR analysis.

## 3-3 RESULT AND DISSCUSION

6EAN and 7EAN, 4EAB and 5EAB were structural isomer of ethyl ester position of carboxyl groups respectively. Combinations of 6EAN and 4EAB that amine and carboxyl groups located at the diagonal position, and adversely 7EAN and 5EAB were selected. The copolymerizations were occurred in DBT at 330°C at a concentration of 2.0% for 6 h with varying molar fraction of EAN in feed ( $\chi_f$ ). Results of the polymerization were presented in Table 3-1. After the polymerization for 6 h, precipitates were obtained in 34-75% of yields and 0.35-0.86 dL·g<sup>-1</sup> of  $\eta_{inh}$  values. Figure 3-1 was IR spectra of precipitates. In the IR spectra of precipitates prepared by copolymerization (Figure 3-1 (a)-(f)), peaks of naphthalene and benzene ring C=C were observed in 1509 and 1490 cm<sup>-1</sup> respectively, it is to confirmed preparation of P(BID-*co*-PI). These two peaks were utilized to estimate of the  $\chi_p$  values defined by molar fraction of BID component in precipitates. The  $\chi_p$  values of precipitates were slightly higher than corresponding  $\chi_f$  values. The oligomers rich in BID moiety are precipitated more rapidly than those rich in PI moiety owing to the lower solubility, causing the difference between the  $\chi_f$  values and the  $\chi_p$  values. The yields and  $\eta_{inh}$  values of P(BID-*co*-PI) prepared from 6EAN and 4EAB were higher than from 7EAN and 5EAB each  $\chi_f$ , these were same trend to homopolymers. And  $\eta_{inh}$  values were increased with decrement of the  $\chi_f$  values. In the copolymerization of EAN and EAB, peak intensities



Table 3-1 Results of polymerization of EAN and EAB <sup>a</sup>

Run No.	Polymerization condition		Yield (%)	$\chi_p^c$ (mol%)	$\eta_{inh}^d$ (dL·g <sup>-1</sup> )	T <sub>10</sub> <sup>f</sup> (°C)	Morpology
	Monomers	$\chi_f^b$ (mol%)					
1	6EAN and 4EAB	70	72	78	0.44	647	PP <sup>g</sup>
2	6EAN and 4EAB	50	70	58	0.62	634	Unclear
3	6EAN and 4EAB	30	75	49	0.86	608	Sphere
4	4EAB	0	70	0	- <sup>e</sup>	678	Ribbon
5	7EAN and 5EAB	70	55	76	0.35	613	PP
6	7EAN and 5EAB	50	43	59	0.45	585	PP
7	7EAN and 5EAB	30	34	45	0.55	564	PP
8	5EAB	0	50	0	-	652	Ribbon

<sup>a</sup> Polymerizations were carried out at 330°C for 6h at a concentration of 2.0% in DBT. <sup>b</sup> Molar ratio of EAN moiety in feed. <sup>c</sup> Molar ratio of PBPI moiety in precipitate. <sup>d</sup> Inherent viscosities were measured in 97% sulfuric acid at 30°C at a concentration of 0.1 g·dL<sup>-1</sup>. <sup>e</sup> Not measured due to insoluble. <sup>f</sup> Temperature of 10% weight loss recorded by a TGA at a heating rate of 10°C/min in nitrogen. <sup>g</sup> Plate-like crystal having protuberances on surface.

of anhydride C=O were decreased according to  $\chi_f$  values. These corresponded to increase of  $\eta_{inh}$  value, and it seems that more efficient solid-state polymerization was occur because mobility of oligomers were enhanced by decrease of BID moiety. However, in copolymerization of 7EAN and 5EAB, differ to 6EAN and 4EAB, peak of anhydride C=O was not disappeared even  $\chi_f$  of 30mol%. And shoulder peak of non-cyclized precursor also appear relatively strong. The oligomers consist of 7EAN were rich in amic acid or amic ester moiety as mentioned in also Chapter 2. These suggest that high miscibility of oligomers for DBT were caused decrement of yields, and strongly interaction of hydrogen bond inhibited solid-state polymerization. The copolymerization influenced the morphology significantly. The rod-like crystals of PBID and the ribbon-like crystals of PPI were formed from 6EAN and 4EAB, respectively. The plate-like crystals having protuberances on the surface were formed by copolymerization of 6EAN and 4EAB at  $\chi_f$  of 70 mol% as shown in

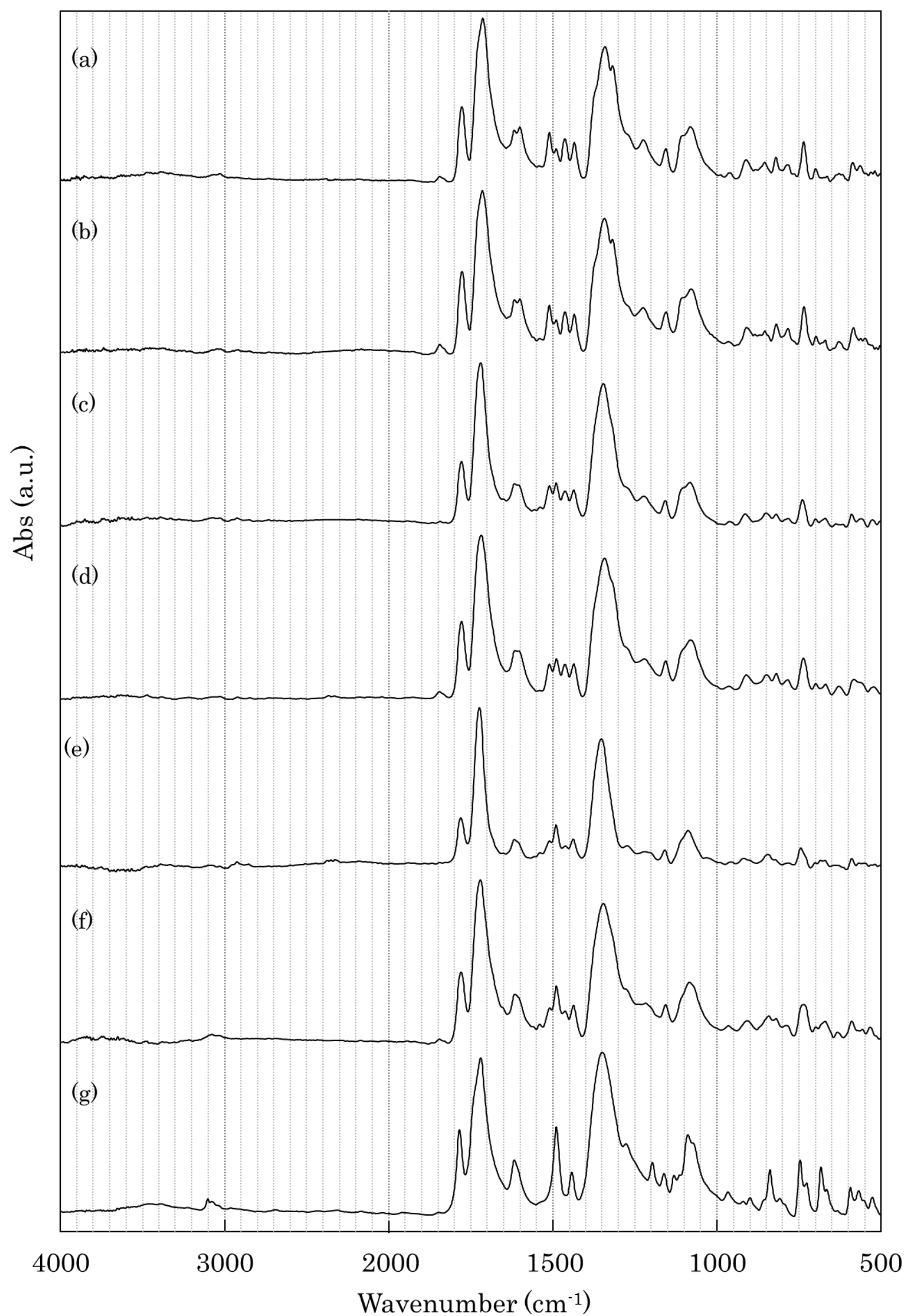


Figure 3-1 FT-IR spectra of P(BID-*co*-PI) precipitates prepared from 6EAN and 4EAB in DBT at 330°C at a concentration of 2.0% at  $\chi_f$  of (a) 70mol%, (c) 50mol%, (e) 30mol% and (g) 0 mol% (PPI). Those prepared from 7EAN and 5EAB at  $\chi_f$  of (b) 70mol%, (d) 50mol% (f) 30mol%.

Figure 3-2 (a). The crystal habit extinguished at  $\chi_f$  of 50 mol%, and spheres fused each other were obtained at  $\chi_f$  of 30 mol% as shown in Figure 3-2 (b) and (c). The clear crystal habit is generally damaged by the copolymerization because of the lack of crystallizability of oligomers. Additionally the freezing point of the oligomers became lower by the copolymerization and the lower freezing point brings about to induce liquid-liquid phase separation rather than crystallization resulting in the formation of spherical precipitates. [10-12] Even though the morphology became spherical and unclear in the middle range of the  $\chi_f$  value, they all possessed high crystallinity as shown in Figure 3-3. The characteristic peaks of the PBID crystals were clearly shown in the P(BID-*co*-PI)s, and those of PPI crystals were gradually visualized with the decrease in the  $\chi_f$  value. But in the 30 and 50 mol% of the  $\chi_f$  value, broadening and shift toward lower angle of peaks were observed, and the  $T_{10}$  values were decreased correspondently in spite of increase of the  $\eta_{inh}$  values. The copolymerizations of 7EAN and 5EAB at  $\chi_f$  of 70 mol% were afforded formation of plate-like crystals having protuberances on the surface as with copolymerization of 6EAN and 4EAB. But in the middle range of the  $\chi_f$  value, in contrast to copolymerization of 6EAN and 4EAB, precipitates of copolymerizations of 7EAN and 5EAB were maintained clear morphology, and there were plate-like crystals having smooth surface as shown in Figure 3-4 (a)-(c). As aforesaid, the oligomers from 7EAN were possessed strong interaction attributed to the hydrogen bonding. Therefore, the crystallization was induced regardless the  $\chi_f$  vales, resulting in the formation of the plate-like crystals. The sizes of plate-like crystals having protuberances on the surface were enlarged substantially with decrement of the  $\chi_f$  vales. It is considered to be as follows: The oligomers rich in amic acid and PI moiety which is more miscible for DBT were formed these conditions. Hence, super-saturation of the polymerization solution was lowered, and only small number of crystal nuclei was generated in early stage. And then oligomers were expended crystal grows without

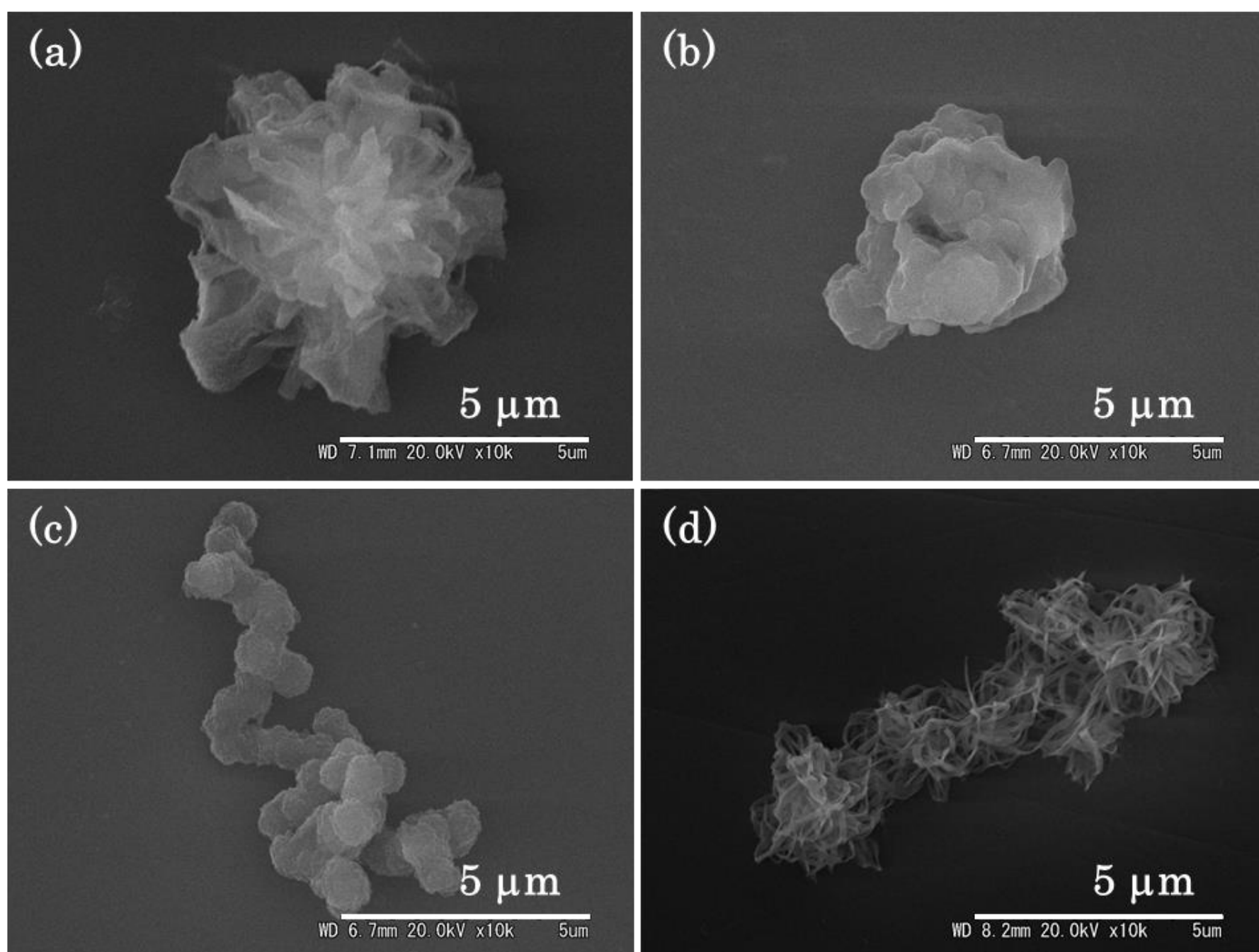


Figure 3-2 Morphology of P(BID-*co*-PI) precipitates prepared from 6EAN and 4EAB in DBT at 330°C at a concentration of 2.0% at  $\chi_f$  of (a) 70mol%, (b) 50mol%, (c) 30mol% and (d) 0 mol% (PPI).

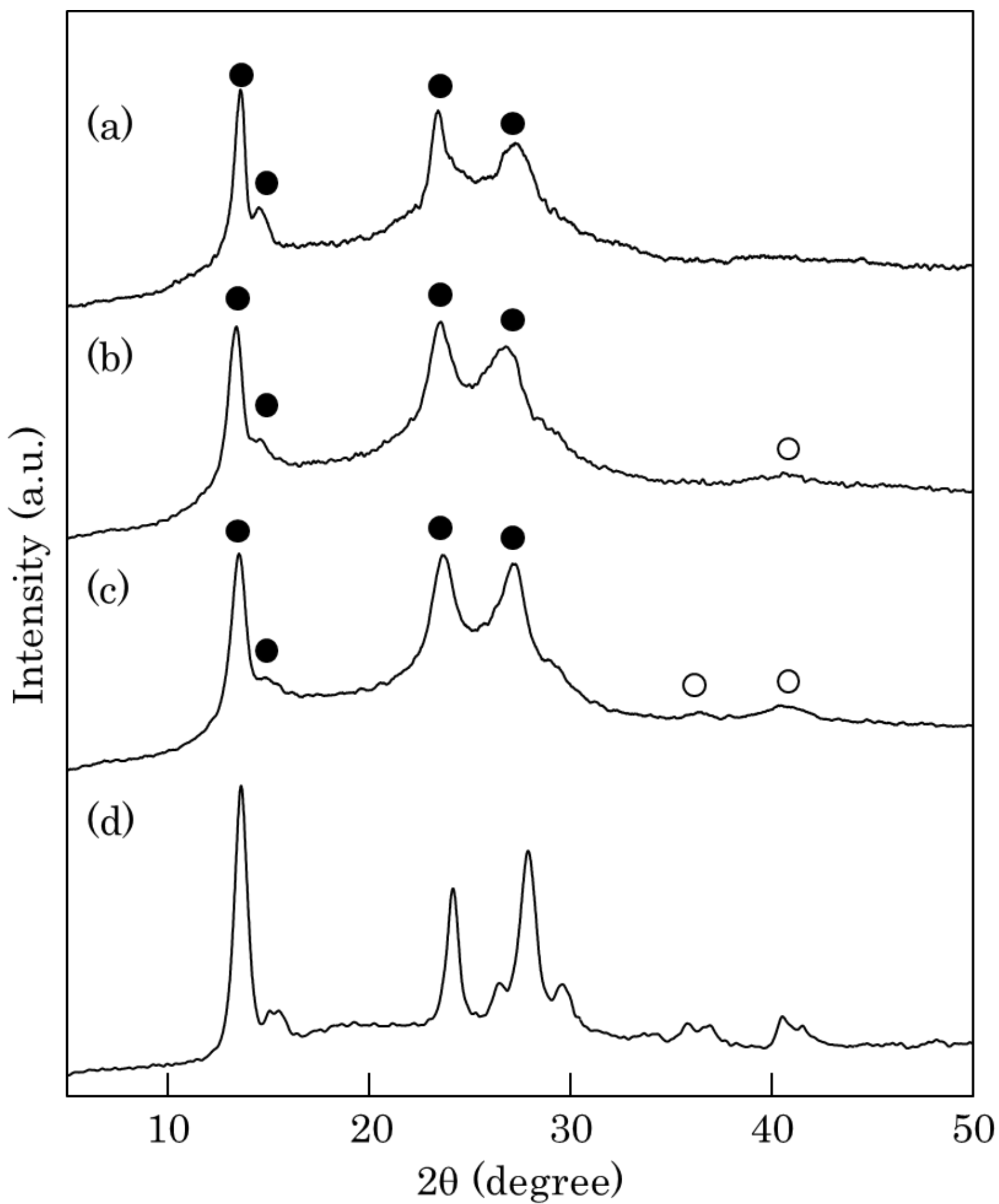


Figure 3-3 WAXS intensity profiles of P(BID-*co*-PI) precipitates prepared from 6EAN and 4EAB in DBT at 330°C at a concentration of 2.0% at  $\chi_f$  of (a) 70mol%, (b) 50mol%, (c) 30mol% and (d) 0 mol% (PPI). Reflection peaks (●) and (○) are derived from PBID and PPI, respectively.

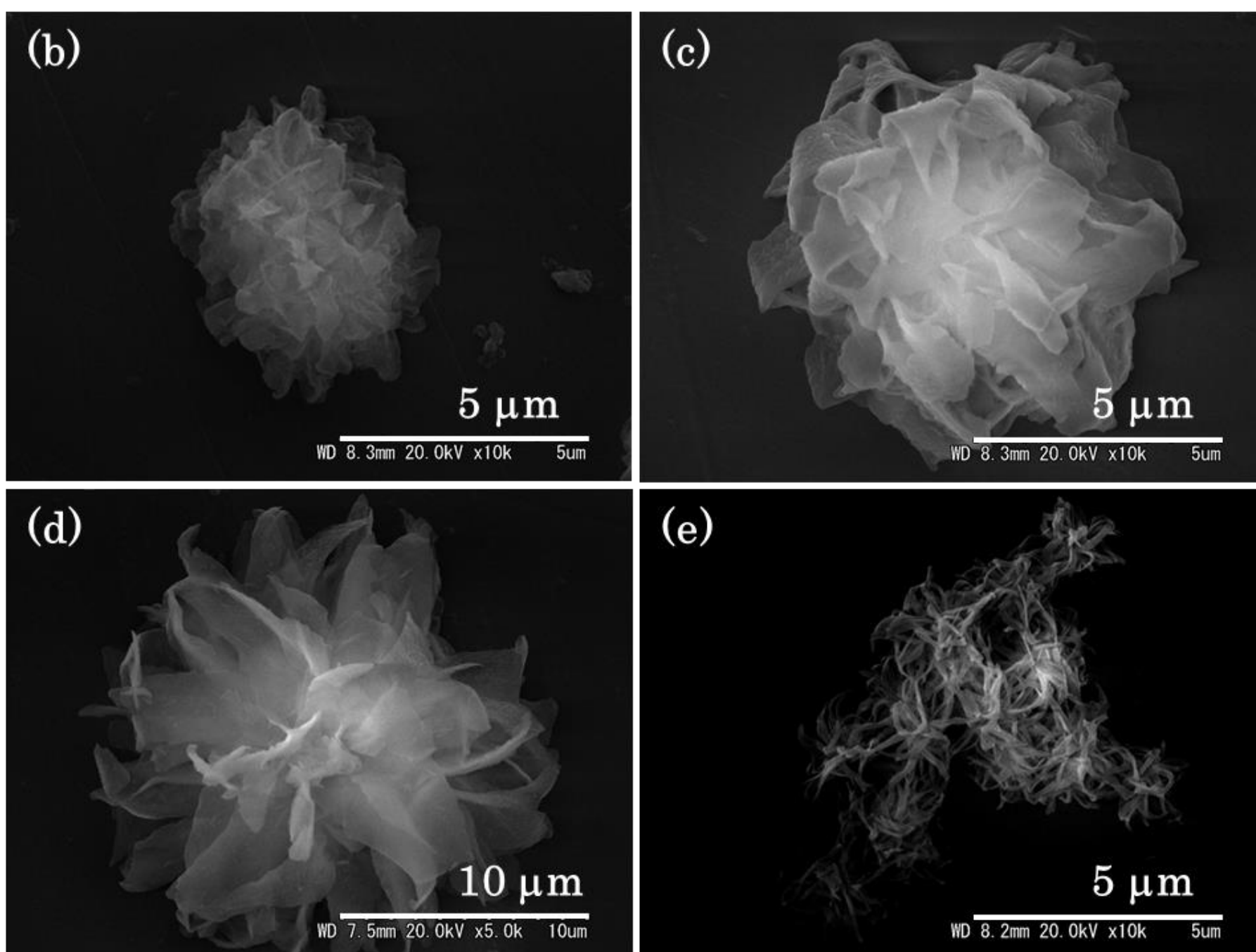


Figure 3-4 Morphology of P(BID-*co*-PI) precipitates prepared from 7EAN and 5EAB in DBT at 330°C at a concentration of 2.0% at  $\chi_f$  of (a) 70mol%, (b) 50mol%, (c) 30mol% and (d) 0 mol%

generation of new nuclei. DSC thermograms of PBID prepared in Chapter 2 and P(BID-co-PI) were shown in Figure 3-5. These exhibited neither  $T_g$  nor  $T_m$  under their decomposition temperature. The imide structure conjugated to naphthalene moiety cannot provide the crankshaft effect sufficiently to reduce the melting temperature under the decomposition.

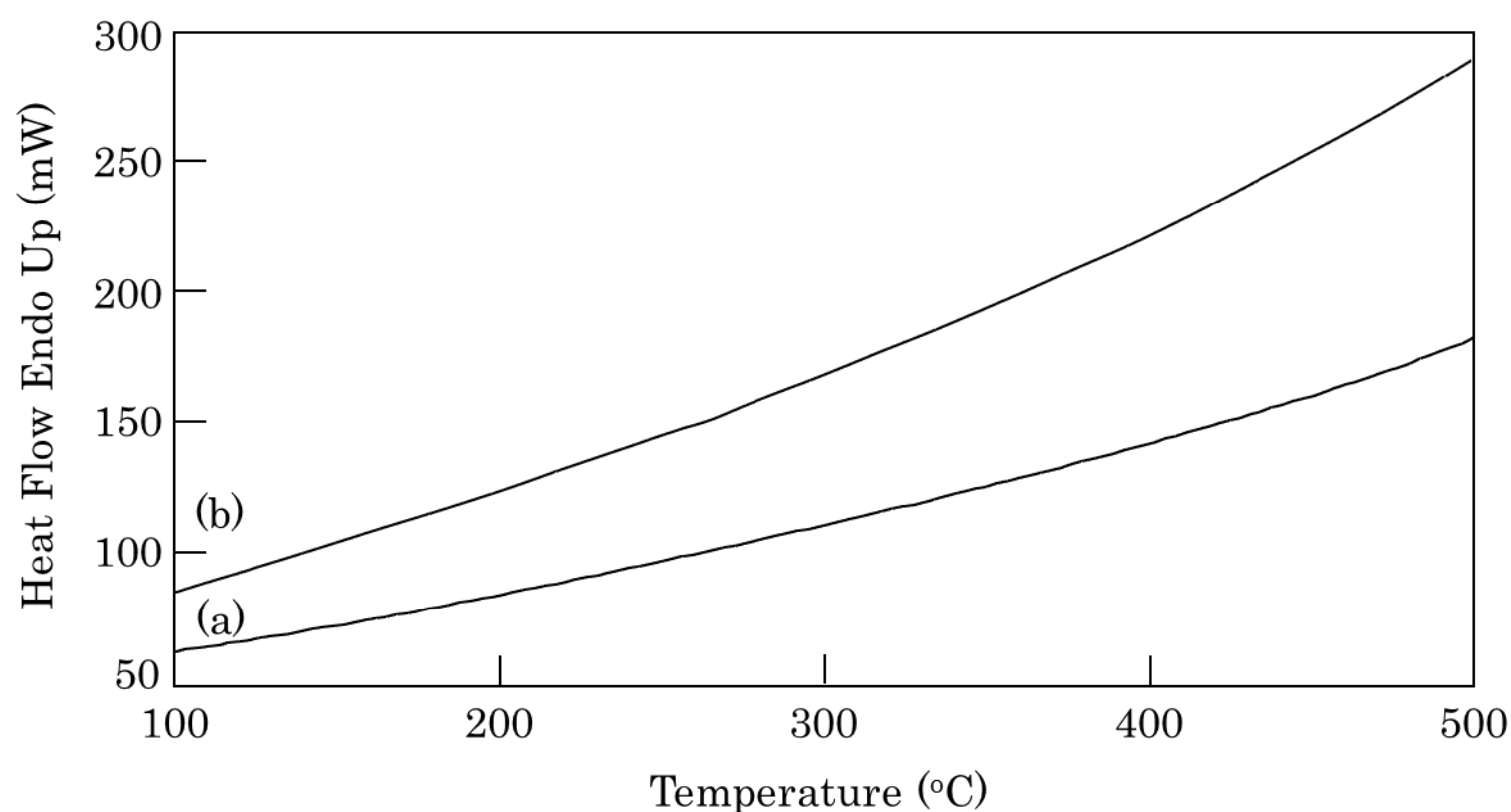


Figure 3-5 DSC thermograms of PBID and P(BID-co-PI) precipitates prepared in DBT at 330°C at a concentration of 2.0% from (a) 6EAN and (b) 6EAN and 4EAB at 30 mol% of  $\chi_f$  value.

### 3-4 CONCLUSIONS

Copolymerizations of EAN and EAB afforded the precipitates, but contrary to expectation they were not fusible. The crankshaft effect of naphthalene moiety was not effective to lower the  $T_m$  under the decomposition temperature in the case of polyimide. The morphology of copolymers was also influenced by not only the value of  $\chi_f$  but also the

structure of the monomer. Generally, copolymerization extinguished the clear morphology, especially in the middle of the  $\chi_f$  value owing to the lower crystallizability of oligomers and the tendency to induce the liquid-liquid phase separation instead of the crystallization. Although the copolymerizations of 6EAN and 4EAB gave the precipitates showing unclear morphology and the spheres at the  $\chi_f$  of 50 and 30%, those of 7EAN and 5EAB did the plate-like crystal having protuberances on surface.

### 3-5 REFERENCE

- [1] Kimura, K.; Kohama, S.; Kuroda, J.; Shimizu, Y.; Ichimori, Y.; Yamashita, Y., *J. Polym. Sci., Part A: Polym. Chem.*, 2006, **44**, 2732.
- [2] Kimura, K.; Ichimori, T.; Wakabayashi, K.; Kohama, S.; Yamazaki, S., *Macromolecules*, 2008, **41**, 4193.
- [3] Ichimori, T.; Yamazaki, S.; Kimura, K., *J. Polym. Sci., Part A: Polym. Chem.*, 2011, **49**, 4613.
- [4] Economy J, Volksen W, *Marcel Dekker, New York*, 1983, 299.
- [5] Calundann, G. W., *US patent*, US 4130545, 1978.
- [6] Chung, T. S.; Cheng, M.; Goh, S. H.; Jaffe, M.; Calundann, G. W., *J. Appl. Polym. Sci.*, 1999, **72**, 1139.
- [7] Wakabayashi, K.; Uchida, T.; Yamazaki, S.; Kimura, K., *Macromolecules*, 2008, **41**, 4607.
- [8] Kimura, K.; Kohama, S.; Yamazaki, S., *Polym. J.*, 2006, **38**, 1005.
- [9] Schwarz, G.; Zemmann, U.; Kricheldorf, H. R., *High Perform. Polym.*, 1997, **9**, 61.
- [10] Kricheldorf, H.R.; Adebahr, T., *J. Polym. Sci., Part A: Polym. Chem.*, 1994, **32**, 159.



- [11] Kricheldorf, H. R.; Loehden, G.; Wilson, D. J., *Macromolecules*, 1994, **27**, 1669.
- [12] Kimura, K.; Nakajima, D.; Kobashi, K.; Yamashita, Y.; Yokoyama, F.; Uchida, T.; Sakaguchi, Y., *Polym. Adv. Tech.*, 2000, **11**, 747.

## CONCLUDING REMAREKS

Self-condensed polyimides are expected to be high performance and high functional materials due to the excellent mechanical properties, thermal stability, chemical resistance, non-linear optical properties and so on derived from the asymmetry rigid-rod structure. However, constraints of synthesis of them are inhibited to avail them as actual materials. One possibility for the synthesis reported previously is the use of condensation agent, but it is unfavorable both environmentally and economically. Additionally, most of them exhibit neither solubility nor meltability, resulting in the difficulty in withdrawing of their potential for industrial usage. Chemical modification had been applied in order to endow them processability, but the excellent properties lost at the same time due to the reduction of molecular chain rigidity. In order to overcome the problem between intractability and properties, morphology control of rigid-rod polymers during polymerization have been eager to be developed since several years. Under these circumstances, new methodology for the morphology control of self-condensed polyimide was examined in this study.

In Chapter 1, morphology control of POPI was examined. POPI spherical aggregates of plate-like crystals, rod-like crystals and fiber-like crystals were obtained by the polymerization of MAPB by means of reaction-induced phase separation of oligomers during polymerization. Most of products were possessed high crystallinity and high molecular weight, and they were prepared in one-step procedure. The spherical aggregates of plate-like crystals were prepared by the polymerization under various conditions. In the polymerization in DBT and BPN, the obtained spherical aggregates diameter was 2 – 5  $\mu\text{m}$ , and the plate-like crystals were grown like crosshatch form. On the other hand, in the polymerization in DPS, obtained spherical aggregates diameter was ca. 8  $\mu\text{m}$ , and the plate-like crystals were oriented in circumferentially. This morphological difference of

spherical aggregate is attributed to miscibility for the solvents. DPS possesses higher miscibility than DBT and BPN to the oligomers, and thus liquid-liquid phase separation was induced to low crystallinity spherical aggregate of plate-like crystals. In the polymerization in DBT/LPF = 5/5 and DBT/LPF = 7/5, rod-like crystals were obtained. This rod-like crystal was composed of small plate-like crystals, in which the plate-like crystals were stacked in rod long direction. Polymerization in DBT at 330°C at a concentration of 0.5 or 1.0%, and 350°C at a concentration of 1.0% were formed fiber-like crystals. The most suitable condition for preparation of the fiber-like crystals was polymerization in DBT at 330°C at a concentration of 1.0%. The fibers prepared in this condition were approximately 250 nm in width and some of them were longer than 15  $\mu\text{m}$ . They were composed of small rectangle crystals as rod-like crystals prepared in DBT/LPF = 5/5 and DBT/LPF = 7/5, and their molecular chains were aligned perpendicular to the long direction of the fibers. The copolymerization usually distinguished the clear morphology, but the precipitates having the clear morphology were formed even at the middle copolymerization ratio ( $\chi_f$ ). The precipitates of one-dimensional structure such as ribbon, cone, rod and fiber were formed by the polymerization in DBT. The oligomers rich in the PPI moiety were initially precipitated to form the crystals served as the nuclei, because the solubility of the oligomers rich in the PPI moiety was lower than that of the oligomers containing the POPI moiety in DBT. The copolymer molecules might align along the long direction of the one-dimensional crystals. The POPI and P(OPI-*co*-PI) crystals were infusible under their decomposition temperature and they exhibited outstanding thermal stability. It is concluded that high molecular and high crystallinity POPI were prepared by reaction induced phase separation of oligomer during polymerization and molecular chains orientation could be controlled by using PPI crystal nuclei as a template.

In Chapter 2, synthesis and morphology control of PBID and influence of monomer

functional group for morphology were observed. Four kinds of monomers, 6EAN, 7EAN, APNI and ANDA were used in this Chapter. 6EAN and 7EAN which are structural isomers mutually produce imide linkage *via* the amic acid or amic ester. On the other hand, APNI and ANDA produce imide linkage in one-step. The morphology of PBID was highly influenced by not only polymerization conditions but also the structure of the monomer. The rod-like crystals and the spherical aggregates of plate-like crystals were formed in DBT at 330°C from 6EAN and 7EAN. This morphological difference was attributed to the degree of imidization of the precipitated oligomers. The rod-like crystals were formed by the spiral growth caused by the screw dislocation in the polymerization of 6EAN due to precipitation of oligomers that are rich in imide content. But in the case of polymerization of 7EAN, the plate-like crystals are formed by the lateral growth of the oligomers that are rich in amic acid or amic ester because the strong interaction between the oligomers through hydrogen bonding strictly prevented the screw dislocation. However, in the polymerization at 350°C, spherical aggregates of plate-like crystals were formed in both monomers. The higher molecular weight oligomers were precipitated at 350°C and they might suppress the occurrence of the screw dislocation, resulting in the formation of the plate-like crystals. The plate-like crystals having protuberances on the surface were formed in TPB from 6EAN. It is suggested that the PBID molecules might align perpendicular to the plate plane, and the fine plate-like crystals of the protuberances possess the same crystal structure as the mother plate-like crystal. The twisted and non-twisted ribbon-like crystals were formed in DBT from APNI owing to precipitation of fully imidized oligomers. Polymerizations of ANDA were afforded needle, fiber and microsphere. These PBID precipitates possessed high crystallinity, and they showed excellent thermal stability and chemical resistance. It is concluded that various morphology of the PBID such as rods, plates have protuberances perpendicular or flat surface, lathes, twisted and non-twisted ribbons, needles, fibers and

micro spheres were fabricated, and their morphologies were highly affected by monomer functional groups

In Chapter 3, synthesis and morphology control of P(BID-*co*-PI) was investigated with the comparison of P(OB-*co*-ON) which is well-known thermotropic wholly aromatic polyesters. The morphology of copolymers was also influenced by not only the value of  $\chi_f$  but also the structure of the monomer. Generally, copolymerization extinguished the clear morphology, especially in the middle of the  $\chi_f$  value owing to the lower crystallizability of oligomers and the tendency to induce the liquid-liquid phase separation instead of the crystallization. In fact, copolymerizations of 6EAN and 4EAB gave the precipitates showing unclear morphology and the spheres at the  $\chi_f$  of 50 and 30%. However, copolymerization of 7EAN and 3EAB did the plate-like crystal having protuberances on surface due to strong interaction attributed to the hydrogen bonding. Contrary to expectation, these precipitates were not fusible. The crankshaft effect of naphthalene moiety was not effective to lower the  $T_m$  under the decomposition temperature in the case of polyimide. It is concluded that copolymerization significantly affects the morphology by not only  $\chi_f$  values but also the kind of isomers, and P(BID-*co*-PI)s were not exhibit thermotropicity such as P(ON-*co*-OB)

Finally, this research for doctoral dissertation has afforded the new methodology for the morphology control of self-condensed polyimides, and the result will contribute significantly to provide the new materials possessing ultimate performance and functions.

## LIST OF PUBLICATIONS

[1] Morphosynthesis of poly[4-(1,4-phenylene)oxyphthalimide] and copolymers prepared by reaction-induced crystallization during polymerization

Takashi Sawai, Kanji Wakabayashi, Shinichi Yamazaki, Tetsuya Uchida, Kunio Kimura, Journal of Polymer Science Part B : Polymer Physics, Volume 50, Issue 18, pages 1293-1303

[2] Synthesis and Morphology Control of Self-condensable Naphthalene-containing Polyimide by using Reaction-induced Crystallization

Takashi Sawai, Kanji Wakabayashi, Shinichi Yamazaki, Tetsuya Uchida, Yoshimitsu Sakaguchi, Ryouhei Yamane and Kunio Kimura, European Polymer Journal, Volume 49, issue 8, pages 2334-2343

[3] Preparation of Novel Naphthalene Polyimide and Its Morphology

Takashi Sawai, Tetsuya Uchida, Shinichi Yamazaki, Kunio Kimura, Journal of Photopolymer Science and Technology, Volume 26, No. 3, pages 341-344

## ACKNOWLEDGMENTS

I would like to express my deepest and heartfelt gratitude to Professor Dr. Kunio Kimura, Department of Environmental Chemistry and Materials, Okayama University, for his proper guidance, untiring efforts, valuable advice, numerous helpful suggestions, constant and warm encouragement and through this work.

I am greatly and deeply indebted to Dr. Shinichi Yamazaki, Associate Professor of the Department of Environmental Chemistry and Materials, Okayama University, for his special guidance, invaluable counsel, numerous fruitful discussion, cordial direction and continuous encouragement throughout this experimental research work.

I am deeply indebted to Emeritus Professor Dr. Yuhiko Yamashita, Department of Environmental Chemistry and Materials, Okayama University, for his valuable advice, helpful suggestions and warm encouragement during this course study.

I am deeply grateful to Emeritus Professor Dr. Kaoru Shimamura, Department of Applied Chemistry, Okayama University, for his useful suggestions and warm encouragement. I wish to thanks Dr. Takumi Okihara, Lecturer and Dr. Tetsuya Uchida, Associate Professor, Department of Applied Chemistry, Okayama University, for their useful suggestions.

I am deeply indebted to Professor Dr. Yukitaka Kimura and Associate Professor Dr. Yutaka Takaguchi, Department of Environmental Chemistry and Materials, Okayama University, for their enlightening comments to improve this manuscript.

I extend my sincere thanks to all members, past and present of Kimura laboratories for their cooperation and friendship throughout my study here.

I extend my special thanks to my family for warm encouragement and support throughout my study.

Takashi Sawai

Graduate school of Environmental Science

Okayama University

3-1-1, Tsushima-naka

Okayama 700-8530

Japan

March 2014